**UNIVERSITA' DEGLI STUDI DI CATANIA**

Dipartimento di Scienze Chimiche

DOTTORATO DI RICERCA INTERNAZIONALE
IN SCIENZE CHIMICHE
XXVIII CICLO

# Synthesis and use of new Porphyrin Derivatives

**PhD Coordinator**: Prof. S. Sortino

**Tutor**: Prof. G. A. Tomaselli

**PhD Student**: Chiara Maria Antonietta Gangemi

2014/2015

*Dedicated to my father,*

*Now as three years ago.*

# Acknowledgements

I would like to thank my family who supported me in numerous ways throughout my life. I could not have achieving this difficult task without their help.

I would like to express my sincere gratitude to my Ph.D advisor Professor G.A. Tomaselli who accepted me into the group and for the continuous support of my Ph.D study and research, for his motivational help and knowledge.

Besides my "official" tutor, I would like to thank my Ph.D co-tutor, Professor R. Purrello, whose expertise, understanding and patience have improved considerably my Ph.D experience and my knowledge in porphyrin chemistry.

A particular thank goes to my mentor Professor Nina Berova, who made my American period at Columbia University rich of human and professional experiences. She always encouraged me to do my best and to widen my research from various perspectives. Thus, she will be an example of hard working scientist and woman.

I would like to express my gratitude to Dr. Alessandro D'Urso and Rosalba Randazzo for their knowledge and helpfulness.

My research would not be easy without the help Dr. Giuseppe Trusso Sfrazzetto and Dr. Andrea Pappalardo. Their suggestions and help with the characterization of my compounds have made my thesis possible; they are colleagues but above all friends. I would to thank all my research group's members: Prof. F. P. Ballistreri, Prof. M.A. Amato, Dr. R.M. Toscano, for their support. In my daily work, I have been gladden by a friendly and cheerful group and enjoyable students.

Finally, I would to thank all collaborators: Prof. M.E. Fragalà (University of Catania) for SEM images and Prof. P. Mineo (University of Catania) for the MALDI spectra, Prof. Koji Nakanishi of the Columbia University, Prof. Liliya A. Yatsunyk of the Swarthmore College, Giorgia Oliviero, Gennaro Piccialli and Giovanni Di Fabio of University of Napoli "Federico II".

# Table of contents

**Appendix A**

**Appendix B**

# 1. Introduction

## 1.1 Porphyrins and their Properties

Porphyrins are an important class of organic molecules largely present in biological world. The word *porphyrin* derives from Greek word "*porphyrá*" which means purple, in fact, often the porphyrins are intensely red or purple coloured, or green when they are metallated or with a protonated core. In many cases, they represent the prosthetic groups or active sites of several proteins, whose function ranges from the oxygen transfer and storage (hemoglobin and myoglobin), to electron transfer (cytochrome c, cytochrome oxidase), to energy conversion (chlorophyll). Porphyrins have attracted considerable attention because they are ubiquitous in natural systems and have prospective applications as mimicking enzymes, in catalytic reactions, in photodynamic therapy, as molecular electronic devices and in the conversion of solar energy. Porphyrins are made up of an aromatic macrocycle ring consisting of four pyrrole molecules (green, Figure 1.1), linked together with four-methine bridging units (red, Figure 1.1).[1]



**Figure 1.1** The porphyrin skeleton. Pyrrole rings are shown in **green** and methine bridges in **red**.

Numbering of the porphyrin nucleus runs along the twenty peripheral carbon atoms and the inner nitrogens are enumerated from 21 to 24 (Figure 1.1). Porphyrins can be peripherally substituted in 12 positions: in eight β-positions on the pyrrolic rings and in four *meso*-positions corresponding to the methine bridges. The unsubstituted porphyrin has named *porphine*.

Porphyrin macrocycle is an aromatic heterocyclic system containing 22 π-electrons, although only 18 of them are delocalized according to the Hückel's rule of aromaticity (4n+2 delocalized π-electrons, where n = 4). In fact, double bonds 7-8 (Δ7) and 17-18 (Δ17) can be easily reduced since they are not involved in aromatic conjunction and thus producing the so-called *chlorin* compounds. The π-electrons delocalization depends on the form of the porphyrin, in fact they are weak bases and they may present as: (i) free base or unprotonated, (ii) fully deprotonated or dianionic form, (iii) metal complex or dicationic form (Figure 1.2).



**Figure 1.2** Delocalization pathway in porphyrin as (i) free base, (ii) dianionic form and (iii) metal complex.

In the unprotonated porphyrin, the two inner protons are mobile and liberally jump among the four nitrogens. The *trans*-(21, 23-H and 22, 24-H) tautomer is energetically preferred to the *cis*- form (22, 23-H and 21, 24-H)(Figure 1.3).

**Figure 1.3** *Cis-/trans-*Porphyrin tautomerism

Porphyrins form a great number of complexes with metal ions and some with non-metals (Figure 1.4). The coordinating environment provided by porphyrins is very flexible and it can be fine-tuned to particular oxidation and spin states by changing peripheral substituents and/or axial ligands. This "*tunability*" is probably the Nature reason to choose porphyrin as its "*workhorse macrocycle*".



**Figure 1.4** Elements known to form complexes with porphyrins **green**. Metals found in nature complexed with porphyrin are showed in **red**.

## 1.1.1 UV-visible Spectra of Porphyrins

Porphyrins typically show very intense absorption bands in the visible region. The absorption spectrum of porphyrins has long been understood in terms of the highly successful *"four-orbital model"* (two highest occupied π orbitals and two lowest unoccupied π*orbitals) firstly applied in 1959 by Martin Gouterman[2] who has proposed, in the 1960s, this model to explain the absorption spectra of porphyrins.



**Figure 1.5** Absorption spectrum of $H_2TPP$ in benzene (~ 4μM, 5 mm).[3]

The electronic absorption spectrum of a porphyrin consists of two distinct regions: in the near ultraviolet and in the visible region (Figure 1.5). The first region encompasses the transition from the ground state to the second excited state ($S_0 \rightarrow S_2$) and the corresponding band is called *"Soret"* or *"B band"*. The range of absorption is between 395-450 nm, with a molar extinction coefficients (ε) of $10^5$ $M^{-1}$ $cm^{-1}$, depending on whether the porphyrin is *β*-or *meso*-substituted. The second region consists, at longer wavelengths in the 500–750-nm range, of a weaker, but still considerably intense transition to the first excited state ($S_0 \rightarrow S_1$). These absorption bands are called *"Q bands"* and they have molar extinction less intense respect to *Soret* band. These favourable spectroscopic features of porphyrins are due to the conjugation of 18 π-electrons and offer the advantage

4

of easy and precise monitoring of guest-binding processes by spectroscopic methods (e.g., UV-visible,[4] CD,[5] fluorescence[6] and NMR spectroscopy[7]).

## 1.1.2 Synthesis of porphyrin

The synthetic world of porphyrins is extremely rich and its history began in the middle of *1930s*. An enormous number of synthetic procedures have been reported until now. For example, tetramerization of pyrroles [3+1] condensation and [2+2] condensation are common methodologies.[8] The most famous monopyrrole polymerization route to obtain symmetrical porphyrins such as tetra-phenylporphyrins, is the acid-catalysed condensation reaction of pyrrole with specific aldehyde, followed by oxidation of the resulting *porphyrinogen*. This procedure was first developed by Rothemund[9a] (Scheme 1.1) and after modifications by Adler, Longo and colleagues,[9] was finally optimized by Lindsey's group.[10] It generally gives around 20% yields for tetra-arylporphyrins. Despite the modest yields, the relative simplicity of this method has made it well suited for preparation of large amounts of tetra-arylporphyrins (*i.e.* >1 g of porphyrin).



**Scheme 1.1** Rothemund's synthesis, in one-step by reaction of benzaldehyde and pyrrole in pyridine

Adler, Longo and coworkers, in the *1960s*[10] re-examined the synthesis of meso-substituted porphyrins and developed an alternative approach (Scheme 1.2). This method involves an acid catalysed pyrrole-aldehyde condensation in glassware open to the atmosphere in the presence of air. The role of acid is to activate aldehyde with protonation of carbonyl group. The reactions were carried out at high temperature, in different solvents and in the concentration range of reactants from 0.01 M to 0.2 M. The yields are in the 30-40% range, although they decrease in the presence of metal salts.



**Scheme 1.2** Adler-Longo's method: acid catalysed pyrrole aldehyde condensation in the presence of air.

Over the period 1979-1986, Lindsey[12] developed a new and innovative *two-step* room temperature method to synthesize porphyrins, motivated by the need for more gentle conditions for the condensation of aldehydes and pyrrole, in order to enlarge the number of aldehydes utilizable and consequently the porphyrins available. This synthesis of porphyrins is based on a sequential process of condensation and oxidation steps (Scheme 1.3). The reactions were carried out under mild conditions in an attempt to achieve an equilibrium during condensation and to avoid side reactions in all steps of the porphyrin-forming process. The maximum yield of tetraphenyl porphyrin is obtained when a solution of dry methylene chloride is charged with benzaldehyde and pyrrole at equimolar concentrations of $10^{-2}$ M. To this solution is added an aliquot of trifluoroacetic acid or $BF_3$-etherate ($10^{-3}$ M). The condensation was found to level

off after 30-60 minutes at room temperature. Then in a second step, the oxidant *2,3-dichloro-5,6-dicyanobenzoquinone* (DDQ) is added in stoichiometric amount and the solution is stirred for 1 h at room temperature.

The Lindsey method has the advantage that it can be used to prepare porphyrins that required the use of acid-unstable aldehydes not generally employed under Adler-Longo conditions.

## 1) Condensation



## 2) Oxidation



**Scheme 1.3** Lindsey's method

The synthesis of the less symmetric porphyrin requires the formation of two types of *meso*-carbons. It is possible to synthesize unsymmetrical substituted porphyrins via *mixed aldehyde* condensations (Scheme 1.4, left). By using a mixture of two different aldehydes as starting materials, in the Adler or Lindsey syntheses, a statistical mixture of products is obtained (Figure 1.6).[11]

**Dipyrromethane + Aldehyde Condensation**

**Mixed Aldehyde Condensation**



A₄-Porphyrin

A₃B-Porphyrin

*trans*-A₂B₂-Porphyrin

*cis*-A₂B₂-Porphyrin

AB₃-Porphyrin

B₄-Porphyrin

1) Acid
2) DDQ

1) Acid
2) DDQ

**Scheme 1.4** Mixed-Aldehyde condensation (left) and a MacDonald-type [2+2] condensation (right).

Thus, mixed aldehyde condensation is a simple and practical way to prepare unsymmetrical porphyrins but the desired porphyrin has to be separated using extensive chromatography. This approach is still used to obtain the different regioisomers (the *trans*- A₂B₂ is the main product), but the yields are usually in 2–4% range and the purification of the six regioisomers formed is quite time consuming.[12]



**Figure 1.6** Porphyrin regioisomers

8

A more convenient method for the direct synthesis of *meso*-substituted trans-$A_2B_2$ porphyrins is the reaction of a dipyrromethane with an aldehyde in acidic conditions proposed by Lindsey (Scheme 1.4, right).[13] Condensation of a dipyrromethane with an aldehyde in a MacDonald-type [2+2] condensation has been used to prepare a wide range of meso-substituted *trans*porphyrins.

Actually, this methodology suffers from three major limitations: (1) the condensation is performed in dilute solution (10 mM). (2) Isolated yields of porphyrin are modest (10-30%). (3) The product of a dipyrromethane-aldehyde condensation is frequently not just the desired *trans*-$A_2B_2$-porphyrin. Due to *scrambling* reactions, a dipyrromethane acidolysis followed by a recombination process (Figure 1.7), we obtain a mixture of porphyrins that can be extremely difficult to separate (especially the t*rans*-$A_2B_2$ and *cis*-$A_2B_2$ isomers).[14] As a result, pure *trans*-porphyrins have been typically available only in limited quantities.



**Scheme 1.5** Substituent scrambling requires two processes: acidolysis (up) and fragment recombination (down).

## 1.1.3 ^{1}H-NMR spectra of porphyrins

Studies performed in the last decades demonstrated that Nuclear Magnetic Resonance (NMR) spectroscopy is a very powerful tool for exploring molecular structure and gives important information about aromatic structures.[7] The presence in the porphyrin macrocycle of an extended delocalized π-electron system gives rise to a strong ring current in the molecules when placed in a magnetic field. In fact, porphyrin aromaticity is most frequently described in terms of the [18]annulene model, proposed by E. Vogel.[15] According to that model the porphyrin is viewed as a bridged diaza[18]annulene, in which the ring current de-shields the external protons (at δ from 9.7 to 11.2 ppm for the *meso*-protons, and at δ from 8.5 to 9.9 ppm for the α-protons). Meanwhile, the inner -NH protons are shifted up-field because they are exocyclic with respect to the local ring currents and *endo*-cyclic with respect to the macrocyclic current. Undoubtedly, the shielding effect of the latter prevails and the signals for the protons of the NH groups are observed at very high field region (at δ from -1.4 to -4.4 ppm). The β-hydrogen atoms of the pyrrole and pyrrolenine fragments are in principle non-equivalent. However, rapid transformations (within the NMR time scale) occur at room temperature and the signals for the β-protons are averaged. Two different peaks corresponding β-CH groups of the pyrrole and pyrrolenine fragments can be observed only at low temperature, -80 °C. In *meso*-arylporphyrins the aryl protons of *meso*-phenyl groups resonate in the range of 7.5-8.5 ppm (-$H_o$ ≈ 8.2 ppm; -$H_m$ and -$H_p$ ≈7.8 ppm) Table 1.1.

**Table 1.1** ^{1}H-NMR chemical shift (δ/ppm) of the free base tetra-arylporphyrins relative to $CHCl_3$.

| Compound | δ -NH | δ $H_{m,p}$ | δ $H_o$ | δ $H_β$ | δ $OCH_3$, δ $CH_3$ |
|---|---|---|---|---|---|
| $H_2$TPP | -2.71 | 7.81 | 8.26 | 8.87 | - |
| $H_2$T(4-Cl)PP | -2.87 | 7.75 | 8.14 | 8.85 | - |
| $H_2$T(4-$CH_3$)PP | -2.77 | 7.56 | 8.11 | 8.86 | 2.71 |
| $H_2$T(4-$CH_3$O)PP | -2.82 | 7.23 | 8.07 | 8.79 | 3.95 |

## 1.2 BODIPYs and their proprieties

The 4,4-Difluoro-4-bora-3a,4a-diaza-s-indacene (hereafter abbreviated to BODIPY) dyes were first discovered in 1968 by Treibs and Kreuzer,[16] but only on late '*90s* the scientists understood the property of these compound.

The IUPAC numbering system for BODIPY dyes is different to that used for classic dipyrromethenes. However, the terms β-, α-positions, and *meso-* are used in the same way for both systems.



"BODIPY core"            "dipyrrin core"            dipyrromethane core
                         of dipyrromethenes

**Figure 1.7** BODIPY, di-pyrromethene and di-pyrromethane IUPAC numbering system

In the last years different BODIPYs were synthetized and studied, they were used in biotechnological and medical field:[17] *e.g.* as sensor, as probes for molecular imaging, or molecular structure[18] or as fluorescent labelling molecules for DNA.[19] In particular, BODIPY dyes have been recognized as a promising platform in these fields for the construction of molecular probes because of their excellent characteristics such as the fluorescence emission spectra with high fluorescence quantum yields, sharp absorption (Figure 1.8), and high photo and chemostability.

They are also relatively insensitive to the polarity and pH of their environment and are reasonably stable to physiological conditions. Therefore, small modifications to their structures enable tuning of their fluorescence characteristics; consequently, these dyes are widely used to label proteins[20] and DNA.[21-22]

**Figure 1.8** Typical absorption (A) and emission (B) spectra of 1,3,5,7-tetramethyl-mesophenyl-BODIPY, $\lambda_{ex}$ = 470 nm.

The low energy band ($\lambda \approx$ 460 nm) in the UV-Vis spectra is due to the $S_0 \rightarrow S_1$ transition (from the ground state to the first excited state) and is characterized by a high molar extinction coefficient ($\varepsilon \approx 10^5$ L mol$^{-1}$ cm$^{-1}$).

At high energy, there is a shoulder due to *out-of-plane* vibrations of the aromatic skeleton. Others bands are due to higher energy forbidden transitions ($S_2$, $S_3$, etc.) with less intense absorptions.[23]

The emission spectrum is specular to the absorption $S_0 \rightarrow S_1$. Quantum mechanical studies show that the geometry of the excited state is similar to the ground state's geometry, so the fluorescent band is characterized by a small Stokes shift. Therefore, the fluorescence is independent by the excitation wavelength, because the emission occurs during the transition between lower vibrational level of the excited state $S_1$, independently of which vibrational level is populated during the process. The intensity and the energy of the emission can be controlled by the insertion of proper substituent e.g. electron-donor groups in 2 or 6 positions move the emission to higher wavelength, while electron-withdraw groups in the same position give the opposite effect.[24]

Aryl or alkyl groups in *meso-* position do not affect the wavelength of the absorption or of the emission, but they decrease the quantum fluorescence yield. The most important effect in this case is due to the groups in *1-* or *7-* position,

because they hinder the rotation of the phenyl group, reducing the no-radiative loss of energy (Figure 1.9).[25]



MeOH, Φ 0.19
$\lambda_{max\ abs}$ 508 nm
$\lambda_{max\ emiss}$ 521 nm

MeOH, Φ 0.65
$\lambda_{max\ abs}$ 498 nm
$\lambda_{max\ emiss}$ 508 nm

**Figure 1.9** *meso*-Phenyl 1,7- substituted and un-substituted BODIPYs

## 1.2.1 Synthesis of BODIPYs

BODIPY's with *meso* groups can be obtained by reaction between pyrrole and acyl chloride or using anhydrides (Scheme 1.6).



**Scheme 1.6** Synthesis of BODIPY from pyrrole and anhydrides

The most useful synthesis to obtain BODIPY derivatives, is the reaction with aldehydes, although in this case is necessary using an oxidant agent such as p-Chloroanilin or DDQ. Aldehyde reacts with pyrrole, used as solvent, at room temperature to give the di-pyrromethane, which is oxidized and after reacts with di BF$_3$·OEt$_2$ (Scheme 1.7).



**SCHEME 1.7** Synthesis of BODIPY from pyrrole and aldehydes

This reaction is preferred to the previous one because is more flexible and is possible to use a wide range of aldehyde.

## 1.3 dsDNA

In the last 20 years it was recognized that changing the biological conditions, DNA can adopt different 3D-conformations in order to execute specific roles during the cell life.

DNA is characterized by an extensive polymorphism as showed by the wide range of structures that it may assume (e.g. A-, B-, Z-DNA, G-quadruplex etc.). Each structure presents different conformation of the sugar, of the backbone and consequently different parameters like helix diameter or base pairs per turn (Figure 1.10).

Usually all these structures are temporarily present in the cell and they can interconvert each other under particular physiological conditions (Figure 1.11).

Obviously, these different conformations affect the interactions with other molecules so the binding studies of DNA with different molecules can provide rational ways to design efficient *"DNA-target"* drugs. Therefore, the design of novel small molecules for specific DNAs targeting is one of the most important goals in modern medicinal chemistry. The roles of these different conformations are not completely known. For example, it has found a correlation between the Z-form of DNA and chromosomal breakpoints in human tumours, it seems that Z-DNA is able to activate the transcription of c-myc gene responsible of the genesis of lymphoid malignancies.[26]

Moreover, it is found that in the Alzheimer disease the β-amyloid aggregates converts the Z-DNA back into the B form.[27]

| A. A-DNA | B. B-DNA | C. Z-DNA |
|---|---|---|
| Twist = 33° | Twist = 36° | <Twist> = -30° |
| Rise = 2.56 Å | Rise = 3.38 Å | <Rise> = 3.7 Å |
| Roll = 6° | Roll = 0° | <Roll> = 0° |
| Inclin. = 21° | Inclin. = -6.0° | <Inclin.> = -6.2° |
| $x$-Dis. = -4.5 Å | $x$-Dis. = 0.23 Å | <$x$-Dis.> = 3.0 Å |
| P-Tw = -7.5° | P-Tw = -4.4° | <P-Tw> = -4.4° |

**Table 1. Comparison of Helices of B-Form and a Variety of Z-DNA Forms**

| parameter[a] | B-form[b] | Z-form[c] |
|---|---|---|
| helical sense | right-handed | left-handed |
| helix diameter | 18.4 | 16.0 |
| base pairs per turn | 10 | 12 |
| helical twist[e] | 36 | −60 |
| helix pitch (rise per turn) | 34.0 | 44.6 |
| mean rise per base pair | 3.40 | 3.72 |
| phosphorus radius: | | |
|   inner | 9.2 | 6.1 |
|   outer | 9.1 | 8.0 |
| mean base inclination | 15.0 | 2.3 |
| sugar pucker | | |
|   G | C2′-*endo* | C3′-*endo* |
|   C | C2′-*endo* | C2′-*endo* |
| glycosidic bond | | |
|   G | *anti-* | *syn-* |
|   C | *anti-* | *anti-* |
| P−P distance across minor groove | | |
|   GpC to CpG (width) | 11.8 | |
|   GpC to GpC (max.) | | 18.1 |
|   CpG to CpG (min) | | 8.6 |

**Figure 1.10** Structures of A-, B-, Z-DNAs (top) and conformational characteristics.
(*Chemical Reviews, 2006, 106, 2045*)

**Figure 1.11** Scheme of the families of naturally occurring DNAs. Transitions between DNA families are induced by changing ionic strength or solvent polarity in solution or changing salt content in fibers. Critical salt or ethanol concentrations give midpoints rather than endpoints of transitions. (*Chemical Reviews, 2006, 106, 2045*)

Among all conformations, the Z-DNA seems to be the most interesting and promising structure, in relation to the biological functions of the cells and thus it is the well-studied. DNA containing an alternation of purine and pyrimidine repeats is able to adopt the Z conformation, a left-handed double helix (Figure 1.10), characterized by a high-energy structure, in which glycosylic bonds of purines are in *syn*- and of pyrimidines are in *anti*-conformation, and with C3'-*endo* and C2'-*endo* for the sugar pucker respectively (Figure 1.12).

**Figure 1.12** Representation of conformation of the glycosylic bond (left) and of the sugar pucker (right)

It has been shown that Z-DNA can exist *in vivo* as a transient structure induced by a biological process and it occurs in a dynamic state, formed as result of physiological conditions, which then relaxes to the right-handed B-DNA.[28] However, the exact biological role of Z-DNA is unknown, yet. *In vitro* the B-Z transition is observed under a variety of conditions including molar concentrations of NaCl, millimolar of $NiCl_2$ (Figure 1.11) or other transition metal complexes $[Co(NH_3)_6]^{3+}$ and micromolar of spermine or chiral binding molecules.[29]

The exact mechanism and/or the kinetics occurring in the transition is not clear although the widely accepted is the *"zipper model"* which involves a two-stage B-Z transition (Figure 1.13).[30]

**Figure 1.13** The zipper model of the B-Z transition. The B-DNA conformation forms a high-energy nucleation step involving two B-Z junctions. The propagation of Z-DNA takes place as the junction migrates in opposite directions along the DNA strands in a cooperative way until all polymer is in the Z-DNA conformation.

Furthermore the B form of poly[d(G-C)•d(C-G)] is more easily transformed into the Z form increasing polymer length.[31] Furthermore, the presence in this sequence of 3 hydrogen bonds for each couple G•C, instead of the 2 H-bonds present in A•T couples (Figure 1.14), contributes to maintain the DNAs in the double strand during the transitions.



**Figure 1.14** Watson and Crick C•G and A•T base pairs with the grooves and the hydrogen bonds (dot line) labelled.

As a high-energy structure a *"not stabilized Z-DNA"* returns into the more stable B form making difficult to study this conformation.

However, the Z-DNA, as high-energy structure, if not stabilized it spontaneously will return in the more stable B conformation, making difficult to study this structure. Therefore, the possibility to induce and stabilize the Z conformation permits to design efficient probes to understand the mechanism involved in the formation of this important structure of DNA.

Different studies are performed in the recognition of B- and Z-DNA; the use of chiral metal complexes or different enantiomers of a ligand displayed structural selectivity in the binding of different forms of DNA.[32] Nevertheless, these ligands cannot be used as chiroptical probes because in these cases, the recognition of the Z or B forms of DNA is not mirrored by distinctive spectroscopic features, such as new CD band, which unequivocally show the detection. Therefore, it is more efficient to use achiral molecules, spectroscopically mute, that give us an unambiguous signal of the specific detection for one of the two conformation of DNA.

Among the DNA ligands, a planar aromatic moiety appears more suitable for the intercalation into DNA. Furthermore, in combination with aromatic groups also the cationic groups, via electrostatic forces, contribute to small molecules ligands-DNA interactions.[33] Some dyes exploiting these interactions, are successful applied in the detection of DNA in solution, in fluorescence imaging techniques, in real-time polymerase chain reaction.

Among the different ligands, porphyrins are one of the most studied DNA binding agents. In particular, water-soluble porphyrins have a natural affinity for DNA, yielding various complexes with it.[34] Moreover, porphyrins interacting with DNA, show an ICD signal in the Soret region, which is free of interference (DNA, cell proteins etc).

One of the best examples of interacting porphyrins with DNA regards the tetra-cationic metal porphyrin (ZnTMPyP4), which has been applied as chiroptical probes for detection of left-handed Z-DNA in a poly(dG·dC) sequence[35] or in small portion of Z-DNA, inside longer sequence of B (Figure 1.15).[36]

**Figure 1.15** a) ZnTMPyP4 structure; b) Interaction of ZnTMPyP4 with poly(dG-dC) in Z-form; c) Modified bromo-guanine poly(dG-dC)in B-Z-B conformation.

In these cases the Z form was achieved using conventional inducers (spermine, $NiCl_2$ and NaCl) before adding the probe and the presence of other species such as the inducer itself could inhibit or change the interactions between the probe and the DNA structure.

At the same time, the possibility to have molecules, which act simultaneously as inducers or stabilizers and as well as probes opens a wide application field, in particular in the medical area.

The BODIPY derivatives for their characteristics can be also usefully applied for the interaction with DNA. As reported in recent studies,[37] a BODIPY cationic derivative (Figure 1.16) was successful used as sensitive fluorescent "turn-on" probes for DNA. In this case, the interaction between the dye and DNA give a substantial increase in fluorescence and this sensitive detection of DNA in aqueous solution it may be

particularly helpful in developing new diagnostics based on fluorescent DNA probes.



**Figure 1.16** *Fluorescence on* BODIPY intercalators

## 1.4 Telomere and G-Quadruplex

Among the different structures that DNA can adopt, triplex and Quadruplex have attracted a deep interest and several research groups have investigated the role of these *"non-canonical"* double helix structures, both in the regulation of the genes translation and in the growth of tumour cells, identifying them as a potential therapeutic targets.[38]

Moreover, G-Quadruplex has an interdisciplinary interest not only in the nucleic acid field but also in genomic, in supramolecular chemistry and in spectroscopy.[39] In guanine rich nucleic acid sequences the formation of a four-stranded structure called G-Quadruplex can occur (Figure 1.17). In this case, four guanines can associate *via Hoogsteen hydrogen bonds,* establishing a square planar structure called *"guanine tetrads"*; therefore, two or more guanine tetrads can stack on top of each other to form a G-quadruplex.[40]



**Figure 1.17** G-quadruplex structure.

G-Quadruplex conformations (GQ) are highly polymorphic and they can classified in term of stoichiometry (uni-, bi- and tetramolecular) and orientation of the strands (parallel, antiparallel and hybrid) (Figure 1.18).[41]

The type of GQs structure depends on the DNA sequence, on the length and on the conditions under which it has been prepared (*i.e.* nature of cations, presence of ligands and annealing conditions).



**Figure 1.18** Classification of G-quadruplex according to the stoichiometry and orientation. *(Chem. Commun., **2012**, 48, 6203)*

In particular, it is known that promoter region of the genes are enriched in quadruplex motifs, in fact more than the 40% of human gene promoters contains one or more quadruplex motifs, proving the key role of these conformations in the regulation of the transcription process.[42] Furthermore, recent researches suggest that *G-quadruplex-forming sequences* are present in important sites such as in proto-oncogene *e.g.* c-myc or bcl-2. For example, the human c-Myc gene is a particularly significant oncogene and its alteration or expression has been associated with many types of cancer, including but not limited to breast, lung, prostate and haematological cancers.[43]

Moreover in 1989 Williamson et al., showed that four contiguous stretch of G-residues were present in a long telomeric DNA sequence, which could fold *in vivo* into GQ conformation, as demonstrated later.[44]

Likewise, it was proved that telomerase protein, which controls the cell duplications and consequently the cell life, is unable to bind structures different from the telomeric single strand DNA.[45]

The telomerase protein allowing the elongation of telomeric DNA,[46] leads to an extension of cell life. In fact, a high level of telomerase activity has been found in embryonic stem cells and associated with cancer cells[47] permitting them to divide virtually forever.

This knowledge has offered the opportunity to design molecules, which bind and stabilize the GQs superstructures.[48] The conversion of the telomeric DNA into a *"non-recognizable"* structure leads to the telomerase inhibition and gives a therapeutic behaviour to these compounds.[49]

An intense development in drug design was carried out after the elucidation of the NMR and crystallographic data of different G-Quadruplex sequences.

Therefore, the binding of small molecules with DNA can occurs via:

(i)     Ionic interaciton

(ii)     π–π stacking

(iii)     H-bonding interactions

Thus, an efficient G-quadruplex binding ligand should have positive charges, a planar conjugated system with heteroatoms capable of acting as H-bond donors, as well as acceptors.

Among them, macrocycles rapidly became popular for interaction with quadruplexes. In fact, the macrocycles favour the stacking interactions with the external G-quartets and the rigid structure maximizes the overlap. Moreover, the possibility to coordinate central metal cations can promote the electrostatic coupling with the negative charges of the DNA. The cationic charges represent both an advantage and a drawback due to the *"lack of specificity"*.

In fact, the electrostatic interactions promote the association with any form of DNA and in particular with duplex DNA, thereby decreasing the binding selectivity.

Porphyrin and metallo-porphyrins were among the first ligands studied in the GQs binding and stabilization. Intriguingly, $H_2$TMPyP4 has early-generated interest among nucleic acid chemists because of its targeting of alternative DNA structures (*i.e.* DNA junctions).[50] This explains also, why $H_2$TMPyP4 was among the very first compounds to be thoroughly studied for its quadruplex interacting properties. Furthermore, $H_2$TMPyP4 having molecular dimensions which resemble a G-tetrads acts as an effective inhibitor of human telomerase in *in vitro* assay.[51]



**Figure 1.19** a) Chemical structure of $H_2$TPyP4. b) NMR solution structure (PDB: 2A5R) of TMPyP4 binding a unimolecular G-quadruplex formed from the modified c-Myc promoter sequence, Pu24I. c) X-ray crystal structure (PDB: 2HRI) of TMPyP4 binding to the bimolecular G-quadruplex formed from the human telomere sequence, TAG3T2AG3[43]

Usually for the porphyrin, it is possible to observe three modes of binding (Figure 1.20) the binding to the top or the bottom of quadruplex (*external stacking* or *capping*),[52] groove binding between strands of G-quadruplexes[53] or intercalation between guanine tetrads within a quadruplex.[54]

**Figure 1.20** Three modes of interaction of small ligands with G -quadruplexes

The binding mode of porphyrin-GQ depends on several factors *i.e.* type of GQ, DNA sequence and the arrangement of strand orientations, in fact the groove sizes depend on the different nature of antiparallel G quadruplexs as well, the structures of the loops and adjacent non G-tetrads might also influence the selectivity of the ligands.

Notwithstanding the good affinity of the $H_2TMPyP4$ towards GQs this porphyrin represent a "*non-selective ligand*" for the GQs because of its inability to discriminate between different DNA structures[55] and its multiple modes of binding. In several cases for example it is been demonstrated also the possibility to obtain complex superstructure between different GQs (Figure 1.21).[56]

27

**Figure 1.21 (a)** Schematic view of the bimolecular quadruplex and TMPyP4 structure (guanine in green, adenine in red, and thymine in cyan). **(b)** View of a column of three consecutive quadruplexes as found in the crystal structure. **(c)** View of the crystal structure along columns of the quadruplex-TMPyP4 complex, showing the porphyrin molecules in space-filling mode (colored orange), the quadruplex backbone (colored yellow) and thepotassium ions (colored cyan), *Biochemistry,* **2007***,46,* 2390-2397.

Thus, the possibility to have a highly selective "*G-Quadruplex-ligand porphyrin"* remains a desirable goal. To address this crucial issue, the functionalization of porphyrin core may help in increasing the selectivity, as it was obtained with a PEG derivative of $H_2$TMPyP4 (called TEGPy) which showed a lower efficiency for duplex interactions compared to the interactions with G-Quadruplex (Figure 1.22).[57]

**Figure 1.22** Chemical structures of TMPyP4 and TEGPy and the schematic of their quadruplex-binding modes through X-ray crystallographic analysis (TMPyP4, upper panel, PDB Id: 2HRI, or qualitative in silico representation (TEGPy, lower panel) *Org. Biomol. Chem.,* **2015,** *13*, 7034**.**

.

## 2. Aim of the work

In the last 3 years our work was aimed to design, synthesize, and test capabilities of new metallated and free base porphyrin-polyamine derivatives and of a BODIPY-Spermine derivative, to interact with different biomolecules and in particular with DNA.

The polyamine arms give a better solubility in aqueous solution to these compounds, displaying a different protonation degree depending of pH and allowing interactions with the anionic backbones of different DNA structures. Among polyamines, we utilized spermine because it shows a good ability to interact and induce a conformational change from B to Z-DNA.[58] As matter of fact, its porphyrin conjugates are used to test their DNA photocleavage abilities.[59]

Furthermore, the new molecules synthesized during my PhD work, were designed to take advantage of polyamines transport system (Figure 2.1) of the cell that affords a selective accumulation of polyamine analogues inside of it and in particular in neoplastic tissues.[60]

In fact, polyamines such as spermine, spermidine and putrescine, are required for cellular growth and their concentrations are particularly high in rapidly proliferating cells. Cancer cells, whose polyamine requirements exceed their biosynthetic capabilities, use a polyamine transport system (PAT) to satisfy their needs. Therefore, the polyamine transport system affords a selective accumulation of polyamine analogues in neoplastic tissues and consequently plays a very attractive role in several anticancer chemotherapeutic strategies.

In polyamine–aromatic conjugates, the cationic polyamine groups likely facilitate binding to the negatively charged tumour cell plasma membranes, while the hydrophobic nature of the porphyrin should facilitate the penetration of the conjugates through the lipid membrane as reported in different works.[61]

**Figure 2.1** Schematic representation of polyamine transport system (PAT)

The central idea of this work was to use one single type of molecules having different biological targets (e.g. dsDNA, G-Quadruplex and telomerase activity) but all converging toward the cure of tumours instead of using a cocktail of different active molecules.

For these purposes, in the last years we have synthesized tetra-, di- and mono-spermine porphyrins and spermine-BODIPY conjugate (schematic representation in Figure 2.2) and after characterization, we have tested their capabilities to interact with dsDNA and G-Quadruplex.

**Figure 2.2** Cartoon representation of polyamine–porphyrin and BODIPY's conjugates

Their dual hydrophilic/hydrophobic nature was designed to turn them into sufficiently water-soluble porphyrins without the loss of aromatic moiety, and in the same time to make them useful to interact as free base with the guanine tetrads and with negative backbone of the GQs. While the insertion of metal core (*i.e.* zinc) in these derivatives was thought to cooperate with the polyamine pendants in the conversion and in the recognition of the Z-Form of the dsDNA.

# 3. Results and discussion

## 3.1 Synthesis of Compounds



**Scheme 3.1** General scheme of synthesis pathway to obtain the porphyrin-conjugates with polyamine's arms

Scheme 3.1 shows the synthetic route to obtain the porphyrin-conjugates with polyamine arms. In the first part of synthetic sequence, we synthesised the tri-BOC-Spermine (**2**) pendant. The differential protection of amine groups allows having only one free amino group, which was used to link the arms with porphyrin core by amide-bonds.

The second part of the work involves the functionalization of 5,10,15,20 *meso*-tetra(4-carboxyphenyl) porphyrin (**H₂TCPP**) with the pendants previously synthesised. Porphyrin-conjugates were obtained *via one-pot reaction* using HATU as condensing agent.

Then, $H_2$TCPP(tri-BOCSpm)4 (**3**) was in part deprotected with trifluoroacetic acid (TFA) in $CH_2Cl_2$ to afford $H_2$TCPPSpm4 (**5**) as trifluoroacetate salt and partially metallated with $Zn(CH_3COO)_2$ obtaining the compound **4** and after it was deprotected to obtain the ZnTCPPSpm4 salt (**6**).

## 3.1.1 Synthesis of tri-BOC-Spermine **2**.

The synthetic procedure reported in the literature provides a *one pot* reaction, which includes a selective protection of spermine, at low temperature (-78 ° C), via trifluoroacetyl group (Tfa), followed by protection of the remaining amino-functions with tert-butoxycarbonylic group (BOC-) and finally by aminolysis of trifluoroacetyl group with $NH_3$/MeOH.[62]



**Scheme 3.2** Synthesis of polyamine pendans.

This protocol has several problems: first precipitation of spermine at -78°C and finally an incomplete hydrolysis of Tfa group. Furthermore, the *one pot* reaction, leads to a formation of many by-products with similar characteristics and thus difficult to purify. For these reasons, we modify the literature method using a two steps procedure (Scheme 3.2).[63] In the first step Spermine was protected on the primary amino functional group by reaction with ethyl trifluoroacetate (-78°C →0°C), to afford a mixture of products including mono-trifluoroacetamide, that was not isolate. Immediately, in this solution, the remaining amino functional groups were quantitatively protected with di-*tert*-butyl dicarbonate to obtain, after column chromatography the fully protected spermine Tfa-tri-BOC-Spm **1** as a yellow oil, which was characterized by ^{1}H-NMR, APT, HMQC, 1D-zTOCSY. In the ^{1}H-NMR spectrum (Figure 3.1) all signals were attributed by using of 1D-zTOCSY.

**Figure 3.1** Selected region of $^1$H-NMR of compound **1** in acetone-$d_6$.

The deprotection of the primary amino group from trifluoroacetyl group with NaOH led to the compound **2**, as a yellow oil, which was characterized by $^1$H-NMR and ESI-MS. The $^1$H-NMR spectrum (Figure 3.2) shows the disappearing of signal at 8.5 ppm (-N$\underline{H}$COCF$_3$); a multiplet at 3.30 ÷ 3.23 ppm (8H) and the appearance of a triplet at 3.17 ppm ($J$ = 7.0 Hz, 2H) attributed to -C$\underline{H}_2$NH$_2$.



**Figure 3.2** $^1$H-NMR of compound 2, in the insert zoom of spectrum that shows signals of **2** (blu) and of **1** (red).

## 3.1.2 Synthesis of H$_2$TCPPSpm4



**Scheme 3.3**

The commercial *meso*-tetrakis(4-carboxyphenyl)porphyrin (H$_2$TCPP) was linked to the tri-BOC spermine pendants (**2**)**,** using HATU *in situ* as carbonyl activating agent in presence of DIPEA and leading to a mixture of products, which were purified by column chromatography to afford the desired compound **3,** characterized by ^{1}H-NMR, APT, HMQC and MALDI-TOF.

The BOC protecting groups of the compound **3** were removed using TFA to afford quantitatively the compound **5**, which was characterized by ^{1}H-NMR, APT, 1D-zTOCSY, ESI-MS and UV-vis. The signals were assigned by 1D-zTOCSY and in ^{1}H-NMR.

In the Figure 3.3 the aromatic signals (in green) were assigned to the β-pyrrolic protons (8.9 ppm, br s, 8H) and to the –H$_o$/-H$_m$ protons of phenyl group (8.4 and 8.33 ppm, d, $J$=8.0 Hz, 16H). While the polyamine portion (in purple) shows a broad triplet (3.7 ppm, 8H) assigned at -C$\underline{H}_2$- in the α position to the amide linkage.



**Figure 3.3** Selected region of $^1$H-NMR of compound **5** in MeOH-$d_4$

By the use of 1D-zTOCSY (Figure 3.4) it was possible to assign the signals (3.3÷3.0 ppm) of the C$\underline{H}_2$ close to the amino groups; and between 1.8 and 2.3 ppm is possible recognize the signals of C$\underline{H}_2$ in the middle of the aliphatic chains. In addition, the compound was characterized by the absorption spectrum in methanol, which showed the typical bands of the free base porphyrin, with an intense Soret band at 414 nm and the four Q Band between 470-670 nm.

**Figure 3.4** ^{1}H-NMR spectrum of compound **5** in MeOH-$d_4$ (**purple**), 1D-selective band zTOCSY 3.71 ppm (**green**), 1D-selective band zTOCSY 3.2 ppm (**blue**), 1D-selective band zTOCSY 1.91 ppm (**red**).

## 3.1.3 Synthesis of ZnTCPPSpm4

The ZnTCPP(tri-BOC)Spm4 (**4**) (Scheme 3.3) was obtained by reaction between H$_2$TCPP(tri-BOC)Spm4 (**3**) and Zn(AcO)$_2$ , which was characterized by ^{1}H-NMR, UV-vis and MALDI-TOF. The metalation of porphyrin was confirmed by UV-Vis absorption spectrum, which shows a shift of the Soret band and the presence of two only Q bands typical for a metallated porphyrin (Figure 3.5).



**Figure 3.5** UV-Vis spectra overlap of compound **3** (**purple solid line**) and compound **4** (**green dashed line**) in MeOH (10μM). The inset shows expansion between 450 and 700 nm (x10).

In the BOC-removal procedure the zinc protected derivative (**4**) reacted with TFA to afford quantitatively the ZnTCPPSpm4 (**6**) as trifluoroacetate salt. This compound was characterized by ^{1}H-NMR, gCOSY and by UV-Vis spectrum. The UV-Vis spectrum confirm the presence of a metal-porphyrin after treatment with TFA (Figure 3.6).

**Figure 3.6** UV-Vis spectrum of compound **6** in MeOH (10 μM). The inset shows expansion between 450 and 700 nm (x10).

## 3.1.4 Synthesis of *mono*-functionalized porphyrin.



**Scheme 3.4** General scheme of synthesis pathway to obtain the porphyrin-conjugate with a polyamine arm

Scheme 3.4 shows the synthetic route followed to synthetize the mono-TCPPSpm (**11**). In the first step we synthetized the 5-mono-(4'-carboxymethyl phenyl)10,15,20-triphenyl porphyrin (**8**) following a literature procedure (Lyndsey's method).[64] Methyl-*p*-benzoate (**7**), previously obtained from 4-formyl-benzoic acid,[65] reacted with pyrrole, freshly distilled, and benzaldehyde, in an appropriate ratio, using $BF_3 \cdot Et_2O$. After oxidation by DDQ, the porphyrin mixture was purified by double chromatographic column, to give the desired mono-functionalized product (**8**), which was characterized by ^{1}H-NMR. This method gave many by-products, such as *tetra*-phenyl porphyrin and many other *di*- tri- substituted porphyrin and it involved a laborious purification's work.



**Figure 3.7** Selected region of ^{1}H-NMR of compound **8** in CDCl₃

In the protonic spectrum the signals were assigned to the β-pyrrolic protons (9.0 and 8.8 ppm, respectively 6H and 2H); to the -$H_o$/-$H_m$ of aromatic phenyl groups between 7.8 and 8.5 ppm and to methyl ester group (-OC$\underline{H}_3$) at 4.1 ppm (Figure 3.7).

The methyl groups were removed by reaction with KOH, in ethanol/water solution[66] to give compound **9,** as confirmed by ^{1}H-NMR (Figure 3.8).



**Figure 3.8** Selected region of ^{1}H-NMR of compound **9** acetone-$d_6$

After deprotection the carboxylic groups of **9** were activated *in situ* using HATU, and reacted with free amino group of Tri-BOC-Spermine (**2**), in the same condition using to obtain H$_2$TCPPSpm4 (**5**), to give us after double chromatographic purification the compound **10**, which was characterized by ^{1}H-NMR, APT, gCOSY and UV-Vis. The signals were assigned by g-COSY experiment (Figure 3.9), which has permitted to identify also the protons of the polyamine chains (Figure 3.10).

**Figure 3.9** Selected region of ^{1}H-NMR of compound **10** acetone-*d₆*



**Figure 3.10** Selected region of ^{1}H-NMR of compound **10** acetone-*d₆*. The inset shows gCOSY of the same compound.

The UV-vis spectrum shows the Soret band at 414 nm and four Q band between 470 and 670 nm.



**Figure 3.11** UV-Vis spectrum of compound **10** (10 μM) in MeOH. The inset shows expansion between 450 and 700 nm (x10).

Compound **11** was obtained after treatment of compound **10** with TFA in $CH_2Cl_2$ and it was characterized by $^1$H-NMR and APT. All signals in this zone of spectrum have similar chemical shifts of $H_2TCPPSpm_4$ but they have a different intensity, as expected.



**Figure 3.12** Selected region of $^1$H-NMR of compound **11** acetone-$d_6$.

## 3.1.5 Synthesis *di*-functionalized porphyrin.



**Scheme 3.5** General scheme of synthesis pathway to obtain the *trans*-porphyrin-conjugates with polyamine arms.

To obtain *trans*-meso-di-functionalized porphyrin we used a [2+2] MacDonald reaction, which involves the use of functionalized dipyrromethane and benzaldehyde.

The dipyrromethane (**12**) was synthetized according to the literature reaction[67] between pyrrole and *p*-methylformyl benzoate (**7**) in aqueous chloridric acid, instead to the classical procedure using pyrrole as solvent.[68] This synthesis give the desired product as a precipitate, pure enough to avoid the chromatographic purification, which is necessary with the second type of synthesis.

The dipyrromethane was used, according to the literature procedure, with benzaldheyde and TFA, to obtain the 5,15 di-functionalized porphyrin (**13**) using DDQ as oxidant agent (Scheme 3.5).[69]

This procedure has three limitations: i) the condensation must be conducted under high dilution conditions, to facilitate the macrocycle closure and avoid polymerization processes; ii) due to secondary reactions such as scrambling, it has been obtained a mixture of differently substituted porphyrins, which involved a difficult purification process; iii) consequently, the yields are usually very low.

The *trans*-di-functionalized porphyrin **13** was obtained after a double chromatographic purification (yield 20%) and it was characterized by $^1$H-NMR. The $^1$H-NMR spectrum shows a typical pattern of an $A_2B_2$ porphyrin system with two doublets for the β-pyrrole protons (8.80 ppm 4H and 8.90 ppm 4H); other two doublets are at 8.45 and 8:31 ppm assigned to $H_o$/$H_m$ protons of *p*-substituted phenyl; at 8.2 and 7.8 ppm there are the signals of the phenyl unsubstituted groups. Finally, at 4.10 ppm there is a singlet of methyl ester and at -2.7 ppm, strongly shielded by the ring current, the core -NH (Figure 3.13).

**Figure 3.13** Selected region of ^{1}H-NMR of 5,10-Di-(4'-carboxymethylphenyl)10,20-di-phenyl porphyrin **13** in CDCl$_3$.

The carboxylic groups of compound **13** were deprotected according to a slight modification of a literature procedure[70] using KOH in a refluxing mixture of EtOH/H$_2$O. The product was extracted with ethyl acetate and washed with a solution of HCl, to give the desired compound **14** as a violet powder, characterized by ^{1}H-NMR (Figure 3.14).

The tri-BOC-Spermine pendants were linked to the free carboxylic groups through amide bonds using HATU as activating agent and DMF as solvent (Scheme 3.5). The desired porphyrin derivative **15** was purified by a double column chromatography and characterized by ^{1}H-NMR, APT and gDQCOSY. All signals of ^{1}H-NMR were assigned using COSY experiment, obtaining for the pendants a similar pattern of the mono and tetra functionalized porphyrins, as showed in the (Figure 3.15).

**Figure 3.14** Selected region of $^1$H-NMR of 5,10-Di-(4'-carboxyphenyl-triBoc-Spm)10,20-di-phenyl porphyrin **15** in acetone-$d_6$.



**Figure 3.15** Selected region of $^1$H-NMR of 5,10-Di-(4'-carboxyphenyl-triBoc-Spm)10,20-di-phenyl porphyrin **15** in acetone-$d_6$.

Compound **16** was obtained after treatment of compound **15** with TFA in $CH_2Cl_2$ and it was characterized by $^1$H-NMR and APT. Similarly to the previous spermine derivatives, the aromatic region of the $^1$H-NMR shows two duplets at 8.88 ppm (d, J= 5Hz, 4H) and at 8.86 ppm (d, J= 5Hz, 4H) assigned to β-pyrrolic protons; three multiplets at 8.6 ppm (4H), at 8.4 ppm (8H) and at 8.0 ppm (6H) assigned to aromatic protons. The protons of polyamine arms are from 3.7 ppm to 1.9 ppm with a triplets at 3.7 ppm (*J*=7.0 Hz, 4H) assigned to C$\underline{H}_2$ in α position to the amido group. Multiplets from 3.25 to 3.05 ppm are assigned to the $CH_2$ near to amino groups and finally up-shielded there are the inner $CH_2$ of the pendants (Figure 3.16).



**Figure 3.16** Selected region of $^1$H-NMR of 5,10-Di-(4'-carboxyphenyl-triBoc-Spm)10,20-di-phenyl porphyrin **16** in methanol-$d_4$

51

## 3.1.6 Synthesis of spermine-BODIPY derivative



**Scheme 3.6** General scheme of synthesis pathway to obtain the BODIPY-conjugates with polyamine's arms.

To synthetize the BODIPY core we used a literature procedure,[71,72] in which methyl-4-formyl-benzoate reacts with 2,4 dimethyl-3-ethyl pyrrole, in presence of TFA as catalyzer, DDQ as oxidant agent and $BF_3 \cdot Et_2O$ to give in a *"one pot reaction"* (Scheme 3.6) the desired compound **17** (BODIPY-COOMe), which was characterized by ^{1}H-NMR as showed in the Figure 3.17.

**Figure 3.17** Selected region of $^{1}$H-NMR of BODIPY-COOMe **17** in CDCl$_3$

The carboxylic group of compound **17** was deprotected using NaOH in MeOH under reflux. The purple solid obtained after evaporation of the solvent, was washed with a solution of HCl and extracted with CH$_2$Cl$_2$, dried over Na$_2$SO$_4$ and the solvent was evaporated to give the compound **18** with 80% of yield. The free carboxylic group of the BODIPY was used to link the tri-Boc-Spermine, using the same procedure applied with porphyrins, in presence of HATU as condensing agent in DMF and at room temperature; obtaining after purification BODIPY-CO-tri-BOC-Spermine **19,** which was characterized by $^{1}$H-NMR (Figure 3.18).

**Figure 3.18** Selected region of ^{1}H-NMR of BODIPY-CO-tri-BOC-Spm **19** in CDCl₃

The BOC-protecting groups were removed using TFA in CH₂Cl₂ to give the free polyamine BODIPY derivative (**20**) in quantitative yield. The compound **20** was characterized by ^{1}H-NMR, gCOSY and APT.



**Figure 3.19** Selected region of ^{1}H-NMR of BODIPY-CO-Spm **20** in D₂O

## 3.2 Study on hierarchically controlled protonation/ aggregation of H$_2$TCPPSpm4[73]

Self-assembly processes in chemistry are important to obtain supramolecular architectures with the desired properties.[74] Recently, two different approaches have been exploited to drive the noncovalent syntheses. One of them foresees a *step-by-step* approach which through the hierarchical addition of rationally designed molecular units, leads to ordered supramolecular architectures (given sequence, stoichiometry, dimensionality and chirality)[75] . The other approach is based on the *sergeant–soldier* principle, according to whom it is possible to drive the system to a predetermined desired final state without a *step-by-step* process.[76] Obviously, the knowledge of the rules governing these processes allows us to control the self-assembly and to synthesize complex supramolecular structures.

Our water-soluble porphyrins could be excellent building blocks for supramolecular architectures,[77] first of all because, in spite of their solubility in an aqueous environment, they maintain the hydrophobic behaviour. This aspect is fundamental because it allows an easy driving of their self-assembly and/or specific aggregation with other similar molecules.

In literature it is known that the self-assembly of porphyrins can be modulated by pH (*e.g. meso*-benzylsulfonated derivatives). In fact, they can form *H*- and *J-aggregates,* after the full core protonation[78] or in other cases the introduction of specific *meso*-substituents opens new self-aggregation pathways, independent from core protonation but fostered by the formation of hydrogen bonds between protonated (H-bond donor) and unprotonated (H-bond acceptor) sites.[76e]

In our derivative the presence of four spermine arms, each having three protonable nitrogen atoms, lets us to obtain a different and *pH-tunable* number of positive charges and in addition to modulate the number of H-bond acceptors (deprotonated amine groups) and donors (protonated amines) sites, which are expected to promote the formation of self-assembled aggregates. In particular the partially protonated forms of H$_2$TCPPSpm4 are potentially able to

spontaneously self-assemble, prompted by the formation of H-bonds between donor and acceptor amino groups.

Four protonation processes are estimated for H$_2$TCPPSpm4: one for the porphyrin core and three for the free amino groups of spermine arms.

In literature, the pK$_a$ values of spermine have been reported in the range 11-7.9.

| | pKa |
|---|---|
| Spe+H$^+$ $\leftrightarrow$ SpeH$^+$ | 10.83 |
| SpeH$^+$+H$^+$ $\leftrightarrow$ SpeH$_2$$^{2+}$ | 9.95 |
| SpeH$_2$$^{2+}$+H$^+$ $\leftrightarrow$ SpeH$_3$$^{3+}$ | 8.77 |
| SpeH$_3$$^{3+}$+H$^+$ $\leftrightarrow$ SpeH$_4$$^{4+}$ | 7.90 |

However, the pK$_a$ values of the spermine arms linked to the porphyrin macrocycle are expected to be different from the free molecule. In fact, each protonation step in the spermine arm causes an increase of the positive charge overall the molecule, shifting to lower pH the following protonation steps. Furthermore, the comparison between the pK$_a$ values of core of cationic porphyrin similar to our derivative, suggests that this protonation step could follow the protonation of the polyamine pendants.

It is known that aggregation can be studied not only from the thermodynamic (analysing binding constant or the interaction involved) but also from the kinetic point of view.[79] The aggregation process in fact depends on the time of coexistence of the species and it starts after a very variable time. This means also, that using the classic continuous titration procedure, it would be possible observe the aggregation process at pH quite different from the pH value at which the aggregate seeds are really formed.

Therefore, to avoid or minimize interference by aggregation in the determination of pK$_a$ we *i)* prepared independent solutions at different pH values and *ii)* performed a very fast continuous titration. The advantage of the first method (independent solutions) is that self-aggregation is avoided because

measurements are performed soon after porphyrin dissolution at a given pH; the main disadvantage is that a thorough experiment requires long reaction time. The second approach (fast continuous titration) is faster than the first one, but can be affected by aggregation processes that have very short time lags.

Thus, we performed both type of titrations by monitoring the UV-vis spectrum of $H_2TCPPSpm4$ (2 mM).

The comparison between the two types of titration shows a hypochromic effect (about 15%) of the absorption in the continuous titration, reporting some aggregation, but there is no pH shift of the curve, thus is not particularly relevant for the determination of the $pK_a$ values (Figure 3.20).

From the continuous titrations, it is possible to derive three different protonation processes. The first one ($pK_{a1}$) is observed at pH~ 8 and it refers to the protonation of the external spermine nitrogen atoms. At pH ~ 5.8 the protonation of the second amino groups ($pK_{a2}$) of the spermine arms occurs; and finally the third protonation process ($pK_{a3}$) at pH ~3.5 corresponds to the porphyrin core protonation, confirmed by the colour change of the solution from purple to green, typically observed for this process. The same $pK_a$ values have been obtained performing fluorescence measurements of the same $H_2TCPPSpm4$ solution by continuous titration methods.

**Figure 3.20** Absorbance vs. pH, for the continuous titration at 414 nm (solid black square)and at 435 nm (red square) and for the independent solutions at 414 nm (open black circle) of 2 mM solution of $H_2TCPPSpm4$. The inset shows a zoom of the UV titration at 435 nm in the 4.3–6.5 pH range.

In order to better understand the dependence of the self-assembly processes by pH, we performed UV-vis absorption measurements of solutions prepared by dissolving $H_2TCPPSpm4$ at pH close to the $pK_a$ (5.0, 6.5 and 8.0) and at pH =1.5 in which $H_2TCPPSpm4$ is fully protonated. To take into account the kinetic aspect of aggregation we recorded the spectra immediately after porphyrin dissolution and 24 h later (Figure 3.21).

**Figure 3.21** UV spectra of 2 mM H$_2$TCPPSpm4 solutions at different pH values (from left 1.5; 5.0; 6.5 and 8.0) as soon as prepared (black curves) and after 24 h (red curves).

Obviously, the inner core protonation of the macrocycles and the positive charges in the side arms disfavours the self-aggregation. This is well supported by the observation of same absorption spectra at pH 1.5 of the solutions just prepared (t = 0 h) and after 24 h. On the contrary, for porphyrins left for 24 h in aqueous solutions at pH 8 it is possible to observe the spectroscopic changes typical of aggregation *i.e.* hypochromicity and broadening of the Soret absorption band (Figure 3.21).

The data concerning pH range 5÷6.5 are quite interesting and help in delineating the delicate dependence of the aggregation processes from the *"pH-tuned hydrogen bond"* scheme. In particular, at pH = 5 (that is under conditions in which pH ~ pK$_{a2}$), after 24 h, H$_2$TCPPSpm4 is aggregated as shown by the hypochromic effect. On the contrary, the data of the solution obtained by dissolving H$_2$TCPPSpm4 at pH 6.5 show that the title porphyrin remains monomeric even after 24 h. This behaviour suggests that skipping the protonation step at pH 5 it is possible to avoid the aggregation of porphyrins and maintain the porphyrin in the monomeric form up to pH 8.

Furthermore, scanning electron microscopy experiments confirm the presence of porphyrin aggregates depending on pH (Figure 3.22). In fact, working at pH 1.5 the substrate surface does not reveal the presence of any aggregates, while a

more structured surface is well evident upon increasing the pH value. In particular, small spherical nanostructures are visible at pH 5, while at pH 8 a high density of particles is well detectable.



**Figure 3.22** SEM images of $H_2TCPPSpm4$ deposited on silicon by drop casting of 100 µl of 100 µM solution at (a) pH=1.5; (b) pH=5.0 and (c) pH=8.0

Further proofs of the relevance of the sequence of protonation steps in the aggregation in the pH range 5–7 is given by fluorescence and RLS[80] measurements performed, monitoring: (i) a solution obtained by dissolving $H_2TCPPSpm4$ (2 mM) directly at pH 6.5 and (ii) a solution at pH 6.5 as a result of a continuous slow pHmetric titration. RLS data show the absence of the aggregation in the solution of $H_2TCPPSpm4$ dissolving the porphyrin directly at pH 6.5. On the contrary, an enhancement of the signal is detected in the slow titration (Figure 3.23), which can be explained recalling that this approach leads to porphyrin assemblies formed during the time of measurements.

Moreover, the presence of aggregates is suggested by the quenching of the fluorescence in the slow titrated solution, differently from the fluorescence spectrum recorded for solution prepared directly at pH 6.5 (Figure 3.23).

**Figure 3.23** RLS (left) and fluorescence (right) spectra of 2 mM H$_2$TCPPSpm4 solutions at pH 6.5 prepared directly by dissolving at desired pH (black curve) and by slow pH titration (red curve).

These differences confirm the presence of an alternative, *"time dependent"* kinetic aggregation path that is *''parallel''* to the thermodynamic protonation pathway and which can be rationally chosen and designed.

These results underline the possibility to choose the aggregation state of a very complex system, by the insertion of appropriate functional groups. The introduction of peripheral groups with protonation steps at pH higher than the inner core protonation, allows to differentiate the two pathways –kinetic (aggregation) and thermodynamic (protonation)– to obtain the desired aggregation state in solution.

## 3.3 Study of interaction with poly(dC-dG)

The conformation of DNA is usually checked by CD measurements, a positive Cotton effect approximately at 280 nm and a negative at 250 nm characterize the B-DNA. On the contrary, the Z-DNA although it is not the enantiomer of the B form, is characterized by a negative signal at 290 nm and a positive at 270 nm (Figure 3.24).



**Figure 3.24** CD-Spectra of (dG-dC)·(dG-dC) 350-mer, 35 μM in bp in buffer solution (Sodium cacodylate 5mM + 10 mM NaCl pH 6.8) at 25°C in B-Form in **red** curve and in Z-Form (Sodium cacodylate 5mM, NaCl 3M, Spermine13 μM) in **black** curve.

To test the ability of our porphyrin as "*Z-form inducer*" towards B-DNA, firstly we tried to induce the conformational change from B to Z with only spermine in two different (dG-dC) length sequences: 100 mer and 350 mer. It is known that the length of the DNA is very important for the conversion process, in fact only the 350 mer  was able to turn into Z- form in the presence of micromolar concentration of polyamine. While to obtain the Z form from a 100 mer dG-dC sequence was necessary to use molar concentration of NaCl and millimolar of $NiCl_2$.

Moreover, the Z form of DNA is a high-energy structure, so the procedure using to convert the B DNA into Z require high temperature (~60°C).

The experiments conducted have not showed any conversion for the 100 mer (Figure 3.25 a)) not even with 55 µM of Spermine. While the conformational change from B to Z was achieved in the longer sequence with the addition of 13 µM of Spermine (Figure 3.25 b)).



**Figure 3.25 a)** Titration of 100 mer 102 µM in bp in buffer solution (sodium cacodylate 5mM + 10 mM NaCl pH 6.8) at 60°C with increasing amount of spermine. **b)** Titration of 350 mer 35 µM in bp in buffer solution (sodium cacodylate 5mM + 10 mM NaCl pH 6.8) at 60°C with increasing amount of spermine.

Therefore, based on these preliminary results we may suppose that our derivatives, through the spermine arms, could act like inducer only with the longer sequence.

## 3.3.1 Titrations with H$_2$TCPPSpm4 and ZnTCPPSpm4

Titrations of 350 mer with H$_2$TCPPSpm4 and ZnTCPPSpm4 at room temperature did not show transition from B to Z but the induced CD signal at 420 nm confirms the interaction with the porphyrins (Figure 3.26).

With H$_2$TCPPSpm4 the shape of multiple ICD seems to be due to a mixed binding modes included aggregation (Figure 3.26 a). With the zinc porphyrin, the ICD is mainly bisegnated probably because the aggregations in this case is reduced by the presence of penta-coordinated zinc (Figure 3.26 b).



**Figure 3.26 a)** Titration of 350 mer 35 µM in bp in buffer solution (sodium cacodylate 5mM + 10 mM NaCl pH 6.8) at 25°C with increasing amount of H$_2$TCPPSpm4. **b)** Titration of 350 mer 35 µM in bp in buffer solution (sodium cacodylate 5mM + 10 mM NaCl pH 6.8) at 25°C with increasing amount of ZnTCPPSpm4.

In order to see if the H$_2$TCPPSpm4 or ZnTCPPSpm4 were able to act as inducer, like spermine, we tried to induce the transition increasing the temperature, so we performed the same titrations of the previous experiments but at 60°C (Figure 3.27).

**Figure 3.27 a)** Titration of 350 mer 35 μM in bp in buffer solution (sodium cacodylate 5mM + 10 mM NaCl pH 6.8) at 60°C with increasing amount of H2TCPPSpm4. **b)** Titration of 350 mer 35 μM in bp in buffer solution (sodium cacodylate 5mM + 10 mM NaCl pH 6.8) at 60°C with increasing amount of ZnTCPPSpm4.

The titration of DNA sequence with $H_2$TCPPSpm4 at 60°C showed a different ICD compared to the same experiment performed at room temperature. At 60° C the multiple ICD disappeared giving a bisegnate signal with a negative Cotton effect at 425 nm and a positive at 440 nm (Figure 3.28).



**Figure 3.28** Comparison between the CD spectra of 350 mer 35 μM in bp in buffer solution (sodium cacodylate 5mM + 10 mM NaCl pH 6.8) at 25°C in presence of 5 μM of $H_2$TCPPSpm4 (**black** curve) and at 60° C in presence of 7 μM of $H_2$TCPPSpm4 (**red** curve).

Furthermore, at high temperature it is not possible to add a concentration of H2TCPPSpm4 higher than 7 µM to the solution of the DNA without inducing the precipitation of the complex DNA-Porphyrin as showed in the Figure 3.29 (violet curve).



**Figure 3.29** Comparison between the CD spectra of 350 mer 35 µM in bp in buffer solution (sodium cacodylate 5mM + 10 mM NaCl pH 6.8) in presence of 7 µM of H2TCPPSpm4 (**green** curve) and of 10 µM of H2TCPPSpm4 (**violet** curve)at 60°C.

The titration with ZnTCPPSpm4 showed, although the high temperature, an intense ICD (Fig. 3.4, b) which increases up to the final addition of porphyrin (10 µM). In addition, in this case the signal exhibits a negative Cotton effect at 425 nm and a positive one at 440 nm. After cooling at 25°C there were no changes in the DNA region neither in the Soret region for both porphyrins derivatives.

The long flexible tentacle arms of H2TCPPSpm4 and ZnTCPPSpm4 probably facilitate the outside interactions and simultaneously permitting a near-optimal electrostatic interaction with the DNA phosphate groups. Moreover, the different shape of the ICD at room temperature and at 60°C suggests at higher temperature the absence of aggregation between the porphyrins, with a more ordered outside binding. Nevertheless, in spite of the high temperature, the interactions are still present, underling the intense interactions between porphyrin and DNA.

## 3.3.2 Partial transition from B to Z

A partial transition from B to Z was induced using a small amount of spermine, just enough to start the conversion at 60 °C. Then, an increasing quantity of our derivatives was added with the aim to find out some additional help in the conformational change or an inhibition of the conversion from B to Z, previously started with the spermine.

The titrations were carried out following a standard protocol. After heating at 60°C the poly(dG-dC) spermine (7 µM) was added directly in the cuvette, inducing a partial transition, pointed out by the negative band at 290 nm and by a red shift of the positive (from 265 to 270 nm). The negative band at 250 nm, typical for the B form of DNA was almost completely disappeared (Figure 3.30 **dotted blue** curve).

The addition of $H_2TCPPSpm4$ (Figure 3.30, red line) produces a decreasing of intensity of the negative band at 290 nm typical for Z-DNA and a red shift of the positive one (from 268 to 271 nm). Further additions of $H_2TCPPSpm4$ (≥7 µM) led to a visible precipitation of the DNA (Figure 3.30 **green** curve).



**Figure 3.30** Titration of 350 mer B form 35 µM in buffer solution (sodium cacodylate 5 mM + 10 mM NaCl pH 6.8) (**black** curve) at 60°C, in presence of 7 µM of Spermine (**dotted blue** curve), with 3 µM $H_2TCPPSpm4$ (**red** curve) and 7 µM of $H_2TCPPSpm4$ (**green** curve) at 60°C.

On the contrary, ZnTCPPSpm4 shows the opposite trend. In fact, the addition of zinc derivative pushes forward the transition from B to Z, acting like a catalyst in the conformational changing. The interaction is underlined also by the ICD in the Soret band region, where is evident the presence of multiple induced signals (Figure 3.31, **red** curve).



**Figure 3.31** Titration of 350 mer B form 35 µM in buffer solution (sodium cacodylate 5 mM + 10 mM NaCl pH 6.8) (**black** curve) at 60°C, in presence of 7 µM of Spermine (**dotted blue** curve), with 3 µM ZnTCPPSpm4 (**red** curve) at 60°C.

Increasing the concentration of the zinc porphyrin (7 µM **green** curve and 10 µM **orange** curve) the negative band become weaker, maybe due to an adaptation between the DNA and the porphyrins system, but nevertheless deeper than the signal with only spermine (dotted blue line) (Figure 3.32).

**Figure 3.32** Titration of 350 mer B form 35 μM in buffer solution (sodium cacodylate 5 mM + 10 mM NaCl pH 6.8) (**black** curve) at 60°C, in presence of 7 μM of Spermine (**dotted blue** curve) with increasing amount of ZnTCPPSpm4 at 60°C.

Cooling down the temperature of the solution containing 10 μM of ZnTCPPSpm4 at 25°C (**brown** curve) the Z-DNA and the ICD were still visible, pointing out that the porphyrin is able to stabilize this high-energy structure of the DNA also when the complex is at room temperature (Figure 3.33).



**Figure 3.33** Titration of 350 mer B form 35 μM in buffer solution (sodium cacodylate 5 mM + 10 mM NaCl pH 6.8) (**black** curve) at 60°C, in presence of 7 μM of Spermine (**dotted blue** curve), with 10 μM of ZnTCPPSpm4 at 60°C (**orange** curve) and at 25°C (**brown** curve).

The inducing effect was more evident using a lower concentration of spermine (6 μM). In this case, the initial conformational changing of DNA is less evident than with 7μM of spermine, and the addiction of ZnTCPPSpm4 led to a complete transition to the Z-Form (Figure 3.34).



**Figure 3.34** Titration of 350 mer B form 35 μM in buffer solution (sodium cacodylate 5 mM + 10 mM NaCl pH 6.8) (**black** curve) at 60°C, in presence of 6 μM of Spermine (**dotted blue** curve), with increasing amount of ZnTCPPSpm4 at 60°C.

The conformational change is stable also at 25°C, as is evident in the figure 3.35.



**Figure 3.35** Titration of 350 mer B form 35 μM in buffer solution (sodium cacodylate 5 mM + 10 mM NaCl pH 6.8) (**black** curve) at 60°C, in presence of 6 μM of Spermine (**dotted blue** curve), with 10 μM of ZnTCPPSpm4 at 60°C (**green** curve) and at 25°C (**pink** curve).

The key experiment was performed using 5 µM of spermine, in this case the conformational change is not evident in the CD spectra (Figure 3.36).



**Figure 3.36** CD spectra of 350 mer B form 35 µM in buffer solution (sodium cacodylate 5 mM + 10 mM NaCl pH 6.8) (**black** curve) at 60°C, in presence of 5 µM of Spermine(**dotted blue** curve).

The addition of ZnTCPPSpm4 at 60°C following the same procedure of the previous experiments showed an initial transition with 3 µM of ZnTCPPSpm4 (Figure 3.37) and increasing the concentration of Zn-porphyrin lead to a deeper negative band at 290 nm and a less intense negative band at 250 nm.
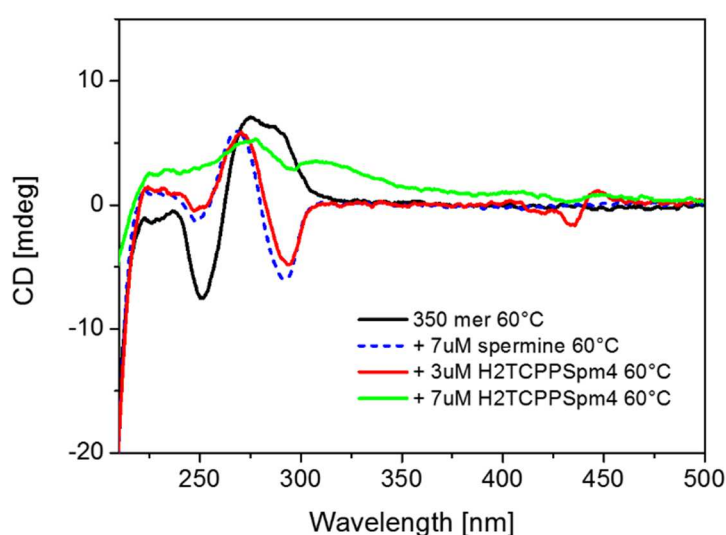
**Figure 3.37** Titration of 350 mer B form 35 μM in buffer solution (sodium cacodylate 5 mM + 10 mM NaCl pH 6.8) (**black** curve) at 60°C, in presence of 5 μM of Spermine (**dotted blue** curve), with increasing amount of ZnTCPPSpm4 at 60°C.

This suggests that the presence of Zn-porphyrin helps the conversion from B to Z. With 7 μM of the Zinc derivative the changing is stable as confirmed by the lack of changes from 7 to 10 μM of ZnTCPPSpm4: the two spectra are in this case almost the same.

## 3.3.3 Probe behavior

Another important goal for our derivatives is the possibility to distinguish the two different forms of DNA. The different ICD signals, shown in the previous experiment with different amount of spermine, suggest that the zinc derivative has a different ICD depending on the percentage of DNA in the two different forms. To confirm these results we induced a complete conversion of the B-DNA into Z-DNA using 13 μM of spermine and it was titrated with ZnTCPPSpm4.
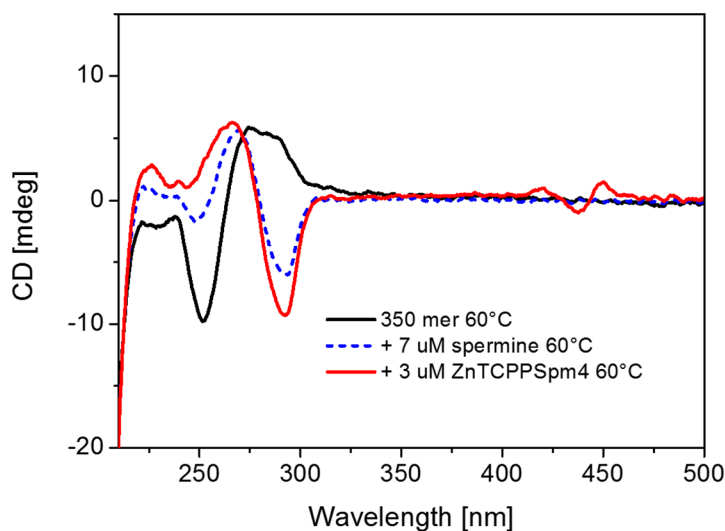
**Figure 3.38** Titration of 350 mer B form 35 µM in buffer solution (sodium cacodylate 5 mM + 10 mM NaCl pH 6.8) (**black** curve) at 60°C, in the Z-Form in in buffer solution (sodium cacodylate 5 mM + 10 mM NaCl pH 6.8, 13 µM spermine (**blue** curve) at 25°C, with increasing amount of ZnTCPPSpm4 at 25°C.

The zinc porphyrin is able to interact with the Z form, as confirmed by ICD in the Soret region (Figure 3.38). From the comparison between the ICD signals of the porphyrin with the B form and the Z-form is evident a different ICD signal, as shown in the figure 3.39. In the interaction with the B form we have: (+)440 nm, (-)425 nm and (-) 410 nm. While for the interaction with the Z-Form the induced CD signal is (+)420 nm; (-)438 nm and (+) 449 nm. The different ICD signal is due to a different type of binding mode that the porphyrin has with the two different structure of DNA. Thus, allowing to the ZnTCPPSpm4 to act not only as an inducer but also as a probe.

**Figure 3.39** CD spectra of 350 mer: in B form 35 µM in buffer solution (sodium cacodylate 5 mM + 10 mM NaCl pH 6.8) (**black** curve) with 10 µM of ZnTCPPSpm4 and in Z form in buffer solution (sodium cacodylate 5 mM + 10 mM NaCl pH 6.8, 13 µM of spermine) (**red** curve) with 10 µM of ZnTCPPSpm4 at 25°C.

## 3.3.4 Stabilizer effect

To support the results according to which the ZnTCPPSpm4 acts as an inducer, we performed the experiment with the only presence of 6 µM spermine, following the same procedure of the other experiments. As the graph shows (Figure 3.40), there was a partial transition from B to Z that did not proceed with time, but went back into the B-form decreasing of temperature (Fig. 3.41, **green** curve). This underline that 6 µM of spermine alone are not enough to induce a *complete* and *stable* conversion of the B-DNA in the Z-form.



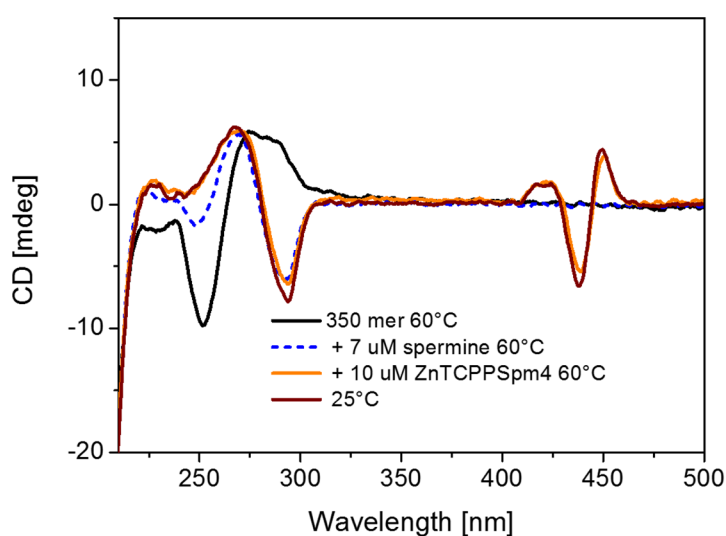**Figure 3.40** Comparison of CD spectra of 350 mer B form 35 µM in buffer solution (sodium cacodylate 5 mM + 10 mM NaCl pH 6.8) (**black** curve) at 60°C, with 6 µM of spermine at 60°C (**dotted blue** curve) and at 25°C (**green** curve).

Specific experiments were performed to study the ZnTCPPSpm4 stabilizer effect on Z-DNA. After inducing a partial transition with 6 µM of spermine, of ZnTCPPSpm4 (7 µM) was added at 60°C and cooled down to 25°C. The experiment shows that in spite of the experiment with only spermine in this case the Z-DNA was still stable at 25°C (Figure 3.42). These results point out not only the ability of the zinc derivative to act as inducer but also to act as a stabilizer towards the Z-form of DNA.
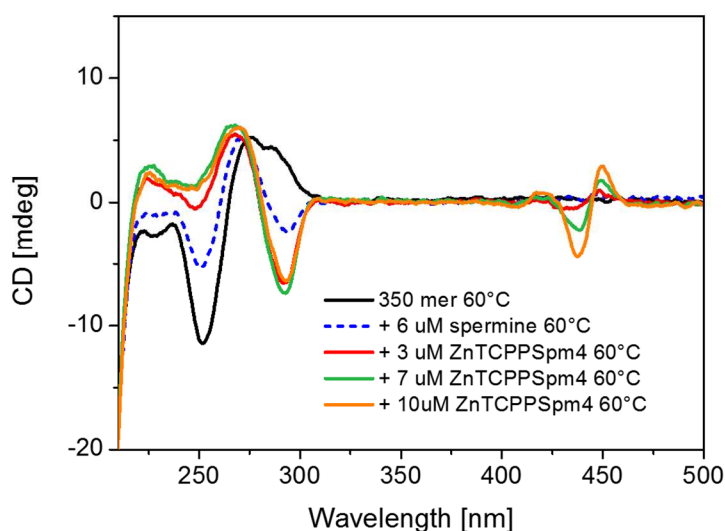
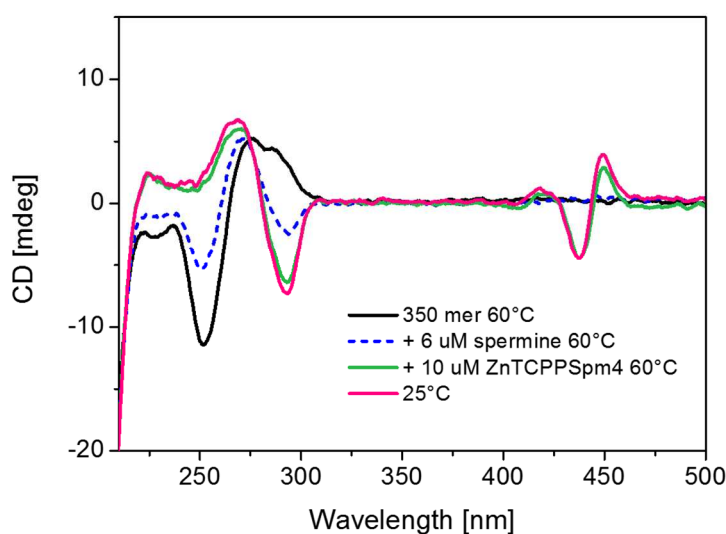**Figure 3.41** CD-spectra of 350 mer 35 µM in buffer solution (sodium cacodylate 5 mM + 10 mM NaCl pH 6.8) (**black** curve) at 60°C, in presence of 6 µM of spermine at 60°C (**dotted blue** curve) and with 7µM of ZnTCPPSpm4 at 60°C (**orange** curve) and at 25°C (**brown** curve).

Another experiment was performed to analyse the stability of Z-DNA with ZnTCPPSpm4. The Z form of DNA obtained with 6 µM of spermine and 7 µM of ZnTCPPPSpm4 at 60°C and cooled at 25°C remained identical for 22 hrs.



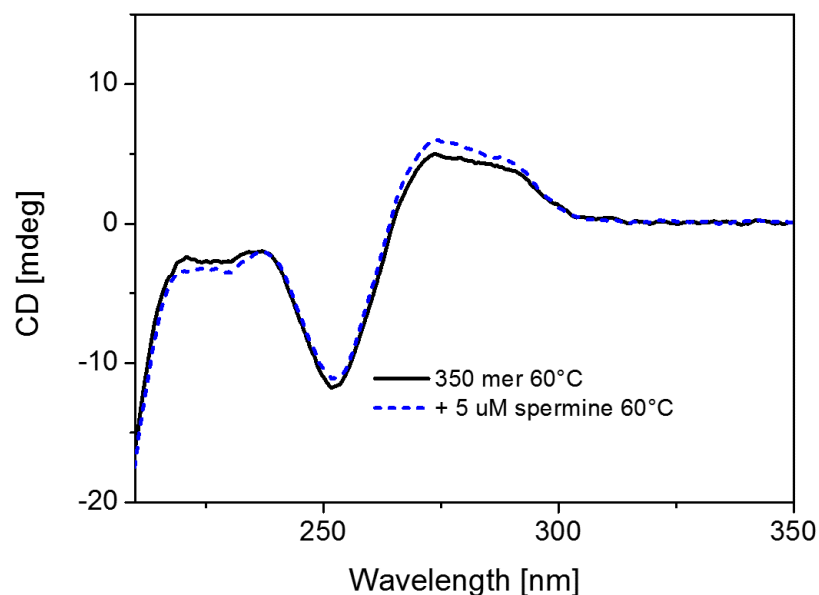**Figure 3.42** CD-spectra of 350 mer 35 µM in buffer solution (sodium cacodylate 5 mM + 10 mM NaCl pH 6.8) (**black** curve) at 60°C, with 6 µM of spermine and 7µM of ZnTCPPSpm4 at 60°C (**blue** curve), during the time.

After a week at 25 °C the reconversion in the B-form was not complete and negative band of the Z form was still visible (Figure 3.43, red dotted curve).

Anyhow, these effects are not ascribable to the independent presence of polyamine arms or of the zinc core. In fact, the same experiment with the H$_2$TCPPSpm4 led to the precipitation of the DNA, maybe due to the formation of macro-aggregates (Figure 3.30).

The experiment performed under the same conditions (6 µM of spermine 60°C) with ZnTMPyP4, a zinc commercial porphyrin, shows that this zinc porphyrin was not able to complete the B to Z transition, neither to stabilize the short Z portion induced by spermine. On the contrary, the increasing quantity of ZnTMPyP4 turns back the DNA into the B form as pointed out by the CD spectra at 25°C after the addition of 7 µM of ZnTMPyP4 in the presence of 6 µM of spermine (Fig. 3.44, orange curve).
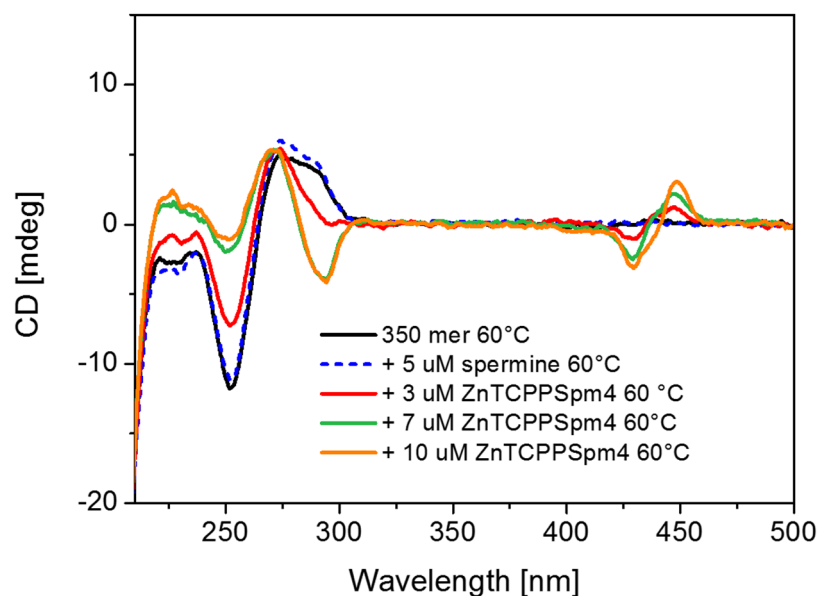


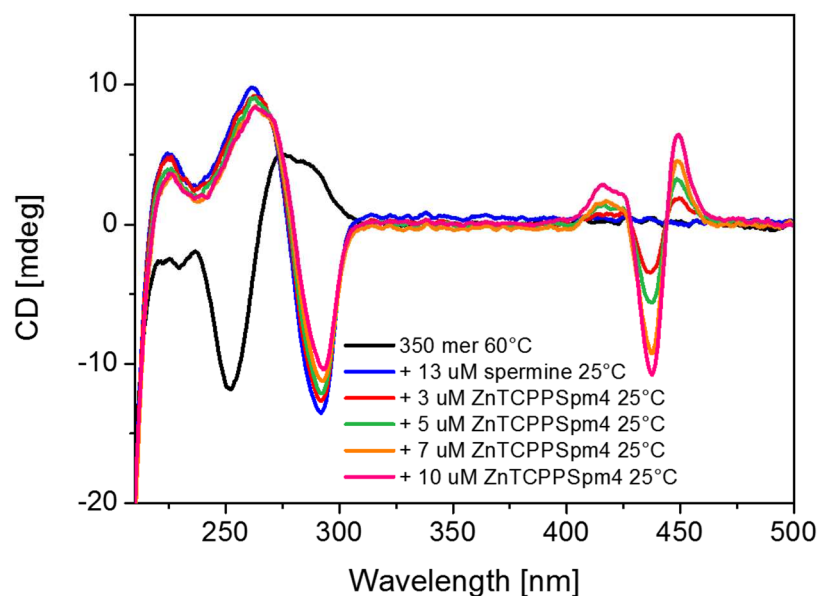**Figure 3.43** Titration of 350 mer B form 35 µM in buffer solution (sodium cacodylate 5 mM + 10 mM NaCl pH 6.8) (**black** curve) at 60°C, in presence of 6 µM of Spermine (**dotted blue** curve), with increasing amount of ZnT4 at 60°C (red and green curve), and at 25°C (orange curve).

Thus, these results points out that it is the contemporary presence in the ZnTCPPSpm4 porphyrin of polyamine arms and Zn, which promote the

conformational changes, maybe through a stabilization of the transition state. These features make our ligand chiroptical probe, with a catalytic effect on the conversion from B to Z and a stabilizer of the Z form.

The impossibility to induce the conformational change without the help of spermine maybe is due to the different charges of the porphyrin pendants compared with the free polyamine. From the literature is known the cooperativity of the spermine in the DNA conformational changes. Therefore, to stabilize and thus to induce the conformational change is necessary that the bigger negative charge of the phosphate backbone in the Z-DNA is counterbalanced by a large number of positive charges, that our spermine derivative does not possess. In fact, one of the amino groups of the spermine is involved in the amide linkage with the porphyrin. Moreover, from our previous study at physiological pH we know that for each arm the average number of positive charges is +2, for this reason we synthetized a longer polyamine pendants with two more amino groups, which will be attached to the porphyrin core and tested on DNA.



**Figure 3.44** Structure of longer polyamine pendants

78

## 3.4 Synthesis of amino propyl spermine pendant



**Scheme 3.7**

To obtain the compound **23,** which will be attached to the porphyrin core, a literature procedure [81] was used starting from the tri-BOC-spermine **2.**

The first step of the synthetic procedure involves the reaction between tri-BOC-Spm (**2**) and N-(3-bromopropyl)-phthalimide, with caesium carbonate. The compound **21** was obtained after purification with 25% of yield and characterized by ^{1}H-NMR, APT, gCOSY and ESI-MS.

The assignments of the ^{1}H-NMR spectra signals of the compound **21** are shown in Figure 3.45; the phthalimidic protons are at 7.83 ppm whereas amide -N$\underline{H}$ near the BOC occurs at 6.0 ppm. Between 4.0÷2.5 ppm we observe the signals of –CH$_2$- protons close to amino and amide groups whereas the *t*-But and –CH$_2$- protons in the middle of propyl- and butyl- aliphatic chains occur in the range ≈ 2.0÷1.3 ppm. The signals of new propyl chain protons occur at 3.76 ppm (*t*, 2H, J=6.70 Hz) at 1.99 ppm (*bs*, 2H) and at 2.82 ppm (*bs*, 2H). The other alkyl chains proton signals can be assigned in the same way using the gCOSY correlations.

**Figure 3.45** Selected region of ^{1}H-NMR of compound **21** in acetone-$d_6$

In the second step, the free amino group of compound **21** was protected with BOC protecting group giving after purification the desired compound **22** (yield 85%), which was characterized by ^{1}H-NMR, ^{13}C-NMR, gCOSY and ESI-MS. In the Figure 3.46 the expansion of ^{1}H-NMR shows the disappearance of the signals at 2.82 and 2.73 ppm which were assigned to the -CH$_2$- close to amino group (compound **21**), converted now in amide group –N$\underline{H}$Boc (compound **22**). In the new compound (**22**), these signals are grouped at 3.22 ppm with the other -CH$_2$- closer to amide groups. The assignment was done by gCOSY.

**Figure 3.46** Selected region of ^{1}H-NMR of compound **22** in acetone-$d_6$

In the final step, the phthalimidic protecting group was removed using hydrazine hydrate to obtain the compound **4** as yellow pale oil (91% yield), characterized by ^{1}H-NMR and ESI-MS.



**Figure 3.47** Selected region of ^{1}H-NMR of compound **23** in acetone-$d_6$

## 3.5 Study of interaction with G-Quadruplex

The porphyrin derivative $H_2TCPPSpm4$ with its positive charges and H-bond donating and acceptor sites has the features to be used for the study of the non-covalent interactions with G-Quadruplex DNA. As model of the GQ structure we used a tetramolecular parallel GQ aptamer with sequence d($TG_3AG$), also called *"Hotoda sequence"*, which seems also acting as an anti-HIV drug (Figure 3.48).[82]



**Figure 3.48** Schematic representation of tetra-molecular TG3AG in G-Quadruplex conformation.

In order to study the stoichiometry of the interaction between our derivative and G-Quadruplex *Hotoda* sequence, we performed an UV-vis titration of the DNA in G-Quadruplex conformation, increasing the amount of $H_2TCPPSpm4$.

Plotting the absorbance of the porphyrin at 412 nm ($\lambda_{max}$ of the Soret band) *vs* the [$H_2TCPPSpm4$]/[GQ] ratio, it is possible to individuate two break points in correspondence of a 1:1 and 2:1 porphyrin/GQ complex (Figure 3.49). Furthermore, the supplementary addition of porphyrin does not show changes in the slope of the graph, which becomes the same of the porphyrin alone, indicating that further additions of porphyrin do not cause any more interaction.

**Figure 3.49** Abs at 412 nm vs [H₂TCPPSpm4] in µM, recorded during the Uv-Vis titration of 8 µM dTG3AG (2 µM in GQ) with increasing amounts of H₂TCPPSpm4.

The UV-Vis spectra of H$_2$TCPPSpm4 and G-Quadruplex in 1:1 ratio, as consequence of the interaction, shows hypochromic effect (H~50%) and a red shift of the Soret Band ~15 nm (Figure 3.50 a). These results are usually reported for intercalation or end-stacking binding modes of tetracationic porphyrin with DNA.[83] In our case we can exclude the porphyrin intercalation due to the steric hindrance of polyamine arms, which prevents the insertion of the porphyrin between the bases, thus at the 1:1 ratio the H$_2$TCPPSpm4 should likely refer to an "*end stacking*" on GQ structure. With more porphyrin *i.e.* 2:1 *ratio* porphyrin /GC the Soret band is more intense than before, with a hypochromic effect of 40% and the presence of a shoulder at higher wavelength (427 nm), which underline a different binding mode (Figure 3.50 b).

**Figure 3.50** Absorbance spectra of H$_2$TCPPSpm4 alone (**black** curves, 2 μM panel (a) and 4 μM panel (b) and in the presence of 2.0 μM GQ (**red** curve).

The CD spectra of d(TG$_3$AG) show the presence of a parallel stranded GQ conformation (positive cotton effect at 263 nm and a negative at 240 nm). Moreover, the negative band at 290 nm suggests the formation of higher ordered GQ- multimers by *end-to-end* stacking interactions. Recently, such type of supra-structures are been reported by Virgilio et al.[84]

After the addition of 1:1 ratio H$_2$TCPPSpm4/GQ the CD spectra changed, with a decrease of the signal at 260 nm and the rice of a trisegnate ICD signal in the Soret band region(positive cotton effect at 436 nm, negative cotton effect at 418 nm and positive at 436 nm), which confirms the interaction between porphyrin and GQ. Moreover, the disappearance of the negative signal at 290 nm supports the hypothesis of the *"end-stacking"* type interaction with tetramolecular GQ and so the destroying the higher ordered GQ-multimers (Figure 3.51).

To clarify and confirm the type of interaction CD titrations were conducted on the dTG$_3$AG, after annealing in 200K buffer. The CD profile of the G-Quadruplex shows a positive band at ~263 nm and a negative one at ~240 nm, which decreased in intensity after the addition of porphyrin with a 1:1 *ratio*. Furthermore, the interaction is confirmed by a strong ICD, observed in the Soret region: with a positive Cotton effect at 436 nm, a negative at 418 nm and a positive one at 400 nm.

**Figure 3.51** CD titration of GQ (2µM in 200K buffer) alone (black curve) and with increasing amount of H₂TCPPSpm4.

The plot of the CD titration data confirms the complex with 1:1 *ratio*, but the decreasing of the signals at 264 nm shows the destabilization of the G-Quadruplex. Moreover, there is no indication of the complex Porphyrin/GC with 2:1 *ratio* (Figure 3.52)



**Figure 3.52** CD intensity at 264 nm (empty blue circles) and 436 nm (red dottes) of CD titration of 8 µM dTG₃AG (2 µM in GQ) with increasing amounts of H₂TCPPSpm4 from 0.5 µM to 6.5 µM.

Moreover, to clarify the different indications obtained by UV and CD spectra, Resonance Light Scattering (RLS) experiments were conducted (Figure 3.53). Porphyrin alone does not give a RLS signal, while the addition of $H_2TCPPSpm4$ to a solution of G-Quadruplex leads to an increasing signal, with a break point at 1:1 *ratio* Porphyrin/GQ, confirming the formation of the complex as showed by the other spectroscopic technique (*i.e.* CD and UV- absorption). Further additions of $H_2TCPPSpm4$ do not lead to a big change in the RLS signal, revealing that with porphyrin/GQ ratios higher than 1:1, the porphyrin excess does not form ordered structures with DNA. Thus, the spectroscopic observations suggest that the CD and RLS data could be affected by transformations which occur after the formation of the complex 1:1 and which could not detected by this technique. In fact, the UV-Vis spectroscopy is faster technique and so is free from kinetic interferences due to the transformation of the complex.



**Figure 3.53 a)** RLS titration of 8 µM $dTG_3AG$ (2 µM in GQ) with increasing amounts of $H_2TCPPSpm4$ from 0.5 µM to 6.5 µM **b)** Plot of RLS intensity at 450 nm of RLS titration of 8 µM $dTG_3AG$ (2 µM in GQ) with increasing amounts of $H_2TCPPSpm4$

To confirm this hypothesis we carried out CD spectra of the two complexes: with 1:1 and 2:1 *ratio* of $H_2TCPPpsm4$/GQ, prepared by direct mixing of the components with the desired concentration (2 µM GQ and 2 µM $H_2TCPPSpm4$ for the *1:1 ratio* complex and 2 µM GQ and 4 µM $H_2TCPPSpm4$ for the 1:2 *ratio* complex). The CD spectra of the complex 1:1 *ratio* obtained after titration and by directly mixing are superimposable. On the contrary, the CD spectra of the 2:1

*ratio* specie shows some changes: the GQ signal is more intense for the specie prepared by mixing directly the components at the final concentration, suggesting either the formation of a different type of complex or a lower destabilizing effect than for the 1:1 species (Figure 3.54).



**Figure 3.54** CD spectra of of 8 µM dTG3AG (2 µM GQ) black curve, 1:1 (red curve) and 2:1 ratio (blue curve) of $H_2TCPPpsm4$/GQ.

Furthermore, we performed CD melting measurements to define the $T_{1/2}$ of $d(TG_3AG)4$ quadruplex (56 °C) in order to estimate the effect of the porphyrin derivative on the thermal stability of the GQ (Figure 3.52).[85] The addition of $H_2TCPPSpm4$ to GQ solution in 1:1 *ratio* decreases the GQ melting temperature $(T_{1/2})$ of ~30 °C, suggesting a strong destabilizing effect on the quadruplex structure, thus confirming the spectroscopic data. On contrary, the melting curve obtained in presence of $H_2TCPPSpm4$ in *2:1 ratio* reveals a biphasic shape, with a first $T_{1/2}$ process at ~ 35 °C and a second one at ~80 °C. The second melting process at higher temperature supports the hypothesis about the formation of a different type of complex in the presence of higher concentration of $H_2TCPPSpm4$ (Figure 3.55).

**Figure 3.55** Melting curves of 4.0 µM GQ alone (black curve) and in the presence of 4 µM H2TCPPSpm4 (red curve) or 8 µM (blue curves) in 200K buffer.

Knowing from the literature[86] that some G-quadruplex sequences with terminal G-quartets are able to generate "*superstructure*" to validate this hypothesis and to better understand this complex system we carried out native PAGE experiments (Figure 3.56). As control we used a four-stranded quadruplex structure, which cannot form GQ superstructures, ending at 3' and 5' position with thymines, *i.e.* d(TG$_4$T) (line 2) and an eight-stranded parallel quadruplexes which forms dimers *i.e.* d(CGGAGGT) (line 6).[87]

**Figure 3.56** Native gel electrophoreses of control TG$_4$T (line 2) and CG$_2$AG$_2$T (line 6), of *Hotoda sequence* (line 3), H$_2$TCPPSpm4/ TG$_3$AG in 1:1 *ratio* (line 4) and H$_2$TCPPSpm4/TG$_3$AG in 2:1 *ratio* (line 5).

The line 3 reporting the Hotoda's sequence d(TG$_3$AG), which in the used buffer runs as a mixture of random coil, probably as tetramolecular and multimeric (likely eight-stranded 2Q species) quadruplex species, in agreement with the above showed CD data. The addition of H$_2$TCPPSpm4 in the 1:1 *ratio* leads to the disappearance of the weak band of the supramolecular quadruplex species. On the other hand, when the porphyrin-quadruplex complex at the 2:1 ratio was added (line 5) only one band is detected, which indicates that at this porphyrin/GQ ratio, the porphyrin derivative promotes the assembly of tetramolecular GQ species as showed by the disappearance of the bands, suggesting the formation of a sandwich-type H$_2$TCPPSpm4–5'-TG$_3$AG-3'–H$_2$TCPPSpm4 complex.

Thus, the melting and PAGE experiments confirm the formation of more stable GQ at 2:1(Porphyrin:GQ) ratio consistent with a T$_{1/2}$ of 80°C.

# 4. Conclusion and outlook

During my research period, new polyamine-porphyrin derivatives have been synthesized and some of them have been used to interact with several biological targets. The porphyrin molecules have been proven to be a versatile scaffold both for self-assembly and for interactions with biopolymers (*e.g.* DNA).

In this thesis, in particular we have focused our attention on the synthesis of porphyrin derivatives with a different number of spermine pendants, in order to combine the hydrophobic and hydrophilic behaviour in a single molecule with the possibility to modulate the two properties, but meanwhile also to have biocompatible features.

To better understanding the role of spermine arms and the interactions with biopolymers a BODIPY-spermine derivative and a longer polyamine pendant have been synthesized.

The results obtained by CD-measurements, UV-Vis, fluorescence and RLS spectroscopy support the good ability of these derivatives (*i.e.* ZnTCPPSpm4) to act like *inducer*, *probe* and *stabilizer* towards the Z-form of DNA. Moreover, they show a good affinity with G-Quadruplex (*i.e.* $H_2$TCPPSpm4) opening the way to several supramolecular structures. In addition, these porphyrins are able to self-assembly under hierarchical control, obtaining the desired aggregation state in solution, by choosing the appropriate pH value.

The collected results do not allow to propose a definitive mechanism of interactions between porphyrin-porphyrin, and porphyrin-DNA and therefore further work is in progress in order to get a rationale which can help in designing *ad hoc* molecules to selectively interact with the target biomolecules.

90

## 5. Experimental section

All of the chemicals and solvents were purchased from Sigma-Aldrich and used without further purification; $H_2TCPP$ was purchased from Frontier Scientific and used as received. Ultra-pure water (18.2 $\Omega M \cdot cm$) obtained from Elga Purelab Flex system by Veolia, at was used in all experiments.

The thin-layer chromatography were carried out on silica gel plates (Merck 60 F254), while the purifications by column chromatography were carried out using as stationary phase silica gel Merck 60 (0.063-0.200 mm).

Positive MALDI-TOF mass spectra were acquired by a Voyager DE (PerSeptive Biosystem) using a delay extraction procedure (25 kV applied after 2600 ns with a potential gradient of 454 V/mm and a wire voltage of 25 V) with ion detection in linear mode. The instrument was equipped with a nitrogen laser (emission at 337 nm for 3 ns) and a flash AD converter (time base 2 ns).

ESI-MS and ESI-MS/MS were acquired by a LCQ DECA (Thermo-Finnigan) and by a API 2000 triple quadrupole equipped with an electrospray ion source.

NMR experiments were carried out at 27 °C on a Varian UNITY Inova 500 MHz spectrometer ($^1$H at 499.88 MHz, $^{13}$C NMR at 125.7 MHz) equipped with pulse field gradient module (Z-axis) and a tuneable 5 mm Varian inverse detection probe (ID-PFG). Unless otherwise stated, NMR spectra were obtained for $CDCl_3$ solutions. The chemical shifts (ppm) were referenced using the residual solvent signal as the internal standard.

JASCO V-630 and V-560 UV/vis spectrophotometer equipped with a 1 cm path-length cell were used for the UV/vis measurement.

Luminescence measurements were carried out using a Cary Eclipse fluorescence spectrophotometer. The emission was recorded at 90° respect to the exciting line beam using 5: 5 slit widths for all measurements. In RLS and fluorescence data, a fluorolog FL-11 Jobin-Yvon Horiba was used.

A JASCO 810 by spectropolarimeter equipped with a temperature controller was used to perform the CD-measurements.

SEM analysis of $H_2TCPPSpm4$ drop casted on silicon substrates at different pHs, has been performed by using a Field

Emission Scanning Electron Microscope (Zeiss Supra 55VP). The EDS analysis has been performed using an Oxford x-Act 10 mm$^2$ SSD detector.

DNA stock solution (350 mer 1.63 mM in bp; 100 mer 10.4 mM in bp) was prepared as required from the frozen sample, by dissolving the polynucleotide in a buffer solution of sodium cacodylate (5mM) and NaCl (10 mM) with hydrochloric acid to pH 6.8. The concentration of the DNA was determined spectroscopically using $\varepsilon_{257}$ =8400 mol$^{-1}$ l cm$^{-1}$ expressed as molarity of phosphate groups.

The annealing of the two sequences was conducted following the standard protocol: heating the DNA's solution tube in a heat block at 91-95 °C for 10 min, and slowly cooled at room temperature in 60 minutes and stored in the refrigerator at 4°C for 1 night before to use.

The stock solution was storage at 4°C and it was diluted the day of the experiment after equilibration at room temperature, to the desired concentration using a buffer solution of cacodylate (5mM) and NaCl (10 mM), pH 6.8.

The porphyrin solutions ($H_2TCPPSpm4$, ZnTCPPSpm4 and ZnTMPyP) in ultra-pure water, were added directly into the cuvette at the desired temperature and concentration. After heating and/or each additions, we waited for 20 min to equilibrate the system, before to acquire the spectra.

Native gel electrophoreses were run on 17% non-denaturing polyacrylamide gels in 1x TBE buffer, pH 7.0, supplemented with 30 mM KCl. ODN samples of 600 µM in single strand, were loaded on the gel and 10% of glycerol was added to each sample just before loading. The gels were run at room temperature at constant voltage (120 V) for 1 h. The bands were visualized by UV shadowing.

## 5.1 Synthesis of H₂TCPPSpm4 **5** and ZnTCPPSpm4 **6**



**Scheme 5.1** General scheme of synthesis pathway to obtain the porphyrin-conjugates with polyamine's arms

## 5.1.1 Synthesis of tfa-tri-BOC-Spermine **1**



**Scheme 5.2**

A solution of Spermine (2.123 g, 10.5 mmol) in MeOH (120 mL) was stirred under a $N_2$ atmosphere at -78 °C. After 10 min ethyl trifluoroacetate (1.24 mL, 10.5 mmol) was added dropwise over 1 hour during which temperature is increased to 0°C. Then a solution of di-tert-butyl dicarbonate (11.46 g, 52.5 mmol) in MeOH (10 mL) was added to reaction mixture during which temperature was brought back to 25°C. After 21 h, the solvent was evaporated and the residue was extracted with dichloromethane. The organic phase was washed with $H_2O$ and then dried over anhydrous $Na_2SO_4$. The solvent was evaporated under reduced pressure. The crude product was purified by column chromatography (CC) (eluent EtOAc) to give the desired product **1** as a yellow oil (3.1 g, 49% yield).

$^1$H NMR (500 MHz, acetone-$d_6$) δ (ppm): 8.54 (br s, 1H); 5.95 (br s, 1H); 3.34-3.24 (m, 10H); 3.07 (m, 2H); 1.82 (br s, 2H); 1.69 (br s, 2H); 1.54-1.41 (m, 31H).

$^{13}$C-NMR (126 MHz, acetone-$d_6$) δ (ppm): 155.7, 155.2, 146.7, 116.2, 84.8, 78.4, 77.5, 46.7, 44.0, 37.5, 36.6, 27.7, 27.6, 26.5, 25.5.

**Figure 5.1** $^1$H NMR of compound **1** in acetone-$d_6$.



**Figure 5.2** APT of compound **1** in acetone-$d_6$.

**Figure 5.3** $^1$D-zTOCSY of compound **1** in acetone-$d_6$, selective band 5.95 ppm

## 5.1.2 Synthesis of tri-BOC-Spermine **2**.



**Scheme 5.3**

The trifluoroacetate protecting group of compound **1** was removed with NaOH after stirring for 15 h at room temperature. The solution was concentrated in vacuum and the residue was extracted with dichloromethane. The organic phase was washed with $H_2O$ and then dried over anhydrous $Na_2SO_4$. The solvent was removed under reduced pressure to give the desired product **2** as a yellow oil (1.089 g, 92% yield).

$^1$H NMR (500 MHz, acetone-d6): δ 5.98 (br s, 1H), 3.30-3.23 (m, 8H), 3.17 (t, J =7.0 Hz, 2H), 3.08 (m, 2H), 1.80 (m, 2H), 1.70 (br s, 2H), 1.53 (br s, 4H), 1.46 -1.41 (m, 27H) ppm.

ESI-MS: 503.4 [M+H]$^+$.



**Figure 5.4** $^1$H-NMR of compound **2** in acetone-d$_6$.

**Figure 5.5** ESI-MS of compound **2**

## 5.1.3 Synthesis of H₂TCPP(tri-BOC-Spm)4 **3**



**Scheme 5.4**

To a solution of H₂TCPP (200 mg, 0.252 mmol) in dry DMF (2 mL), a solution of HATU (445 mg, 1.17 mmol in 1 mL of DMF) was added dropwise and stirred for 20 min at room temperature under nitrogen atmosphere. Then a solution of **2** (510 mg, 1.02 mmol) in dry DMF (2 mL) was added to the reaction mixture. After 40 min *N,N*-diisopropylethylamine (200 μL, 1.17 mmol) was added to the reaction, which was stirred for 24 hrs at rt. The solvent was removed under reduced pressure and CH₂Cl₂ was added obtaining a precipitate that was removed by filtration. The resulting solution was concentrated under vacuum and purified by column chromatography (CH₂Cl₂/EtOH 90:10) to afford the desired compound **3** as a purple powder (107.6 mg, 16% yield).

$^1$H-NMR (500 MHz, CDCl₃): δ 8.84 (s, 8H), 8.31(br s, 16H), 3.63-3.00 (br s, 48H), 1.91 (br s, 8H), 1.69 (br s, 8H), 1.55-1.28 (m, 124 H), -2.72 (s, 2H) ppm.

$^{13}$C-NMR (126 MHz, CDCl₃) 134.5, 125.5, 80.1, 79.6, 55.5, 46.8, 43.5, 37.5, 28.5, 28.47, 28.43, 27.7 ppm.

MALDI: *m/z* 2729 [M+H]$^+$

**Figure 5.6** ^{1}H-NMR of compound **3** in CDCl$_3$



**Figure 5.7** APT of compound **3** in CDCl$_3$

**Figure 5.8** MALDI of compound **3**



**Figure 5.9** UV-VIS of compound **3** in methanol (10 µM).

## 5.1.4 Synthesis of ZnTCPP(tri-BOC-Spm)4 **4**



**Scheme 5.5**

To a solution of **3** (27 mg, 0.010 mmol) in $CH_2Cl_2$ (1 mL), $Zn(CH_3COO)_2 \cdot 2H_2O$ (12.1 mg, 0.055 mmol) in $CH_2Cl_2$ (500 μL) was added and the reaction mixture was refluxed for 24 hrs. Then $H_2O$ was added and the desired compound **4** was obtained as a purple solid (quantitative yield).

^{1}H-NMR (500 MHz, $CDCl_3$) δ 8.84 (br, s, 8H), 8.21 (br, s, 16H), 3.89-2.57 (br, s, 48H), 1.62-1.28 (m, 140H).

MALDI *m/z*: 2791 [M+H]$^+$

**Figure 5.10** ^{1}H-NMR of compound **4** in CDCl₃



**Figure 5.11** MALDI of compound **4**

103

**Figure 5.12** UV-Vis of compound **4** in methanol (10 µM).

## 5.1.5 Synthesis of H$_2$TCPPSpm4 **5**



**Scheme 5.6**

To a solution of **3** in CH$_2$Cl$_2$ (0.04 mmol in 1.5 mL), TFA (20 eq.) was added dropwise under nitrogen and the reaction was stirred at rt for 2 hrs. The reaction was monitored by TLC (CH$_2$Cl$_2$/EtOH 90:10) and the solvent was removed under reduced pressure affording the corresponding trifluoroacetate salt compound **5** as a green-purple solid in nearly quantitative yield.

$^1$H-NMR (500 MHz, CD$_3$OD): δ 8.88 (br, s, 8H), 8.37 (d, *J* = 8.0 Hz, 8H), 8.33 (d, *J* = 8.0 Hz, 8H), 3.71 (br, s, 8H), 3.26-3.06 (m, 40H), 2.19-2.09 (m, 16H), 1.91 (br, s, 16H) ppm.

$^{13}$C-NMR (126 MHz, CD$_3$OD): δ 170.8, 136.4, 135.2, 127.3, 146.5, 121.4, 46.6, 45.8, 37.8, 27.8, 25.3, 24.4, 24.3 ppm.

ESI-MS *m/z* 1527.7 [M+H]$^+$ (100%), 1453.7 [M-(C$_3$H$_9$N$_2$)]$^+$, 1399.6 [M-(C$_7$H$_{17}$N$_2$]$^+$, 1325.6 [M-(C$_{10}$H$_{26}$N$_4$]$^+$.

**Figure 5.13** ^{1}H-NMR of compound **5** in methanol-$d_4$



**Figure 5.14** [1]D-zTOCSY of compound **5** in MeOH-$d_4$ selective band at 1.91 ppm

**Figure 5.15** [1]D-zTOCSY of compound **5** in MeOH-*d₄* selective band at 3.01 ppm



**Figure 5.16** [1]D-zTOCSY of compound **5** in MeOH-*d₄* selective band at 3.71 ppm

**Figure 5.17** APT of compound **5** in methanol-$d_4$



**Figure 5.18** ESI-MS of compound **5**



**Figure 5.19** UV-Vis of compound **5** in methanol (10μM)

**Figure 5.20** UV–vis spectra of a solution of H$_2$TCPPSpm4 **5** (2 μM, in H$_2$O) increasing the pH from 1.3 to 11.1



**Figure 5.21** Fluorescence spectra ($\lambda_{ex}$) 424 nm of a solution of H$_2$TCPPSpm4 **5** (2 μM, H$_2$O) increasing the pH from 1.3 to 11.1.

## 5.1.6 Synthesis of ZnTCPP(tri-BOC-Spm)4 **6.**



**Scheme 5.7**

To a solution of **4** in $CH_2Cl_2$ (0.04 mmol in 1.5 mL), TFA (20 eq.) was added dropwise under nitrogen and the reaction was stirred at rt for 2h. The reaction was monitored by TLC ($CH_2Cl_2$/EtOH 90:10) and the solvent was removed under reduced pressure affording the corresponding trifluoroacetate salt compound **6** as a green solid in nearly quantitative yield.

^{1}H NMR (500 MHz, $CD_3OD$) δ 8.84 (br, s, 8H), 8.36-8.20 (m, 16H), 3.71 (br, s, 8H), 3.28-3.07 (m, 40H), 2.16- 2.00 (m, 16H), 1.90 (br, s, 16H).

ESI-MS *m/z* 738.9 $[M-C_6H_{13}N_2]^{2+}$, 709.89 $[M-C_9H_{20}N_3]^{2+}$, 681,36 $[M-C_{12}H_{27}N_4]^{2+}$

**Figure 5.22** ^{1}H-NMR of compound **6** in methanol-*d₄*



**Figure 5.23** ^{1}H-^{1}H gCOSY of compound **6** in methanol-*d₄*

**Figure 5.24** UV-Vis of compound **6** (10 µM) in methanol

## 5.2 Synthesis of *mono*-functionalized porphyrin **11**



**Scheme 5.8**

## 5.2.1 Synthesis of Methyl 4-formylbenzoate **7**



**Scheme 5.9**

To a suspension of 4-formylbenzoic acid (2.5g; 16.7mmol) in MeOH (65 ml) was added dropwise $SOCl_2$ (4ml, 55.1 mmol) and stirred for 2 days. The solvent was removed in vacuum, by co-evaporation with dichloromethane (2 x100 mL) to remove the excess of thionyl chloride. The residue was stirred with dilute aqueous HCl for 1h. The obtained white solid was washed with water and dried to give desired compound **7** (77% yield).

^{1}H-NMR (500 MHz, $CDCl_3$) δ 10.10 (s, 1H); 8.20 (d, *J*= 8.0 Hz, 2H); 7.96 (d, *J*= 8.0 HZ, 2H); 3.96 (s, 3H).



**Figure 5.25** ^{1}H-NMR of compound **7** in $CDCl_3$

## 5.2.2 Synthesis of 5-mono-(*p*-phenyl-COOMe)10,15,20-Tri-phenyl porphyrin **8**.



**Scheme 5.10**

To a solution of pyrrole (2.52 ml, 36 mmol), in $CHCl_3$ (500 ml) benzaldehyde (3.64 ml, 36 mmol) and methyl-p-formylbenzoate **7** (985.0 mg, 6 mmol) were added and purged with nitrogen (1 hour) in the dark. After boron trifluoride etherate (0.69 ml, 5.4 mmol) was added and the reaction allowed to stir at room temperature. After one hour DDQ (8.14 g, 36 mmol) was added and stirred for 16 hours. Reaction mixture was concentrated in vacuum and was purified by double column chromatography ($CH_2Cl_2$) to give a solid purple powder **11** (yields 3%).

^{1}H-NMR (500 MHz, $CDCl_3$) δ 8.88 (m, 6H); 8.80 (d, *J*= 5.0 Hz, 2H), 8.45 (d, *J* = 8.0 Hz, 2H) 8.32 (d, *J* = 8.0, 2H); 8.23 (d, *J*= 7.0 Hz, 6H); 7.78 (m, 9H) 4.12 (s, 3H); -2.76 (2H).

**Figure 5.26** $^1$H-NMR of compound **8** in CDCl$_3$

## 5.2.3 Synthesis Synthesis of 5-mono-(*p*-phenyl-COOH)-10,15,20-Tri-phenyl porphyrin **9**.



**Scheme 5.11**

To a suspension of **8** (77.5 mg, 0.12 mmol) in EtOH (5 mL) was added a solution of KOH (2 N, 10 mL) and the suspension was refluxed for 24 hrs. Cooled to room temperature, the reaction mixture was acidified with HCl$_{acq}$ up to a pH≈5. The compound is extracted with ethyl acetate (3x20 ml). The organic phase was collected and was dried with anhydrous $Na_2SO_4$. The solvent was removed in vacuum obtaining desired product **9** as violet powder. (95% yield).

^{1}H-NMR (500 MHz; Acetone-*d₆*) δ: 8.90 -8.91 (m, 8H), 8.52 (d, *J*= 8.0 Hz, 2H), 8.43 (d, *J*= 8.0 Hz, 2H), 8.28 (m, 6H), 7.86 (m, 9H).



**Figure 5.27** ^{1}H-NMR of compound **9** in acetone-*d₆*

## 5.2.4 Synthesis of 5-mono-(*p*-phenylCOtriBOCSpm)-10,15,20-Tri-phenyl porphyrin **10**.



**Scheme 5.12**

To a solution of compound **9** (75.7 mg, 0.115 mmol) in DMFdry (1 mL), under a $N_2$ atmosphere and at room temperature, HATU (50.7 mg, 0.133 mmol) in DMFdry (1 mL) was added dropwise and stirred for 20 min. Then to reaction mixture a solution of tri-BOC-Spm (57.8 mg, 0.115 mmol) in DMF$_{dry}$ (500 µL) was added. After 40 min N,N-diisopropylethylamine (20 µL, 0.115 mmol) was added to reaction mixture and it was stirred at r.t under $N_2$ for 54 h. Then $H_2O$ was added and the precipitate was dried and after purified by double chromatographyc column (CHCl$_3$/EtOH) to give desired compound **10** (yield 28%).

UV-Vis (CH$_3$OH): $\lambda_{max}$ (logε) 413 (5.57); 512 (4.29); 548 (4.00); 590 (3.81); 645 (3.60).

$^1$H-NMR (500 MHz; Acetone-$d_6$) δ: 8.87 (br s, 8H); 8.31-8.29 (dd, 4H); 8.24 (m, 6H); 7.82 (m, 9H); 5.95 (br s, 1H); 3.60-3.40 (br m, 4H); 3.35-3.22 (m, 6H); 3.08 (m, 2H) 1.93 (m br, 2H); 1.71 (m br, 2H); 1.60 (m br, 4H); 1.51 (s, 9H); 1.47 (s, 9H); 1.39 (s, 9H); -2.72 (s, 2H).

$^{13}$C-NMR (125 MHz, Acetone-$d_6$) δ: 166.0, 155.7, 150.1, 149.6, 146.2, 144.7, 143.3, 141.9, 134.5, 134.3, 131.7, 131.6, 131.6, 131.3, 127.9, 127.4, 126.8, 126.5, 125.6, 125.2, 120.72, 120.4, 120.3, 119.2, 78.5, 77.5, 46.7, 44.2, 37.5, 27.8, 27.8.

ESI-MS: *m/z* 1143.87 [M+H]$^+$

**Figure 5.28** $^1$H-NMR of compound **10** in acetone-$d_6$



**Figure 5.29** APT of compound **10** in acetone-$d_6$

**Figure 5.30** dqCOSY of compound **10** in acetone-$d_6$



**Figure 5.31** UV-Vls of compound **10** (10 µM) in MeOH.

**Figure 5.32** ESI-MS of compound **10**

## 5.2.5 Synthesis of 5-mono-(*p*-phenylCOSpm)10,15,20-Tri-phenyl porphyrin **11**.



**Scheme 5.13**

To a solution of 5-mono-(4'carbossiphenyl-Tri-Boc-Spm)-10,15,20-triphenyl porphyrin **10** ( 20.6 mg, 0.018 mmol) in $CH_2Cl_2$ (3 ml) was added 40 µL of TFA ( 0.52 mmol). After about 8 hours you add another 60 µL of TFA and 4 ml of $CH_2Cl_2$ and allowed to react overnight. After about 24hrs the solvent was removed in vacuum to obtain the desired product **11** (95% yield).

^{1}H-NMR (500 MHz, $CD_3OD$) δ: 8.87 (m, 8H), 8.71 (d, *J* = 8.0 Hz, 2H), 8.60 (d, *J* = 6,5 Hz, 6H), 8.53 (d, *J* = 8.0, 2H), 3.74 (t, *J* = 6.5 Hz, 2H), 3.27 (t, *J* = 7.0 Hz, 2H), 3.18 (m, 6H), 3.08 (t, *J* = 7.5 Hz, 2H), 2.20 (m, 2H), 2.12 (m, 2H), 1.92 (m,4H).

^{13}C-NMR (125 MHz, $CD_3OD$) δ: 169.3, 150.1, 143.7, 143.3, 140.4, 136.4, 134.3, 132.6, 131.3, 130.5, 129.6, 129.3, 129.1, 128.1, 127.0, 126.4, 126.0, 122.3, 122.1, 120.2, 46.9, 45.3, 44.5, 36.4, 29.3, 29.0, 26.5, 23.9, 23.0, 22.9.

**Figure 5.33** $^1$H-NMR of compound **11** in acetone-$d_6$



**Figure 5.34** APT of compound **11** in acetone-$d_6$

**Figure 5.35** ESI-MS of compound **11**

## 5.3 Synthesis of di-functionalized porphyrin



**Scheme 5.14** General scheme of synthesis pathway to obtain the porphyrin-conjugates with polyamine's arms.

125

## 5.3.1 Synthesis of di-pyrromethane **12**



**Scheme 5.15**

To a solution of methyl-4-formyl-benzoate **7** (2.5 g, 15.3 mmol) in pyrrole (25 mL, 382.5 mmol), under a $N_2$ atmosphere and at room temperature, Trifluoroacetic acid (220 µL, 2.89 mmol) was added dropwise and stirred for 1.5 h. Then to reaction mixture $Et_3N$ (600 µL, 3.83 mmol) was added. After 30 min toluene (70 mL) was added and the organic phase was washed with a $NaCl_{aq}$ saturated solution, then dried over anhydrous $Na_2SO_4$. The solvent was evaporated at reduced pressure to give the crude product, which was purificated by column chromatography (CC) (eluent $CH_2Cl_2$). The desired product was further purified by treatment with diethyl ether to give a white powder **12** (1.39 g, 33% yield).

^{1}H-NMR (500 MHz, CDCl₃) δ 7.98 (*d*, *J*=8.5 Hz , 2H, 7.29( *d*, *J*= 8.5 Hz, 2H), 6.72 (*broad m*, 2H) 6.17 (*d*, *J*=3.0 Hz 2H), 5.89 (*broad m*, 2H), 5.53 (s,1H), 3.91(s,3H).

**Figure 5.36** ^{1}H-NMR of compound **12** in CDCl₃.

## 5.3.2 Synthesis of 5,15-di(*p*-phenyl-COOMe)10,20-diphenyl porphyrin **13**



**Scheme 5.16**

To a solution of dipirromethane **12** (225.9 mg; 0.81 mmol) in $CHCl_3$ (128 ml) under a nitrogen atmosphere and at room temperature, benzaldehyde (82 μL, 0.81 mmol) was added dropwise and stirred for 0.5 h. Then TFA (62 μl; 0.81 mmol) was slowly added for 24h; After DDQ (227mg, 0.22 mmol) was added and stirred for 2 hours then $Et_3N$ (2 ml; 14.4 mmol) was added and reacted for 20 min. Reaction mixture was filtered and the solvent was evaporated at reduced pressure. The crude product was purified by double column chromatography ($CHCl_3$ and $CHCl_3$/ Ethyl acetate 95:5) to give a solid purple powder of the compound **13** (yields 20%).

$^1$H-NMR (500 MHz, $CDCl_3$) δ: 8.87 (m, 4H), 8.80 (m, 4H), 8.45 (*d*, *J* = 8.0 Hz, 4H), 8.31 (*d*, *J* = 8.0 Hz, 4H), 8.21 (*m*, 4H), 7.75 (*m*, 6H), 4.10(s, 6H), -2.7 (*bs*, 2H).

**Figure 5.37** ^{1}H-NMR of compound **13** in CDCl₃

## 5.3.3 Synthesis of 5,15-di(*p*-phenyl-COOH)10,20-diphenyl porphyrin **14**



**Scheme 5.17**

A suspension of compound 5,15-di-(4'carboxymethylphenyl)10,20 di-phenyl porphyrin (**13**) (84.8 mg; 0.12 mmol) reacted with $KOH_{acq}$ (15 mL, 2N) in EtOH (7 ml) under reflux for all weekend (~90 h). The purple precipitate was extracted with ethyl acetate, washed with a solution of HCl, pH ~3 and then dried over anhydrous $Na_2SO_4$. The solvent was evaporated at reduced pressure to give the desired compound **14** as a violet powder (yield, 93%).

^{1}H-NMR (500MHz, $CDCl_3$/DMSO-$d_6$ 3/2): 8.78 (s br, 4H), 8.82 (s br, 4H), 8.36 (br d,4 H), 8.24 (br d, 4H), 8.14 (br d, 4H), 7.75 (br d, 6H).

**Figure 5.38** $^1$H-NMR of compound **14** in CDCl$_3$/DMSO-$d_6$

## 5.3.4 Synthesis of 5,15-di(*p*-phenylCOtriBOCSpm)-10,20-di-phenyl porphyrin **15**



**Scheme 5.18**

To a solution of 5,15-di-(4'carboxyphenyl)10,20 di-phenyl porphyrin (**14**) (95.8 mg; 0.14 mmol) in $DMF_{dry}$(1 mL) a solution of HATU (145 mg, 0.38 mmol in 500 μL $DMF_{dry}$) was added dropwise under nitrogen atmosphere and at room temperature. After 20 min a solution of triBOCSpm (**2**) (163 mg, 0.325 mmol) in 500 μL $DMF_{dry}$ was added to the reaction mixture. After 20 min DIPEA (80 μl, 0.46 mmol) was added, and after 5 gg we added 5 ml of water and the precipitate was filtered and dried. The crude product was purified by column chromatography ($CH_2Cl_2$ → $CH_2Cl_2$/MeOH 97:3) and after by PLC ($CH_2Cl_2$/MeOH 97:3), to give the desired compound (**15**) (yield, 9%).

UV-Vis ($CH_3OH$): $\lambda_{max}$ (logε) 414 (5.53); 512 (4.14); 548 (3.89); 590 (3.68); 645 (3.47).

$^{1}$H-NMR (500 MHz, Acetone-$d_6$) δ: 8.88 (*s*, 8H); 8.34 (*br s*, 8H); 8.30 (*d*, *J*=6.5 Hz, 4H); 7.84 (*m*, 6H); 5.96 ( *br s*, 2H); 3.60-3.20 (*m*, 20H); 3.08 (*m*, 4H) 1.97 ( *br s*, 4H) 1.71 (*br s* , 4H); 1.61 (*br s*, 8H); 1.51( *s*, 18H); 1.47 (*s*, 18H); 1.39 (*s*, 18H); -2.73 (*s*, 2H).

$^{13}$C-NMR (125 MHz, Acetone-$d_6$) δ: 173.2, 166.4, 155.8, 150.1, 149.6, 146.3, 144.6, 143.4, 141.8, 134.6, 134.3, 131.7, 127.9, 126.8, 126.5, 125.6, 125.2, 120.4, 119.4, 78.5, 77.6, 46.8, 44.3, 37.9, 33.7, 27.8, 27.8.

ESI-MS: *m/z* 1673.07 [M+H]$^{+}$

**Figure 5.39** ^{1}H-NMR of compound **15** in methanol-*d₄*



**Figure 5.40** APT of compound **15** in methanol-*d₄*

**Figure 5.41** $^1$H-$^1$H gCOSY of compound **15** in methanol-$d_4$



**Figure 5.42** UV-Vis absorption spectra of compound **15** in methanol

**Figure 5.43** ESI-MS of compound **15**

## 5.3.5 Synthesis of 5,15-di(*p*-phenylCOSpm)-10,20-di-phenyl porphyrin **16**



**Scheme 5.19**

To a solution of 5,15-di(4'carboxy-tri-BOC-spm-phenyl)10,20-diphenyl porphyrin **7** (19.3 mg, 0.012 mmol) in $CH_2Cl_2$ (1.5 ml) was added 110 µL of TFA (1.2 mmol). After about 24h the solvent was removed in vacuum to obtain the desired product **8** (95% yield).

$^1$H-NMR (500 MHz, methanol-$d_4$) δ: 8.88 (d, J= 5Hz, 4H), 8.86 (d, J= 5Hz, 4H), 8.6 (m, 4H), 8.4 (m, 8H), 8.0 (m, 6H), 3.7 (t, *J*=7.0 Hz, 4H), 3.25-3.0 (*t*, *J*=7.5 Hz, 4H; *m*, 12H; *t*, *J*=8 Hz, 4H), 2.2 (*m*, $J_{1,2}$=7.0 Hz, $J_{2,3}$= 7.5 Hz, 4H), 2.1 (*m*, $J_{1,2}$=7.5 Hz, $J_{2,3}$= 8.0 Hz, 4H), 1.85(*bm*, 8H).

$^{13}$C-NMR (125 MHz, methanol-$d_4$) δ 173.2, 154.4, 153.7, 146.7, 143.7, 141.5, 141.3, 138.7, 133.8, 133.7, 133.1, 131.9, 130.8, 126.9, 125.2, 50.8, 49.3, 48.4, 40.4, 33.2, 30.4, 28.8, 27.9, 27.0.

**Figure 5.44** ^{1}H-NMR of compound **16** in methanol-*d₄*



**Figure 5.45** APT of compound **16** in methanol-*d₄*

## 5.4 Synthesis of BODIPY-spermine derivative



**Scheme 5.20** General scheme for the synthesis of spermine BODIPY derivative

## 5.4.1 Synthesis of BODIPY-COOMe **17**



**Scheme 5.21**

To a solution of methyl-4-formyl-benzoate **7** (1.16 g, 7.0 mmol) in $CH_2Cl_2$ (700 mL), under a nitrogen atmosphere and at room temperature, 2,4-dimethyl-3-ethylpyrrole (1.89 mL, 14 mmol) and trifluoroacetic acid (40 µL) were added dropwise and stirred overnight. Then DDQ (1.58 g, 7mmol) was added and the mixture was stirred for 1 h. After $Et_3N$ was added (17 ml, 122 mmol) dropwise and stirred for 20 min, then $BF_3 \cdot Et_2O$ (17 ml, 137 mmol). After stirring for 1 h, the reaction mixture was washed with water and dried over $Na_2SO_4$. The solvent was evaporated at reduced pressure to give the crude product, which was purificated by column chromatography (CC) (eluent *n*-hexane/ $CH_2Cl_2$ from 7/3 to 6/4) to give the desired product **17** (yield 33%).

**Figure 5.46** ^{1}H-NMR of compound **17** in CDCl₃

## 5.4.2 Synthesis of BODIPY-COOH **18**



**Scheme 5.22**

To a solution refluxing solution of BODIPY-COOMe **17** (600 mg, 1.37 mmol) in MeOH (200 ml) NaOH$_{aq}$ (2N, 45 ml) was added. After 4 hrs the solvent was evaporated at reduced pressure and the reaction mixture re-dissolved in water, the pH was adjusted at pH 7 with HCl solution. The product was extracted by using of CHCl$_3$ and dried over anhydrous Na$_2$SO$_4$. The solvent was removed under pressure to give the desired product **18** (yield 80%).

^{1}H-NMR (500 MHz; CDCl$_3$) δ: 8.24 (d, *J*=8.5 Hz, 2H), 7.40 (m, 2H), 2.53 (s, 6H), 2.29 (q, *J*=7.5 Hz 4H), 1.25 (s, 6H), 0.97 (t, *J*=7.5 Hz 6H).

**Figure 5.47** ^{1}H-NMR of compound **18** in CDCl₃



**Figure 5.48** UV-Vis absorption spectra of compound **18** in methanol.

## 5.4.3 Synthesis of BODIPY-CO-tri-BOC-Spm **19**



**Scheme 5.23**

To a solution of **18** BODIPY-COOH (255 mg, 0.6 mmol) in $DMF_{dry}$ (3mL), HATU (270 mg, 0.71 mmol) was added and the reaction mixture was stirred under nitrogen for 20 min at room temperature. Then a solution of tri-BOC-Spermine **2** (510 mg, 1.02mmol) in $DMF_{dry}$ (1.5 ml) was added, after 20 min DIPEA (130 µL, 0.78 mmol) and the reaction mixture was stirred at r.t. for 48 hrs. $H_2O$ (30 ml) was added and the precipitate was filtered and dried. The crude product was purified by column chromatography (ciclohexane/Ethyl acetate 5:5) to give the desired product **19** (yield, 9.4%).

^{1}H-NMR (500 MHz, $CDCl_3$); 8.04 (br. s), 7.38 (d, 2H), 3.03-3.53 (m, 12H), 2.53 (s, 6H), 2.29 (q, J=7.5 Hz, 4H), 1.80 (br.s, 2H), 1.66 (m, 2H), 1-49-1.41 (31H), 1.26 (s, 6H), 0.97 (t, J= 7.5 Hz; 6H).

^{13}C-NMR (126 MHz, $CDCl_3$); 166.28, 156.98, 156.11, 154.15, 139.28, 138.98, 138.38, 134.98, 133.06, 130.58, 128.74, 127.94, 80.25, 79.75, 46.92, 46.43, 44.38, 44.04, 43.36, 37.84, 35.96, 29.81, 28.59, 27.65, 26.14, 17.18, 14.70, 12.64, 12.00.

**Figure 5.49** $^1$H-NMR of compound **19** in CDCl$_3$



**Figure 5.50** APT of compound **19** in CDCl$_3$

**Figure 5.51** UV-Vis absorption spectra of compound **19** in methanol.



**Figure 5.52** Emission spectra of compound **19** in methanol.

## 5.4.4 Synthesis of BODIPY-CO-Spm **20**



**Scheme 5.24**

To a solution of **19** (51 mg, 0.056 mmol) in 2.5 ml of $CH_2Cl_2$ $CF_3COOH$ (154μL, 2 mmol) was added. The mixture was stirred at r.t for 48 h and after the solvent was removed under pressure to give the desired product **20** with a quantitative yield.

^{1}H NMR (500 MHz, methanol-$d_4$) δ 8.03 (d, J=8.0 Hz , 2H), 7.50 (dd, $J_{1,1}$= 8.0Hz, $J_{1,2}$= 20.5Hz, 2H), 3.55 (t, J=7.0 Hz, 2H), 3.10 (m, 10H),2.6-2.3 (m, 10H) 2.10 (*m*, $J_{1,2}$=8.0 Hz, $J_{2,3}$= 7.5 Hz, 2H) 2.0 ppm (*m*, $J_{1,2}$=7.5 Hz, $J_{2,3}$= 7.0 Hz, 2H),1.83 (m, 4H),1.65 (bs, 3H), 1.31(s, 3H) 1.10 (t, J= 7.5 Hz, 3H), 0.98 (t, J=7.5 Hz, 3H)

^{13}C NMR (126 MHz, methanol-$d_4$) δ 168.40, 153.93, 150.89, 144.26, 139.72, 139.33, 139.21, 138.04, 137.13, 134.38, 133.64, 130.19, 128.66, 127.99, 127.77, 46.82, 45.20, 44.65, 36.36, 26.34, 26.23, 23.92, 22.90, 22.81, 16.82, 16.37, 13.53, 13.20, 12.49, 11.20, 11.02, 10.74.

**Figure 5.53** $^{1}$H-NMR of compound **20** in methanol-$d_4$



**Figure 5.54** $^{1}$H-$^{1}$H gCOSY of compound **20** in methanol-$d_4$

**Figure 5.55** APT of compound **20** in methanol-*d₄*



**Figure 5.56** ESI-MS of compound **20** in methanol

148

# 5.5 Synthesis of pendant



**Scheme 5.25** General scheme of synthesis to obtain N-propyl- tetra-BOC-Spm **23**

## 5.5.1 Synthesis of compound **21**



**Scheme 5.26**

To a solution of **2** (730 mg; 1.45 mmol) in CH$_3$CN dry (35 mL) Cs$_2$CO$_3$ (840 mg; 2.8 mmol) was added; to the refluxing mixture N-(3-bromopropyl)phthalimide (350 mg; 1.30 mmol) was added and stirred for 12 hrs. After evaporations, the crude product was poured into water (100 mL) and extracted with Ethyl acetate (3x70 ml). The organic phase was dried over Na$_2$SO$_4$ and evaporated. The crude product was purified by chromatographic column on SiO$_2$ and eluted with a gradient of pure CH$_2$Cl$_2$ to CH$_2$Cl$_2$/MeOH 9:1 to yield after evaporation 287.5 mg of desired compound **21** as colorless oil (Yield 29%).

$^1$H-NMR (500 MHz; Acetone-$d_6$) δ 7.83 (*d*, *J*=8.0 Hz , 4H), 5.99 (*br s*, 1H), 3.76 (*t*, J= 7.0 Hz, 2H), 3.25 (*br m*, 8H), 3.05 (*br m,* 2H), 2.82 (*br m*, 2H), 2.73 (*br t*, 2H), 1.99 (*br s,* 2H), 1.82 (*br m*, 2H), 1.68 (*br m*, 2H), 1.51 (*br s*, 4H), 1.42-1.43 (*s*, 27H).

$^{13}$C-NMR (125 MHz; Acetone-$d_6$) δ 170.58, 158.28, 136.7, 134.9, 125.4, 81.05, 80.1, 54.0, 53.7, 48.9, 38.7, 38.2, 35.9, 32.4, 30.5, 30.4, 28.6, 24.9

ESI-MS: [M+H]$^+$= 690 *m/z* ; [M+H+31]$^+$ 721.9 *m/z*

N-propyl-Pht-Tri-BOC-Spm



**Figure 5.57** ^{1}H-NMR of compound **21** in Acetone-$d_6$



**Figure 5.58** ^{1}H-^{1}H-gCOSY of compound **21** in Acetone-$d_6$

151

**Figure 5.59** APT-NMR of compound **21** in Acetone-$d_6$



**Figure 5.60** ESI-MS of compound **21**

## 5.5.2 Synthesis of compound **22**



**Scheme 5.27**

To a solution of **21** (287.5 mg; 0.417 mmol) in THF dry (6mL) $BOC_2O$ (230 mg; 1.06 mmol) was added and stirred for 2 days. After evaporations, the crude product was poured into water (50 mL) and extracted with Ethyl acetate (3x40 ml). The organic phase was dried over $Na_2SO_4$ and evaporated. The crude product was purified by chromatographic column on $SiO_2$ and eluted with a gradient of pure n-Esane to n-Esane/Ethyl acetate 5:5 to yield after evaporation 275.8 mg of the desired compound **22** as colorless oil (Yield 84%).

$^1$H-NMR (500 MHz; Acetone-$d_6$) δ 7.86 (*m*, 4H), 5.94 (*br s*, 1H), 3.68 (*t*, J= 7.0 Hz, 2H), 3.25 (*br m*, 12H), 3.05 (*br m,* 2H), 1.97 (*m*, 2H), 1.79 (*m*, 2H), 1.69 (*br s,* 2H), 1.52 (*br s*, 4H), 1.45-1.41 (*s*, 36H).

$^{13}$C-NMR (125 MHz; Acetone-$d_6$) δ 168.8, 156.6, 155.8, 135.0, 133.2, 123.7, 79.4, 79.2, 78.44, 60.5, 47.6, 47.2, 45.7, 44.9, 38.4, 36.4, 28.6, 26.8, 26.4.

ESI-MS: $[M+H]^+$= 790 *m/z* ; $[M+Na]^+$= 812 *m/z*

N-propylPht-Tetra-BOC-Spm



**Figure 5.61** $^1$H-NMR of compound **22** in Acetone-$d_6$



**Figure 5.62** $^1$H-$^1$H-gCOSY of compound **22** in Acetone-$d_6$

**Figure 5.63** $^{13}$C-NMR of compound **22** in Acetone-$d_6$



**Figure 5.64** ESI-MS of compound **22**

## 5.5.3 Synthesis of compound **23**



**Scheme 5.28**

To a solution of **22** (275.8 mg; 0.350 mmol) in absolute ethanol (10 mL) $NH_2NH_2$ (100 µL; 3.14 mmol) was added and refluxed for 4 hrs. After evaporations, the crude product was poured into water (30 mL) and extracted with Ethyl acetate (3x20 ml). The organic phase, was washed with water (2x10 ml), dried over $Na_2SO_4$ and evaporated. The desired compound **23** was obtained as colorless oil (91% yield).

$^1$H-NMR (500 MHz; Acetone-$d_6$) δ 5.94 (*br s*, 1H), 3.30, 3.15 *(m*, 14H), 3.05 (*br m*, 2H), 1.79-1.61 (*m*, 6H), 1.53 (*br s*, 4H), 1.45-1.40 (s, 36H).

ESI-MS: $[M+H]^+=660$ *m/z*; $[M+K]^+=698$ *m/z*

**Figure 5.65** ¹H-NMR of compound **23** in Acetone-*d₆*



**Figure 5.66** ESI-MS of compound **23**

# 6. Bibliography

[1] Milgrom, L.R., The Colours of Life, OUP, Oxford, **1997**; The Porphyrins, ed. D. Dolphin, AcademicPress, New York, 1978.

[2] Weiss, C.; Kobayashi, H.; Gouterman, M.; *J. Mol. Spectrosc.*, **1965**, 16, 415-450

[3] Uttamlal, M., Holmes-Smith A. S.; *Chem. Phys. Lett.*, **2008**, 454, 223-228.

[4] a) Yang, R.; Wang, K.; Long, L.; Xiao, D.; Xiaohai Yang, X.; Tan, W., *Anal. Chem.*, **2002**, *74*, 1088-1096. b) Gulino, A.; Mineo, P.; Bazzano, S.; Vitalini, D.; Fragalà, I.; *Chem. Mater.*, **2005**, *17*, 4043-4045. c) Di Natale, C.; Salimbeni, D.; Paolesse, R.; Macagnano, A.; D'Amico, A., *Sens. Actuators B*, **2000**, *65*, 220-226. d) Di Natale, C.; Paolesse, R.; D'Amico, A., *Sens. Actuators B*, **2007**, *121*, 238-246.

[5] a) Scolaro, L. M.; Romeo, A.; Pasternack, R.F., *J. Am. Chem. Soc.*, **2004**, *126*, 7178-7179. b) Balaz, M.; Holmes, A.E.; Benedetti, M.; Rodriguez, P.C.; Berova, N.; Nakanishi, K.; Proni, G., *J. Am. Chem. Soc.*, **2005**, *127*, 4172-4173.

[6] a) Zhang, Y.; Yang, R. H.; Liu, F.; Li, K.A., *Anal. Chem.*, **2004**, 76, 7336-7345 b) Zhou, H.; Baldini, L.; Hong, J.; Wilson, A. J.; Hamilton, A.D., *J. Am. Chem. Soc.*, **2006**, *128*, 2421-2425.

[7] a) Shundo, A.; Labuta, J.; Hill, J.P.; Ishihara, S.; Ariga, K., *J. Am. Chem. Soc.*, **2009**, *131*, 9494-9495. b) Tong, Y.; Hamilton, D.G.; Meillon, J.-C.; Sanders, J.K.M., *Org. Lett.*, **1999**, *1*, 1343-1346.

[8] a) Rothemund, P. *J. Am. Chem. Soc.*, **1935**, *57*, 2010-2011. b) Arsenault, G. P.; Bullock, E.; MacDonald, S. F. *J. Am. Chem. Soc.*, **1960**, *82*, 4384-4389. c) Nguyen, L. T.; Senge, M. O.; Smith, K. M. *J. Org. Chem.*, **1996**, *61*, 998-1003.

[9] Adler, A.D.; Longo, F.R.; Finarelli, J.D.; Goldmacher, J.; Assour, J.; Karsakoff, L., *J. Org. Chem.*, **1967**, *32*, 476.

[10] Lindsey, J. S.; Schreiman, I.C.; Hsu, H.C.; Kearney, P.C.; Marguerettaz, A.M., *J. Org. Chem.*, **1987**, *52*, 827-836.

[11] Iengo, E.; Zangrando, E.; Minatel R.; Alessio, E.; *J. Am. Chem. Soc.*, **2002**, *124*, 1003-1013.

[12] Zhu, X.-J.; Wang, P.; Leung, H. W. C.; Wong, W.-K.; Wong, W.-Y.; Kwong, D. W. J.; *Chem. Eur. J.*, **2011**, *17*, 7041-7052.

[13] Littler, B. J.; Ciringh, Y.; Lindsey, J. S.; *J. Org. Chem.*, **1999**, 64, 2864-2872.

[14] Geier III, G. R.; Littler, B. J.; Lindsey, J. S.; *J. Chem. Soc., Perkin Trans. 2*, **2001**, 701–711.

[15] E. Vogel , *Pure Appl. Chem.*, **1993**, *65*, 143; b) E. Vogel , *J. Heterocycl. Chem.*, **1996**, *33*, 1461-1487.

[16] Treibs, A.; Kruzer, F. H.; Liebigs, J.; *Ann. Chem.*, **1968**, *718*, 208-223.

[17] a) Metzker, M. L.; Lu, J.; Gibbs, R. A.; *Science*, **1996**, *271*, 1420-1422. b) Farber, S. A. ; Pack, M.; Ho, S-Y.; Johnson, I. D.; Wagner, D. S.; Dosch, R.; Mullins, M. C.; Hendrickson, H. S.; Hendrickson, E. K.; Halpern, M. E.; *Science,* **2001**, *292*, 1385-1388. c) Reents, R.; Wagner, M.; Kulhmann, J.; Waldmann, H.; *Angew. Chem. Int. Ed.,* **2004**, *43*, 2711-2714.

[18] Brizet, B.; Bernhard, C.; Volkova, Y.; Rousselin, Y.; Harvey, P.D.; Goze, C.; Denat, F.; *Org. Biomol. Chem.,* **2013**, *11*, 7729-7737.

[19] Zhao, C.; Zhang, Y.; Wang, X.; Cao, J. ; *J. Photochem. Photobiol. A*, **2013**, *264, 41-47.

[20] A) Karolin, J.; Johansson, L. B.-A.; Strandberg, L.; Ny, T. *J. Am. Chem. Soc.,* **1994**, 116, 7801-7806. b) Haugland, R. P. *Handbook of Fluorescent Probes and Research Chemicals*, 6th ed.; Molecular Probes, Eugene, OR, **1996.** c) Tan, K.; Jaquinod, L.; Paolesse, R.; Nardis, S.; Di Natale, C.; Di Carlo, A.; Prodi, L.; Montalti, M.; Zaccheroni, N.; Smith, K. M. *Tetrahedron* **2004**, *60*, 1099-1106. d) Yee, M.-C.; Fas, S. C.; Stohlmeyer, M. M.; Wandless, T. J.; Cimprich, K. A.; *J. Biol. Chem.* **2005**, 280, 29053- 29059. e) Wagner, R. W.; Lindsey, J. S. *Pure Appl. Chem.* **1996**, 68, 1373-1380.

[21] Metzker, M. L. WO Patent WO/2003/066812, 2003.

[22] Kim, K. T.; Kim, B. H.; *Chem. Commun*., **2013**, 49, 1717-1719.

[23] Lòpez Arbeloa, F.; Banuelos, J.; Martinez, V.; Arbeloa, T.; Lòpez Arbeloa, I.; *Int.Rev.Phys.Chem.,* **2005**, *24*, 339-374.

[24] a) Nepomnyashchii, A.B.; Pistner, A. J.; Bard, A.J.; Rosenthal, J.; *J. Phys. Chem. C*, **2013**, *117, 5599-5609*. b) Bañuelos Prieto, J.; López Arbeloa, F.; Arbeloa López, T.; Martínez Martínez, V.; López Arbeloa, I. *"In Chromic Materials, Phenomena and their Technological Applications"*, Applied Science Innovations Pvt. Ltd., India, 2012, 641-677.

[25] Lu, H.; Mack, J.; Yang, Y.; Shen, Z.; *Chem. Soc. Rev.,* **2014**, *43*, 4778-4823

[26] Chi V. Dang, *Mol. Cell. Biol.,* **1999**, *19,*1-11

[27] a) Vasudevaraju, P.; Guerrero, E.; Hegde, Muralidhar L.; Collen, T. B.; Britton, Gabrielle B.; Rao, K. S., *J. Pharm. BioAllied Sci.*, **2012**, *4*, 1-13. b) Govindaraju, M.; Monica, F. S.; Berrocal, R.; Sambasiva Rao, K. R. S.; Rao, K. S., *Curr. Trends Biotechnol. Pharm.*, **2012**, *6*, 204-209. c) Geng, Jie; Zhao, Chuanqi; Ren, Jinsong; Qu, Xiaogang, *Chem. Commun.,* **2010**, *46*, 7187-7189. d) Vasudevaraju, P.; Bharathi; Garruto, R. M.; Sambamurti, K.; Rao, K. S. J., *Brain Res. Rev.,* **2008**,*58*,136-148.

[28] a) Adachi, M; Tsujimoto, Y. *Oncogene*, **1990**, *5*, 1653-1657. b) Boehm, T.; Mengle-Gaw, L.; Kees, U. R.; Spurr, N.; Lavenir, I.; Forster, A.; Rabbitts, T. H. *EMBO Journal*, **1989**, *8*, 2621-2631.

[29] a) Parkinson, A.; Hawken, M.; Hall, M.; Sanders, K. J.; Rodger, A. *Phys. Chem. Chem. Phys.*, **2000**, *2*, 5469-5478. b) Qu, X. G.; Trent, J. O.; Fokt, I.; Priebe, W.; Chaires, J. B. *Proc.*

*Natl. Acad. Sci. USA*, **2000**, *97*, 12032-12037. c) Xu, Y.; Zhang, Y. X.; Sugiyama, H.; Umano, T.; Osuga, H.; Tanaka, K. *J. Am. Chem. Soc.*, **2004**, *126*, 6566-6567. d) Behe, M. J.; Felsenfeld, G.; Szu, S. C.; Charney, E. *Biopolymers*, **1985**, *24*, 289-300. e). Loprete D. M; Hartman, K. A.; *Biochemistry,* **1993**, *32*, 4077-4082. f) Keller, P. B.; Loprete, D. M.; Hartman, K. A.; *J. Biomol. Struct. Dyn.,* **1988**, *5,* 1221-1229.

[30] Fuertes, M. A.; Cepeda, V.; Alonso, C.; Pérez, J. M., *Chem. Rev.*, **2006**, *106*, 2045-2064.

[31] a) Manzini, G.; Xodo, L. E.; Quadrifolglio, F. ; van Boom, J. H.; van der Marel, G. A. *J. Biomol. Struct. Dyn.,* **1987**, *5*, 651-668. b) Chen, F.-M. *Nucleic Acids Res.,* **1988**, *16*, 2269-2281.

[32] a) Tsuji, G.; Kawakami, K.; Sasaki, S. *Bioorg. Med. Chem.*, **2013**, *21*, 6063-6068. b) Dubois M.-A.; Grandbois, A.; Collins, S. K; Schmitzer, A. R. *J. Mol. Recognit.*, **2011**, *24*, 288-294. c) Li, L-Y.; Jia, H-N; Yu, H-J.; Du, K-J; Lin, Q-T.; Qiu, K-Q.; Chao, H.; Ji, L.-N *J. Inorg. Biochem.*, **2012**, *113*, 31-39. d) Medina-Molner, A.; Rohner, M.; Pandiarajan, D.; Spingler, B. *Dalton T.*, **2015**, *44*, 3664-3672. e) Medina-Molner, A.; Spingler, B. *Chem. Commun.*, **2012**, *48*, 1961-1963. f) Wu, Z.; Tian, T.; Yu, J.; Weng, X.; Liu, Y.; Zhou, X. *Angew. Chem., Int. Ed.*, **2011**, *50*, 11962-11967. h) Doi, I.; Tsuji, G.; Kawakami, K.; Nakagawa, O.; Taniguchi, Y.; Sasaki, S. *Chem. Eur. J.*, **2010**, *16*, 11993-11999.

[33] a) Rescifina, A.; Zagni, C.; Varrica, M. G.; Pistarà, V.; Corsaro, A.; *Eur. J. Med. Chem.,* **2014**, *74*, 95-115. b) Strekowski, L.; Wilson, B.; *Mutat. Res. Fund. Mol. Mech. Mut.*, **2007**, 623, 3-13. c) Sirajuddin, M.; Ali, S.; Badshah, A.; *J. Photochem. Photobiol. B,* **2013**, *124*, 1-19.

[34] a) Pasternack, R.F.; Gibbs, E.J.; Villafranca, J.J.; *Biochem.*, **1983**, 22, 2406-2014. b) D'Urso, A.; Fragalà, M. E.; Purrello, R. Non-Covalent Interactions of Porphyrinoids with Duplex DNA. In *Top. Heterocycl. Chem.*; Springer-Verlag Berlin Heidelberg 2013; Vol. 34, pp 139-174. d) Fiel, R.J.; Howard, J.C.; Datta Gupta, N.; *Nucleic Acids Res.,* **1979**, 6, 3093-3118.

[35] Balaz, M.; De Napoli, M.; Holmes, A. E.; Mammana, A.; Nakanishi, K.; Berova, N.; Purrello, R. *Angew. Chem. Int. Ed.*, **2005**, *44*, 4006–4009.

[36] a) D'Urso, A.; Holmes, A. E. ; Berova, N.; Balaz, M.; Purrello, R.; *Chem. Asian J.*, **2011**, 6, 3104 – 3109. b) D'Urso, A.; Choi, J. K.; Shabbir-Hussain, M.; Ngwa, F. N.; Lambousis, M. I.; Purrello, R.; Balaz, M.; *Biochem. Biophys. Res. Commun.*, **2010**, *397*, 329–332.

[37] Zhao, C.; Zhang, Y.; Wang, X.; Cao, J.; *J. Photoch. Photobio. A,* **2013**, 264, 41-47

[38] Biffi, G.; Tannahill, D.; McCafferty, J.; Balasubramanian, S.; Nat. Chem., **2013**, *5*, 182-186.

[39] a) Davis, J. T. *Angew. Chem., Int. Ed.*, **2004**, *43*, 668–698. b) Pu, F.; Wu, L.; Ran, X.; Ren, J.; Qu, X.; *Angew. Chem.* Int. Ed., **2015**, *54*, 892–896.

[40] Zahler, A. M.; Williamson, J. R.; Cech, T. R.; Prescott, D. M.; *Nature*, **1991**, *350*, 718-720.

[41] Seanger, W.; Principles of Nucleic Acid Structure, Springer-Verlag, **1988**, New York.; H. Yaku, T. Fujimoto, T. Murashima, D. Miyoshi and N. Sugimoto, Chem. Commun., 2012, 48, 6203.

[42] Huppert, J. L.; Balasubramanian, S.; *Nucleic Acids Res.*, **2007**, *35*, 406–413.

[43] Le, H. T.; Miller, M. C.; Buscaglia, R.; Dean, W. L.; Holt, P. A.; Chaires, J. B. ; Trent, J. O.; *Org. Biomol. Chem.*, **2012**, *10*, 9393 – 9404.

[44] Schaffitzel, C.; Berger, I. ; Postberg, J.; Hanes, J. ; Lipps H. J.; Plückthun, A.; *Proc. Natl. Acad. Sci. U. S. A.*, **2001**, *98*, 8572-8577.

[45] a) Zaug, A. J. ; Podell, E. R.; Cech, T. R. ; *Proc. Natl. Acad. Sci. U. S. A.*, **2005**, *102*, 10864-10869. b) Lei, M.; Zaug, A. J. ; Podell, E. R.; Cech, T. R.; *J. Biol. Chem.*, **2005**, *280*, 20449-20456.

[46] a) Hackett, J. A.; Feldser, D. M.; Greider, C. W.; *Cell,* **2001**, *106*, 275-286. b) Hayflick, L.; Moorhead, P. S.; *Exp. Cell. Res.,* **1961**, *25*, 585-621.

[47] a) Bearss, J.; Hurley, L. H.; Von Hoff, D. D.; *Oncogene*, **2000**, *19*, 6632-6641. b) Shay, W.; Bacchetti, S.; *Eur. J. Cancer*, **1997**, *33*, 787–791.

[48] a) Monchaud, D.; Teulade-Fichou, M.-P.; *Org. Biomol. Chem.,* **2008**, *6*, 627-636. b) Arola, A.; Vilar, R.; *Curr. Top. Med. Chem.*; **2008**, *8*, 1405-1415. c) Franceschin, M.; *Eur. J. Org. Chem.,* **2009**, *14*, 2225-2238 d) Neidle, S.; *Curr. Opin. Struct. Biol.,* **2009**, *19*, 239-250.

[49] a) Lavelle, F.; Riou, J.F.; Laoui, A.; Mailliet, P.; *Crit. Rev. Oncol. Hemat.,* **2000**, *34*, 111-126; b) Mergny, J.L.; Lacroix, L.; Teulade-Fichou, M.P.; Hounsou, C.; Guittat, L.; Hoarau, M.; Arimondo, P.B.; Vigneron, J.P.; Lehn, J.M.; Riou, J.F.; Garestier, T.; Hélène, C.; *Proc. Natl. Acad. Sci. USA.*, **2001**, *98*, 3062-3067; c) Zimmermann, S.; Martens, U.M.; *Cell. Mol. Life Sci.,* **2007**, *64*, 906-921; d) Olaussen, K.A.; Dubrana, K.; Domont, J.; Spano, J.P.; Sabatier, L.; Soria, J.C.; Crit. Rev.Oncol. Hemat, **2006**, *57,* 191-214. d) Siddiqui-Jain, A.; Grand, C. L.; Bearss, D. J.; Hurley, L. H.; *Proc. Natl. Acad. Sci. USA*, **2002**, 99, 11593-11598.

[50] a) Guo, Q.; Lu, M.; Churchill, M. E. A.; Tullius T. D.; Kallenbach, N. R.; *Biochemistry,* **1990**, 29, 10927-10934; b) Lu, M.; Guo, Q.; Kallenbach, N. R.; *Crit. Rev. Biochem. Mol. Biol.*, **1992**, *27*, 157-190.

[51] a) Pradines, V.; Pratviel, G.; *Angew. Chem. Int. Ed.*; **2013**, *52*, 2185-2188. b) Wheelhouse, R. T.; Sun, D.; Han, H.; Han, F. X.; Hurley, L. H.; *J. Am. Chem. Soc.*; **1998**, *120*, 3261-3262.

[52] Dixon, I. M.; Lopez, F.; Tejera, A. M.; Esteva, J-P.; Blasco, M. A.; Pratviel, G.; Maunier, B.; *J. Am. Chem. Soc.*, **2007**, *129*, 1502-1503.

[53] a) Zhang, J.; Wang, X-F.; Wang, P.; Pang, S-P.; Ai, X-C.; Zhang, J-P.; *Sci. China Ser. B:Chem.;* **2008**, *51*, 452. b) A.K. Jain, S.Bhattacharya, *Bioconjugate Chem.*, **2011**, *22*, 2355–

2368. c) Gai, W. ; Yang, Q.; Xiang, J.; Jiang, W.; Li, Q.; Sun, H.; Guan, A.; Shang, Q.; Zhang, H.; Y.Tang, *Nucleic Acids Res.*, **2013**, *41*, 2709–2722.

[54] a) Lubitz, I.; Borovok, N.; Kotlyar, A.; *Biochem.*; **2007**, *46*, 12925-12929. b) Hecht, C.; Friedrich, J.; Chang, T-C., *J. Phys. Chem. B,* **2004**, *108*, 10241-10244. c) Teixeira, S. C. M.; Thorpe, J. H.; Todd, A.K.; Powell, H. R.; Adams, A.; Wakelin, L. P. G.; Denny, W. A.; Cardin, C. J., *J. Mol. Biol.*, **2002**, 323, 167-171.

[55] a) Ren, J.; Chaires, J. B.; *Biochemistry*, **1999**, *38*, 16067- 16075; b) White, E. W. ; Tanious, F.; Ismail, M. A.; Reszka, A. P.; Neidle, S.; Boykin, D. W.; Wilson, W. D.; *Biophys. Chem.*, **2007,** *126*, 140-153; c) Stefan, L. ; Bertrand, B.; Richard, P.; Le Gendre, P.; Denat, F.; Picquet, M.; Monchaud, D. ; *ChemBioChem,* **2012**, *13*, 1905-1912.

[56] Parkinson, G. N.; Gosh, R. Neidle, S.; *Biochemistry*, **2007**, *46*, 2390-2397.

[57] Laguerre, A.; Chang, Y. ; Pirrotta, M.; Desbois, N.; Gros, C. P.; Lesniewskab, E.; Monchaud, D.; *Org. Biomol. Chem.,* **2015**, *13*, 7034-7039.

[58] D'Urso, A.; Mammana, A.; Balaz, M.; Holmes, A.E.; Berova, N.; Lauceri, R.; Purrello, R.; *J. Am. Chem. Soc.,* **2009**, *131*, 2046-2047.

[59] Garcia, G.; Sarrazy, V.; Sol, V.; Le Morvan, C.; Granet, R.; Alves, S.; Krausz, P.; *Bioorg. Med. Chem.*, **2009**, *17*, 767-776.

[60] a) Cullis, P. M.; Green, R. E; Merson-Davies, L.; Travis, N., *Chem. Biol.,* **1999**, 6, 717- 729. b) Wang, C.; Delcros, J.-G.; Biggerstaff, J.; Phanstiel, O., IV *J. Med. Chem.*, **2003**, 46, 2663-2671. c) Wang, C.; Delcros, J.-G.; Biggerstaff, J.; Phanstiel, O., IV *J. Med. Chem.*, **2003**, 46, 2672-2682.

[61] Dinesh, N. V. S.; Bhupathiraju, K.; Graça, M.; Vicente, H.; *Bioorg. Med. Chem.*, **2013**, *21*, 485-495.

[62] a) Geall, A. J.; Blagbrough, I. S.; *Tetrahedron,* **2000**, *56*, 2449-2460. b) Blagbrough I. S. ; Geall, A. J.; *Tetrahedron Lett.,* **1998**, 39, 439-442.

[63] Sunil, A.D.; Dutta, A.; U.S. Pat. Appl. Publ., **2007**, US2007/0197658A1.

[64] Brewer, A.; Siligardi, G.; Neylond, C.; Stulz, E.; *Org. Biomol. Chem.,* **2011**, *9,* 777-782.

[65] a) Balasubramanian, G.; Thanasekaran, P.; Rajagopal, S.; Kuppusamy, B.; Kachhadia, V.; Radhakrishnan, V.; Sivasudar, V.; Narayanan, S.; Bhonde, M.; Rajendran, P. PCT Int. Appl.,2010; WO2010/043953; c) Sharma, S.K.; Tandon, M. ; Lown, J. W.; *Eur. J. Org. Chem.,* **2000**, *11*, 2095-2103.

[66] a) Matile, S.; Berova, N.; Nakanishi, K.; Fleischhauer, J.; Woody, R. W.; *J. Am. Chem. Soc.,* **1996,** *118*, 5198-5206. b) Balaz, M.; Holmes, A. E.; Benedetti, M.; Proni, G.; Berova, N.; *Bioorg. Med. Chem.*, **2005**, *13*, 2413-2421.

[67] Rohand, T.; Dolusic, E.; Ngo, T. H.; Maes, W.; Dehaen, W.; *Arkivok*, **2007**, *10*, 307-324.

[68] Littler, B.J.; Miller, M. A.; Hung, C.H.; Wagner, R. W.; O'Shea, D. F. ; Boyle, P. D.; Lindsey, J. S.; *J. Org. Chem.,* **1999**, *64*, 1391 -1396.

[69] a) Geier III, G. R.; Littler,B. J.; Lindsey, J. S.; *J. Chem. Soc., Perkin Trans*, **2001**, *5*, 701-711. b) Arsenault, G. P.; Bullock, E.; McDonald, S. F.; *J. Am. Chem. Soc.,* **1960**, 82, 4384-4389. c) M. K., Panda, G. D., Sharma, K. R. J., Thomas, A. G., Coutsolelos; *J. Mat. Chem*., **2012**, 22, 8092-8102.

[70] Saha, S.; Johansson, E.; Flood, A. H.; Tseng, H.-R.; Zink, J. I.; Stoddart J. F.; *Chem. Eur. J.,* **2005**, *11*, 6846 – 6858.

[71] Eggenspiller, A.; Takai, A.; El-Khouly, M. E.; Ohkubo, K.; Gros, C. P.; Bernhard, C.; Goze, C. Denat, F.; Barbe, J.-M.; Fukuzumi, S.; *J. Phys. Chem. A.* **2012**, 116, 3889-3898.

[72] Brizet, B.; Bernhard, C.; Volkova, Y.; Rousselin, Y.; Harvey, P. D.; Goze, C.; Denat, F.; *Org. Biomol. Chem.,* **2013**, 11, 7729-7737.

[73] C. M. A. Gangemi, R. Randazzo, M. E. Fragala`, G. A. Tomaselli, F. P. Ballistreri, A. Pappalardo, R.M. Toscano, G. Trusso Sfrazzetto, R. Purrello, A. D'Urso, *New J. Chem*., 2015, **39**, 6722-6725.

[74] Lehn, J.-M.; *Angew. Chem., Int. Ed. Engl.*, **1988**, *27*, 89-112.

[75] a) D'Urso, A.; Fragalà, M. E.; Purrello, R.; *Chem. Commun.*, **2012**, *48*, 8165-8176; b) Guo, D.S.; Chen, K.; Zhang, H.-Q.; Liu, Y.; *Chem. –Asian J.,* **2009**, *4*, 436-445.

[76] a) Lehn, J.-M.; Supramolecular Chemistry Concepts and Perspective, VCH, Weinheim, Germany, 1995. b) Elemans, J. A. A. E.; Rowan, A. E.; Nolte, R. J. M.; *J. Mater. Chem.*, **2003**, *13*, 2661-2670. c) Smulders, M. M. J.; Schenning, A. P. H. J.; Meijer, E. W.; *J. Am. Chem. Soc.*, **2008**, *130*, 606-611. d) Destoop, I.; Xu, H.; Oliveras-Gonzalez, C.; Ghijsens, E.; Amabilino, D. B.; De Feyter, S.; *Chem. Commun.,* **2013**, *49*, 7477-7479. e) De Napoli, M.; Nardis, S.; Paolesse, R.; Vicente, M. G. H.; Lauceri, R.; Purrello, R.; *J. Am. Chem. Soc.,* **2004**, *126*, 5934-5935.

[77] a) Medforth, C. J.; Wang, Z.; Martin, K. E.; Song, Y.; Jacobsen, J. L.; Shelnutt, J. A.; *Chem. Commun.*, **2009**, *47*, 7261-7277; b) Drain, C. M.; Varotto, A.; Radivojevic, I.; *Chem. Rev.*, **2009**, *109*, 1630-1658.

[78] a) Akins, D. L.; Zhu, H.-R.; Guo, C.; *J. Phys. Chem.,* **1996**, *100*, 5420-5425. b) Micali, N.; Mallamace, F.; Romeo, A.; Purrello, R.; Monsu` Scolaro, L.; *J. Phys. Chem. B,* **2000**, *104*, 5897-5904. c) Koti, A. S. R.; Taneja, J.; Periasamy, N.; *Chem. Phys. Lett.,* **2003**, *375*, 171-176. d) Rubires, R.; Crusats, J. ; El-Hachemi, Z. ; Jaramillo, T.; Lopez, M.; Valls, E.; Farrera, J.-A.; Ribò, J. M.; *New J. Chem.,* **1999**, *23*, 189-198. e) Ohno, O.; Kaizu, Y.; Kobayashi, H.; *J. Chem. Phys.,* **1993**, 99, 4128-4139. f) Short, J. M.; Berriman, J. A.; Kübel, C.; El-Hachemi, Z.; Naubron, J.-V.; Balaban, T. S.; *ChemPhysChem.,* **2013**, *14*, 3209-3214.

[79] Romeo, A.; Castriciano, M. A.; Occhiuto, I.; Zagami, R.; Pasternack, R. F.; Monsù Scolaro, L.; *J. Am. Chem. Soc.*, **2014**, *136,* 40-43.

[80]a) Pasternack, R. F.; Collings, P. J.; *Science*, **1995**, *269*, 935-939. b) Collings, P. J.; Gibbs, E. J.; Starr, T. E.; Vafek, O.; Yee, C.; Pomerance, L. A.; Pasternack, R. F.; *J. Phys. Chem. B,* **1999**, *103*, 8474-8481.

[81] Imbert, T.; Guminski, Y.; Barret, J.-M.; Kruczynski, **2010,** WO2010020663 A1

[82]a) Chou, S.H.; Chin, K.H.; Wang, A.H.; *Trends Biochem Sci*, 2005, **30**, 231-234. b) Hotoda, H.; Koizumi, M.; Koga, R.; Kaneko, M.; Momota, K.; Ohmine, T.; Furukawa, H.; Agatsuma, T.; Nishigaki, T.; Sone, J.; *et al. J Med Chem*,**1998**, *41*, 3655-3663. c) Pedersen, E. B.; Nielsen, J. T.; Nielsen, C.; Filichev, V.V.; *Nucleic Acids Res.*, **2011**, *39*, 2470-2481.

[83] Pasternack, R. F.; *Chirality*, **2003**, *15*, 329-332. b) Parkinson, G. N.; Ghosh, R.; Neidle, S. *Biochemistry*, **2007**, *46*, 2390-2397

[84] Virgilio, A.; Varra, M. ; Scuotto, M.; Capuozzo, A.; Irace, C. ; Mayol, L.; Esposito, V.; Galeone, A.; *ChemBioChem*., **2014**, *15*, 652–655.

[85]a) Rachwal, P.A.; Fox K.R.; *Methods,* **2007**, *43,* 291-301. b) Mergny, J-L.; De Cian, A.; Ghelab, A.; Sacca, B.; Lacroix, L.; *Nucl. Acids Res.,* **2005,** *33,* 81-94.

[86]a) Sen, D.; Gilbert, W. *Biochemistry*, **1992**, *31*, 65-70; b) Krishnan-Ghosh, Y.; Liu, D.; Balasubramanian, S.; *J. Am. Chem. Soc.*, **2004**, *126*, 11009-11016. c) Kato, Y.; Ohyama, T.; Mita, H.; Yamamoto, Y.; *J. Am. Chem. Soc.*, **2005**, *127*, 9980-9981. d) Poon, K.; Macgregor, R. B. *Biopolymers*, **1998**, *45*, 427-434. e) Chen, F. M.; *Biophys. J. ,* **1997**, *73*, 348-356. f) Guo, Q.; Lu, M.; Kallenbach, N. R. *Biochemistry,* **1993**, *32*, 3596-3603. g) Marsh T. C.; Henderson, E.; *Biochemistry,* **1994**, *33*, 10718-10724.

[87] Borbone N.; Amato J.; Oliviero G.; D'Atri V.; Gabelica V.; De Pauw E.; Piccialli G.; Mayol L.; *Nucleic Acids Res.,* **2011**, **39**, 7848-7857. i) Oliviero G.; Piccialli G.; D'Atri V.; Borbone N.; Amato J.; Gabelica V.; D'Errico S.; Mayol L.; *Biochimie*, **2014**, 99, 119-128.

## Papers:

- C. M. A. Gangemi, A. Pappalardo, G. Trusso Sfrazzetto, *"Applications of supramolecular capsules derived from resorcin[4]arenes, calix[n]arenes and metallo-ligands: from biology to catalysis"* RSC Adv., **2015**, *5,* 51919-51933

- C. M. A. Gangemi, R. Randazzo, M. E. Fragalà, G. A. Tomaselli, F. P. Ballistreri, A. Pappalardo, R. M. Toscano, G. Trusso Sfrazzetto, R. Purrello, A. D'Urso *"Hierarchically controlled protonation/aggregation of a porphyrin–spermine derivative"*; New J. Chem., **2015**, *39,* 6722-6725.

- C. M. A. Gangemi, A. Pappalardo, G. Trusso Sfrazzetto *"Assembling of Supramolecular Capsules with Resorcin[4]arene and Calix[n]arene Building Blocks"*; Curr. Org. Chem. **2015**, *19,* 2281-2308.

## REVIEW

# Applications of supramolecular capsules derived from resorcin[4]arenes, calix[n]arenes and metallo-ligands: from biology to catalysis

Chiara M. A. Gangemi,[a] Andrea Pappalardo[*ab] and Giuseppe Trusso Sfrazzetto[*a]

Supramolecular architectures developed after the initial studies of Cram, Lehn and Pedersen have become structurally complex but fascinating. In this context, supramolecular capsules based on resorcin[4]arenes, calix[n]arenes or metal–ligand structures are dynamic assemblies inspired by biological systems. The reversible formation of these assemblies, combined with the possibility to modify their dimensions and shapes in the presence of a guest (concepts of reversibility and adaptivity) make them similar to biological macromolecules, such as proteins and enzymes. The small space inside a supramolecular capsule is characterized by different properties compared to the bulk solution. This review describes concrete applications of capsular supramolecular self-assemblies in the biomedical field, in catalysis and in material science.

## Introduction

The enhancements in the noncovalent synthesis of macrocyclic molecules have led to the development of supramolecular chemistry, a field that has attracted increasing attention in the last few decades.[1–7] Many important aspects have been investigated by supramolecular chemistry including molecular self-assembly,[8] folding,[9] molecular recognition, host–guest

[a]Department of Chemical Sciences, University of Catania, Viale A. Doria 6, 95125 Catania, Italy. E-mail: andrea.pappalardo@unict.it; giuseppe.trusso@unict.it
[b]I.N.S.T.M. UdR of Catania, Viale A. Doria 6, 95125 Catania, Italy

chemistry,[10] mechanically-interlocked molecular architectures,[11] and dynamic covalent chemistry.[2] Researchers have explored the host–guest interactions by employing several classical macrocyclic hosts, comprising crown ethers, cyclodextrins, calixarenes, cavitands and cucurbiturils. Since the pioneering studies of Donald J. Cram, Jean-Marie Lehn and Charles J. Pedersen (Nobel Prizes for Chemistry in 1987), researchers started to survey exciting areas of material chemistry and nanoscience, with many potential applications in polymer science,[12] organic photovoltaics,[13] as well as *in vitro* and *in vivo* biological imaging.[14] In particular, supramolecular chemistry built on weak and reversible non-covalent

*Chiara M. A. Gangemi was born in Catania, Italy in 1983. She received her master degree in Organic Chemistry in 2012, 110/110 cum laude. Actually, she is a PhD student in Chemical Science, at the University of Catania. She spent 6 months at Columbia University in the group of Prof. Nakanishi and Berova, where she studied the interactions of organic molecules with DNA. Her research is* focused on the synthesis and spectroscopic investigations of organic molecules (e.g. porphyrins derivatives) and their interactions with biomolecules.

*Andrea Pappalardo was born in Catania, Italy in 1974. After receiving his BS degree in Chemistry and Pharmaceutical Technologies from Catania University in 1999, he continued his PhD study in Catania under the supervision of Prof. Gaetano Tomaselli. In 2004 he had a Post-Doc position at the Department of Organic and Biological Chemistry of the University of Messina under the supervision* of Prof. Melchiorre Parisi. From 2007, he is a researcher at the Department of Chemical Science of the University of Catania. His research interest is focused on calixarene macrocycles and their use as receptors in the supramolecular host/guest chemistry.

interactions has emerged as a powerful and versatile strategy for the fabrication of new materials, due to its facile accessibility, extraordinary reversibility and adaptivity.

Supramolecular capsules represent a branch of these new materials: the inner space inside them shows unique properties, different from the bulk solution, making them new attractive and useful "supramolecular tools" in different fields. Cram's work was concerned with the formation of molecular capsules (carcerands or hemicarcerands), by covalently linking two resorcin[4]arene units.[15] The high stability of these capsules associated with the covalent nature of their formation, represent a main advantage. However, the low yielding syntheses and the difficulty to encapsulate/release a specific guest have compelled the researchers to develop a different strategy to obtain containers, able to self-assembly in solution, thus leading to the "supramolecular capsules". Hydrogen bonding is one of the strongest driving forces for a well-defined self-aggregation. Rebek *et al.* firstly reported on the formation of a supramolecular capsule, exploiting the formation of several hydrogen bonds between two bis-glycoluril derivatives.[16] A remarkable key aspect of the supramolecular strategy to generate a capsules is the dynamic nature of the self-assembly, which leads to the mutual modification of the molecular structures of host and guest.[17–21] As a consequence, physical–chemical properties of guests included inside a container are altered with respect to the free molecules in solution. For these reasons, supramolecular cages have found applications in different fields, as alternative route to the classic chemistry in solution.

A fundamental contribute to the study and characterization of supramolecular capsules was provided by the development of sophisticated NMR techniques, particularly diffusion NMR.[22–27] Diffusion ordered spectroscopy (DOSY)[28] was used to characterize and determine dimensions and structure of several host–guest systems,[29–39] organometallic complexes,[40–44] supramolecular systems,[45–49] and supramolecular polymers.[50–53] Recently, Cohen and Avram reported on the applications of the diffusion NMR to study cages and container molecules, describing some methodological and practical aspects.[54] In general, three

strategies for the self-assembly of supramolecular capsules are employed: hydrogen bonding, metal coordination and hydrophobic effect. The success of these approaches is warranted by the strong and highly directional non-covalent interactions that lead to the product formation. However, the inclusion of a guest inside the capsule facilitates the self-assembly process. As a result of the formation of supramolecular complex, encapsulated guests should diffuse as a single entity with the capsule, causing a clear change of the diffusion coefficient of the included guest. An additional significant contribute for the understanding of supramolecular systems was also given by Dynamic Light Scattering techniques (DLS).[55]

This review collects the applications of supramolecular capsules assembled from calixarenes, resorcinarenes and metallo-cage building blocks. In particular, the applications of these capsular supramolecular assemblies as nanoreactors for specific organic reactions are analyzed and discussed, without neglecting the applications of some hosts as new materials in AFM analysis and in the biomedical field as drug delivery systems.

# Biomedical applications

Calix[*n*]arenes and cavitands have been used for biomedical applications,[56] albeit they are macrocyclic hosts that show hydrophobic properties and poor water solubility. To overcome this drawback, researchers have spent considerable effort to prepare hydrophilic and water-soluble hosts. For example in calix[*n*]arene derivatives, sulfonation,[57] the introduction of carboxylic acid groups at the lower rim,[58] and the functionalization with polar groups at the upper rim[59] are the most common strategies to prepare water-soluble hosts. Furthermore, by using click chemistry, cationic, anionic, and non-ionic hydrophilic calixarene macrocycles have been efficiently synthesized.[60] In terms of biocompatibility, water-soluble calixarene derivatives exhibit low toxicity, and the *in vivo* dosage can reach up to 100 mg kg$^{-1}$ without any toxic effect in mice.[61] On the basis of these considerations, the formation of supramolecular structures capable of encapsulating guest molecules into the host cavities has become an attractive topic. Although biomedical applications of cyclodextrins are widely diffused,[62] no reports have so far appeared in the literature concerning concrete applications of cyclodextrin capsules. Furthermore, the binding constants of calix[*n*]arenes and resorcin[4]arene cavitands toward guest molecules are usually higher than those with cyclodextrins. In this context, Nau and co-workers reported on the possibility to encapsulate guest drugs into calixarene derivatives.[63]

Supramolecular approach has been used in drug delivery, mainly to solve the problems associated with the low solubility of hydrophobic drugs in aqueous solution, and the difficulty of anticancer drugs to penetrate the cancer cell membranes.[64–66] Chemical activity of drugs might be improved by their inclusion into the inner space of a capsule and, upon external stimuli, (*i.e.* thermal change, pH variation, or competitive binding) the encapsulated drugs can be released from the cavity, leading to prolonged therapeutic effects.[67]

*Giuseppe Trusso Sfrazzetto was born in Catania in 1981. He received his Master Degree in 2007 with 110/110 cum laude and PhD Degree in 2011 at the University of Catania working in the group of Prof. Gaetano Tomaselli on the synthesis and applications of new chiral cavitand hosts for the enantioselective molecular recognition of amino acid derivatives. He started his Post-Doc research on the design and synthesis of fluorescent sensors for bio-imaging. His research interests is focused on supramolecular chemistry, molecular recognition and fluorescent sensors for metal ions.*

## Drug delivery

Menon and co-workers prepared a *para*-sulfonatocalix[4]resorcinarene **1** able to encapsulate several drugs including the poorly soluble mycophenolate mofetil – an immunosuppressant drug used to prevent rejection in organ transplantation – by forming the 2 : 1 host–guest complexes (Fig. 1).[68–70]

Xiao reported on a new amphoteric calix[8]arene **2** that displays a pH-triggered drug releasing behavior (Scheme 1).[71] The upper rim of the calix[8]arene is functionalized with sulfonate groups, while the lower rim presents positive charges due to the presence of quaternary ammonium groups.

Hydrophobic model drug, ciprofloxacin, was included into the calixarene cavity at neutral pH, self-assembling into superstructures through electrostatic interactions between the upper and lower rims (Scheme 1). At higher or lower pH values, the capsule disassembles releasing the ciprofloxacin. Such pH-responsive drug delivery system shows great potential for future theranostic applications.

Very recently, Lippard *et al.* reported on an innovative application of the tetrahedral metal-cage **3** (M = Pt) as nanocontainer of a *cis*-platinum prodrug able to exhibit high cellular uptake (Fig. 2 and Scheme 2).[72]

The metallo-cage **3**, reported by Fujita in 1995, is one of the first capsular systems based on the metal coordination, assembled from four tridentate nitrogen-based ligands, six metal (palladium or platinum) ions, and six ethylendiamine ligands.[73] This cage can accommodate several guests, including tripeptides *via* a series of π–π and CH–π interactions and intramolecular guest–guest interactions.[74–77]



Scheme 1 Model of pH-triggered drug loading and releasing procedure developed by Xiao. Adapted from Y. Xue, Y. Guan, A. Zheng and H. Xiao, *Colloids Surf., B*, 2013, **101**, 55–60, with permission from Elsevier.

In particular, the delivery systems constituted by cytotoxic Pt(IV)-prodrugs and the hexanuclear Pt(II) cage **3** possess low toxicity, and an excellent cellular uptake due to the presence of twelve positive charges (Scheme 2).

To explicate anticancer activity, cisplatin must be released from this host–guest system upon reduction with ascorbic acid. The supramolecular cage **3** displays micromolar potency, comparable to cisplatin, against several cancer cell lines (lung carcinoma, ovarian carcinoma, and ovarian carcinoma).

## Applications in catalysis

### Metallo-cage capsules

The inclusion of two molecules within such a small volume leads to a high concentration of the guests and, consequently, to an increased likelihood of reaction between them. Fujita and co-workers used metallo-cage **3** to catalyze reactions of normally unreactive species, or to induce asymmetric reactions into the cavity of the cage, which possesses a chiral element attached to the metal center.[78] The enhancement of "activity" of the guests inside a similar supramolecular cage is demonstrated by the



Fig. 1 Drugs used by Menon and co-workers to form the host–guest complexes with *para*-sulfonatocalix[4]resorcinarene **1**.



Fig. 2 Tetrahedral cage **3**.

Scheme 2   Assembly of supramolecular complex **3** and release of Pt(ɪᴠ)-drug in presence of ascorbic acid. Adapted from Y. Zheng, K. Suntharalingam, T. C. Johnstone and S. J. Lippard, *Chem. Sci.*, 2015, **6**, 1189. Published by The Royal Society of Chemistry.

Diels–Alder reaction between the triphenylene and maleimides shown in Scheme 3,[79] and by the photocatalytic reaction between *o*-quinone and 4-(1-adamantyl)-toluene reported in Scheme 4.[80]

Ramamurthy *et al.* reported also on the reaction of photodimerization of *trans*-cinnamic acid esters inside the capsular system **3**, leading to both the monomeric *cis*-isomer, in considerably reduced yield with respect to the reaction in absence of the cage **3**, and dimeric products in a range of 21–63% yield.[81] The same research group has also examined how host **3** can afford the exclusive formation of *syn* head–head dimers of several coumarin derivatives, while in free aqueous solution *syn* head–head, *syn* head–tail, and anti head–head dimers are obtained.[82] Photodimerization was also investigated using acenaphthylene as guest.[83]

Raymond's group developed a new tetrahedral metallocage **4** consisting of a series of metal ions (*e.g.* Ga(ɪɪɪ), Al(ɪɪɪ), In(ɪɪɪ), Ti(ɪᴠ)



Scheme 4   Photocatalytic reaction catalyzed by supramolecular cage **3**.



Scheme 3   Dies–Alder reaction catalyzed by supramolecular cage **3**.



Scheme 5   Reactions of iridium complex inside the cage **4**.

Fig. 3  Raymond's tetrahedral capsule 4.

and Ge(IV)) and six catecholamide-based ligands (Fig. 3). The metal cation determines the kinetic stability of the capsule, which can include a wide range of guests.[84–87]

The gallium complex 4 is able to encapsulate in water media the (CpRuCl(cod)) (Cp = cylopentadiene, cod = 1,5-cyclooctadiene), a catalyst used for the formation of C–C bonds.[88] Raymond and co-workers studied the applications of tetrahedral metallocage 4 as nanoscale reactor. In particular, the reactivity of encapsulated mono-cationic half-sandwich iridium guests was analyzed (Scheme 5).[89] The reactivity of this complex into 4 shows highly specific size and shape selectivities in the C–H bond activation of aldehydes and ethers.

The catalytic properties of other metal transition complexes inside the supramolecular cage 4 were further examined. In particular, a series of bisphosphine rhodium–diene cations were encapsulated, affording the hydrated active catalyst (Rh(PMe$_3$)$_2$(D$_2$O)$_2$) 5 (Scheme 6).[90]

This host–guest complex [4·5] is stable within 12 hours, and catalyzes the isomerization of allylic substrates exhibiting substrate selectivity depending on the steric hindrance (Scheme 6): only prop-2-en-1-ol and its methyl ether were isomerized, while larger substrates are isomerized only by the non-encapsulated catalyst.

Also [RuCp(PMe$_3$)(MeCN)$_2$]$^+$ 6 was encapsulated by 4, leading to the supramolecular catalyst [4·6] capable to isomerize allylic alcohols to the corresponding aldehydes or ketones showing a similar substrates selectivity. In fact, the larger 1-phenylprop-2-en-1-ol does not react with the encapsulated catalyst (Scheme



Scheme 7  Isomerization of allylic substrates with supramolecular catalyst [4·6].



Scheme 8  Intramolecular cyclizations of an allen-ol and of an en-yne, catalyzed by supramolecular catalyst [4·(Au−P(CH$_3$)$_3$)].

7).[91] Notably, the supramolecular catalyst [4·6] shows a TON higher than those obtained for the non-encapsulated catalyst. The same supramolecular catalyst was used in association with enzymes, like esterases, lipases and alcohol dehydrogenases, to perform cascade reactions. In a one-pot reaction, the aliphatic alcohol was obtained starting from the corresponding allylic alcohol.[92] This result demonstrates that metal complex encapsulation can prevent the degradation of the catalyst.

Furthermore, supramolecular complex [4·(Au–P(CH$_3$)$_3$)], assembled by the tetrahedral cage 4 and monophosphine gold ion, is able to catalyze the intramolecular cyclization of an allen-ol and of an en-yne (Scheme 8).[93,94] The use of the bromide salt of the gold complex in the reaction with allen-ol results in an acceleration rate of eight times, and an increase of TON value of 67. Whereas, in the case of cyclization of en-yne, the formation of the product is selective only in the presence of the supramolecular catalyst, the tetrahedral cage around the gold complex controls the coordination sphere of the gold, acting as a phase transfer reagent, enhancing the reaction rate and tuning the regioselectivity of the reaction.

In addition, Raymond's group reported on the ability of cage 4 to catalyze the 3-aza Cope rearrangements showed in Scheme 9, observing an acceleration of the reaction into the range 5–854 times with respect to the normal conditions.[95,96]

Capsule 4 can also accommodate basic amines, phosphines, and (super basic) azaphosphatranes, since these guests are internalized in the protonated state.[97] This phenomenon is ascribed to a shift of the p$K_a$ values of the guests into the host



Scheme 6  Isomerization of allylic substrates with supramolecular catalyst [4·5].

**Scheme 9** The 3-aza Cope rearrangements inside the cage **4**.

**Scheme 10** Photochemical products obtained by the photolysis of stilbene derivatives in free solution and inside the OA capsule **7**.



**Fig. 4** Water soluble cavitands **7–10**. Adapted from Z. Laughrey and B. C. Gibb, *Chem. Soc. Rev.*, 2011, **40**, 363, with permission of The Royal Society of Chemistry.

environment. Searching on a plausible explanation of how host **4** can shift the p$K_a$ of an encapsulated guest, Raymond reported on an acid catalysis in basic solution. The formate esters, normally stable in neutral and basic conditions, were rapidly hydrolyzed at pH 11, with a catalytic amount of host **4**, showing an acceleration rate of *ca.* 650–890 times with respect to the non-catalyzed reaction.[98] Furthermore, cage **4** has been used as catalyst for the hydrolysis of acetals and ketals at pH 10, with an acceleration rate higher than 1000 times.[99,100]

**Supramolecular capsules assembled *via* hydrophobic effect**

In addition to metal coordination, also hydrophobic effect can induce the formation of supramolecular capsules, exploiting the desolvation of hydrophobic surfaces of the single molecules.[101,102] Few examples of self-assembled capsules driven by the hydrophobic effect have been described (compounds **7–10**, Fig. 4).[103–106]

The octa acid (OA) derivative **7** is the first example of water soluble deep cavitands based on a resorcin[4]arene scaffold, able to provide supramolecular dimeric capsules in presence of several guests.[107] Octa acid cavitands **7–10** differ from similar opened containers (such as micelles, open cavitands, cyclodextrins, cucurbiturils and Pd nanocages) because they are closed containers. Unlike micelles and open cavitands, the entire guest molecule is enveloped within a hydrophobic container. Interestingly, **7** can include propane and butane with a 2 : 2 stoichiometry from the gas phase and the aqueous phase.[108] Due to the high difference of binding constant values between propane and butane, capsule **7** can selectively extract butane from a propane/butane mixture. Ramamurthy and coworkers used the OA capsule **7** as chemical reactor in aqueous solution,[109] for the generation of singlet oxygen,[110,111]

the photodimerization of acenaphthylene,[112] and the photo-induced rearrangement of dibenzylketone.[109,113] Furthermore, this nano-capsule can affect the photochemistry of α-(*n*-alkyl) dibenzyl ketones depending on the dimension of the guests:[114] different kinds of packing motif lead to diverse photochemical behaviors. With the smallest guests a simple decarbonylation is observed, whereas, rearrangement products became prominent with the guests that possess bulkier alkyl groups. To clarify the mechanism of this rearrangement, optically pure α-deoxybenzoins were used as guests contained into OA capsule.[115] In addition, analysis with stilbene derivatives as substrate demonstrated that photophysical and photochemical properties of the encapsulated guests are strongly influenced by the formation of the capsule.[116,117] In particular, as shown in Scheme 10, the inner space of the capsule mainly leads to the formation of the trans pseudo-photostationary state of the stilbenes, which precludes the cyclization into the final product. The general ability of the capsule to control photodimerization reactions has been also studied with methyl cinnamates, *p*-methyl styrene, indene, and 4,4-dimethylcyclohex-2-enone.[118]

Ramamurthy reported on another example of how the inner space of octa acid capsule alters the outcome of some photochemical reactions. By photochemical reaction, cyclohexyl-phenyl ketones can afford Type I and Type II Norrish



**Scheme 11** Type I and Type II Norrish photochemical reaction of cyclohexyl-phenyl ketone.

Scheme 12   Reactivity of carbenes generated within the OA capsule.

products. Cyclobutanol, the Type II Norrish product, is formed in free solution of acetonitrile, while only the Type I products are obtained with octa acid capsule (Scheme 11).[119]

The inner space of octa acid container 7 can also influence the chemical behavior of incarcerated carbenes generated by photolysis of adamantanediazirines.[120]

In free solution, formation of alcohol and ketone was observed, while carbene generated into OA capsule furnished the azine derivative in high yield (Scheme 12).

Gibb has also reported that OA 7 controls the product distribution during photo-Fries rearrangement of naphthyl esters in water by restricting the mobility of primary singlet radical pair.[121] In normal condition, ester 11 in hexane upon irradiation affords eight products, while, after inclusion into the cavity of 7, only compound 12 is formed in 99% yield (Scheme 13).

The same *ortho*-rearrangement was observed with other ester compounds. The high selectivity was attributed to the limited movement of the guest inside the capsular assembly, and the rapid recombination of the radicals.

Gibb's group described the kinetic resolution of pairs of constitutional isomers of long chain esters using the octa acid capsule 7, that cannot be resolved since they react at similar rates.[122] Their strategy was based on the higher affinity of one guest to be preferentially encapsulated into the capsule 7, leaving the other molecule to undergo hydrolysis in solution. The resolution is determined by a competitive binding equilibrium in which the stronger binder mainly occupies the inner space of the capsule, whereas the weaker binding ester mostly resides in the bulk hydrolytic medium.

Supramolecular cage 7 has been used to carry out diastereoselective photoreactions. In particular, photocyclization of tropolone ethers and the oxa-di-π-methane rearrangement of cyclohexadienones within the capsule revealed good diastereoselectivities inside the capsule (17%) in comparison with the bulk solution (3%) (Scheme 14).[123]

A higher enhancement of diastereoselectivity inside the capsule 7 (73%) with respect to the free solution (4%) was obtained by Gibb and co-workers, while studying the photoelectrocyclization of pyridones.[124]

Recent studies highlighted how these water soluble capsules can act as active species in some photochemical reactions.[125] In fact, combining octa acid cavitand 7 with a resorcinol-capped octa acid cavitand (devoid of carboxylic groups at the upper rim and with four resorcinol groups at the lower rim), a heterocapsule was formed and able to act as triplet sensitizers towards aromatic guests, leading to different products depending on the type of excitation (Scheme 15).

Recently, Ramamurthy emphasized how the guests inside OA 7 capsule undergo a pre-orientation effect, because all parts of the enclosed guest molecules are exposed only to a hydrophobic inner space, thus excluding any orientation from hydrophobic–hydrophilic interactions, characteristics of other opened molecular reactors. This feature is particularly important in the regio- and stereo-selectivity of the reaction catalyzed inside the capsule.[126] In the photodimerization of indene in acetonitrile (Scheme 16), four possible reaction products are possible. However, in the presence of OA 7, anti-head–tail dimer is exclusively formed inside the cavity.

An interesting application of capsule 7 was recently reported by Ramamurthy's research group. They explored the feasibility of opening the capsule in order to release its contents in an aqueous media.[127] In particular, *p*-methoxyphenacyl esters were photo-hydrolized in *ca.* 90 minutes leading to the



Scheme 13   Photo-Fries reactions within the capsule 7.



Scheme 14   Diastereoselective rearrangement photoinduced inside 7.



Scheme 15   Photochemistry of benzonorbornadiene in solution.



Syn head-head        Syn head-tail

Anti head-head       Anti head-tail

Scheme 16   Photodimerization of indene and possible reaction products.

Scheme 17  Mechanism for the photorelease of carboxylic acids into OA capsule 7.



Scheme 18  Resorcin[4]arene 13 and relative hexameric capsule 14. Adapted with permission from *J. Am. Chem. Soc.*, 2008, **130**, 2344–2350. Copyright 2008 American Chemical Society.



Scheme 19  Wittig reaction catalyzed by hexameric capsule 14.



Scheme 20  Hydration of 4-phenyl-butyne catalyzed by hexameric capsule 14 containing gold complex.

corresponding acid derivatives as main products, and the disassembly of the capsule, hence releasing the products in solution. This system presents potential applications in the selective photo-release of molecules for pharmaceutical purposes.

Ramamurthy's group have explored the properties of the OA 7 as photo-reactor on the silica surface.[128] They demonstrated that the properties of photo-reactor are maintained in the heterogeneous system, and that capsular assemblies are stable on silica surface.

Very recently, Ramamurthy and co-workers reported on the photorelease of different carboxylic acids hosted into the OA capsule 7, after a rapid photo-Favorskii rearrangement of *p*-hydroxyphenacyl esters (Scheme 17).[129]

In particular, the acids were esterified with photoremovable protecting groups (PPGs), which upon irradiation >300 nm for 50 minutes undergo to the hydrolysis of the ester bonds. The absence of radical attack on the OA capsule 7 by *p*-hydroxyphenacyl ester photolysis is a clear evidence that the photorelease mechanism for OA encapsulated *p*-hydroxyphenacyl esters differs from that of the *p*-methoxyphenacyl esters.

## Hexameric supramolecular capsules

By the formation of multiple hydrogen bonds, in apolar solvents, the resorcin[4]arene 13 can self-assembly to the hexameric capsule 14 (Scheme 18), which was reported for the first time by Atwood in 1997.[130,131]

With an internal volume of *ca.* 1400 Å$^3$, hexameric capsule 14 represents one of the largest hydrogen-bonded molecular capsules. The presence of eight water molecules is essential to

the formation of this assembly.[132] The formation of the capsule and the encapsulation of different guests have been extensively investigated in solution.[133–142]

Tiefenbacher and Zhang reported on the first catalytic application of capsule 14: due to the value of p$K_a$ (approximately 5.5–6), the capsule acts as a strong Brønsted acid.[143] The authors explored the possibility to protonate a stabilized Wittig ylide inside the capsule 14 (Scheme 19). Ylide 15 is included inside the hexameric capsule 14, as confirmed by NMR spectroscopy. Even the addition of an excess of propanal (10 equiv.) did not produce any alkene product, although the uptake of propanal into the capsule is demonstrated by the appearance of characteristic signals in the NMR spectra.

With the larger Wittig ester 16, which is not able to fit the inner space of the capsule, the formation of alkene 17 occurred, indicating that the protonation of the Wittig ylide outside the capsule is reversible and does not prevent conversion to the alkene. Furthermore, the authors explored the potential use of the hexameric capsule as a selective enzyme-like catalyst, investigating the hydrolysis of acetals. They proved that a catalytic conversion is indeed possible with the capsule and that the reaction takes place inside the cavity. In addition, comparing the results obtained by using different substrates, they concluded that hexameric capsule 14, due to the stabilization of cationic intermediates and transition states in the hydrolysis process, enables reactions under mild conditions that are not possible in the solution phase.

Reek and co-workers used hexameric capsule 14 to include gold complexes, obtaining a supramolecular catalyst for the hydration of 4-phenyl-butyne (Scheme 20).[144]

**Scheme 21** Synthesis of amide derivatives encapsulated into hexameric capsule **14**.



**Fig. 5** Scheme of the single-molecule force spectroscopy experiment and typical force–distance curve. Reproduced with permission of T. Schröder, S. N. Sahu, D. Anselmetti and J. Mattay, *Isr. J. Chem.*, 2011, *51*, 725–742.

This reaction normally occurs with Markovnikov addition of water, leading to the corresponding ketone, or 1,2 dihydronaphtalene in absence of water. In the presence of hexameric capsule **14** the formation of aldehyde is observed, as well as the ketone and 1,2 dihydronaphtalene with different ratio respect to the normal reaction in solution. Afterward, the same research group evaluated the impact of steric hindrance and structural rigidity of the guests on the rate of reaction.[145] Interestingly, the reaction rates of the Au-catalyst in absence of the hexameric capsule show an opposite trend respect to the supramolecular catalyst.

Very recently, Scarso and co-workers reported on the use of **14** as a nanoreactor in the synthesis of several amide derivatives, differing for the length of substituent $R_1$ and $R_2$ (Scheme 21).[146]

The capsule acts as nanoreactor that imparts steric restriction to the encapsulated reagent. In particular, the capsule includes the cationic carbodiimide activator, and preferentially select the shorter acidic and amine reagents leading to the shorter amide derivatives. In absence of the supramolecular cage, scarce product selectivities were detected, thus demonstrating the active role of the hexameric capsule.

## AFM applications

AFM (Atomic Force Microscopy) is a powerful technique, applied mainly to the material science, with several applications in imaging and manipulation of the surfaces at nanoscale level.[147,148] The basic principle is based on a small force sensor (cantilever) and a piezo scan tube positioned onto the sample. The sharp tip of the cantilever, which has a radius of *ca.* 10 nm, interacts with the substrate *via* a wide range of weak forces, and this phenomenon leads to a minimal deflection of the sensor (Fig. 5). Furthermore, nano-scale objects can be precisely manipulated with the cantilever tip by applying very low forces (in the range of pN = 10–12 N), which is the magnitude of weak intermolecular bonds. A typical AFM-SMFS (AFM-single molecule force spectroscopy) mechano-chemistry experiment consists in the monitoring of interactions between two molecules, *i.e.* a host and a guest, using this technique. The tip of the cantilever is functionalized with a flexible linker (typically a PEG spacer) bearing one of the molecules object of the study. At the same time, the surface is covered by the other "partner" molecule.[149–151]

A precise determination of the forces between host and guest occurs, following the deflection on the cantilever. For this reason, the development of new synthetic receptors able to exploit non-covalent interactions using different weak forces is of primary importance in this technique. The first problem to solve is the covalent anchoring of host.

One of the most common strategies is the functionalization of the lower rim with sulfur-containing groups for its attachment onto a gold surface.[152,153] For SMFS experiments, Schindler's research group immobilized a tetra-(carboxyl)cavitand with a PEG linker to the cantilever, to add steric freedom to the system and allowing the complex formation to take place (Fig. 6).[154]

The spacer was further modified introducing a new type of linker *via* "click chemistry".[155] The first set of experiments were carried out using a tetra-(pyridyl)cavitand covalently attached on the gold surface, and a tetra-(carboxyl)cavitand immobilized on the cantilever. All measurements were carried out in *p*-xylene, which is encapsulated during the assembly process. Because of the high concentration of the tetra-(pyridyl)cavitand in the surface, multiple interactions due to simultaneous formation of several supramolecular capsules were detected.

Moreover, mixed self-assembled monolayers (SAMs) containing alkyl sulfides without functional groups can be used to realize a functionalized surface at low density, thus ensuring single-molecule recognition.[156,157] The force–distance curve observed contains only one distinct force jump, associated to



**Fig. 6** Tetra-(carboxyl)cavitand immobilized with a PEG linker to the cantilever.

the dissociation of a supramolecular capsule formed between the two hosts and p-xylene. Plotting the detected dissociation forces in a force histogram, a narrow distribution of forces characteristic for single-molecule force spectroscopy experiments was observed, allowing for a precise determination of the dissociation force, along with the mechanical stability and the dynamics of the dissociation process of this supramolecular capsule in a quantitative manner.

Recently, AFM measurements were employed to quantitatively evaluate drug–receptor interactions,[158] and drug–cell interactions[159] for analytical applications. Furthermore, these studies had lead to the development of new drugs with higher efficiency and also give fundamental insight into the mechanism of molecular level interactions in biological systems.

## Conclusion and outlook

In this review we detailed supramolecular capsules based on resorcin[4]arenes, calix[n]arenes and metal–ligands, having concrete applications in biomedical field, catalysis and material science. The inner space of these self-assembled structures represents a unique environment, with chemical–physical properties different with respect to the bulk solution. For this reason, one (or more) guest molecule encapsulated in this nanospace can undergo a different "chemistry" relative to the normal conditions. This feature is of particular interest in catalysis, leading to nanoreactors able to catalyze reactions not allowed in normal solution, or with the classical organometallic catalysts, or in biomedical applications, obtaining efficient drug-delivery system with potential theranostic properties. Although these supramolecular systems are known since '80, the research interest to design new and efficient (supra) molecular architectures, with practical uses in medicinal and materials, is still today an important and active field.

## Acknowledgements

## Notes and references

1 T. Ogoshi and T. Yamagishi, Pillararenes: versatile synthetic receptors for supramolecular chemistry, *Eur. J. Org. Chem.*, 2013, 2961–2975.

2 J.-M. Lehn, Perspectives in chemistry—aspects of adaptive chemistry and materials, *Angew. Chem., Int. Ed.*, 2015, **54**, 3276–3289.

3 L. F. Lindoy, K.-M. Park and S. S. Lee, Metals, macrocycles and molecular assemblies – macrocyclic complexes in metallo-supramolecular chemistry, *Chem. Soc. Rev.*, 2013, **42**, 1713–1727.

4 K. Kirkorian, A. Ellis and L. J. Twyman, Catalytic hyperbranched polymers as enzyme mimics; exploiting the principles of encapsulation and supramolecular chemistry, *Chem. Soc. Rev.*, 2012, **41**, 6138–6159.

5 *Supramolecular Chemistry: From Molecules to Nanomaterials*, ed. P. Gale and J. Steed, Wiley-VCH, Weinheim, 2012.

6 D. M. Bassani, Supramolecular chemistry: Molecular wires get connected, *Nature*, 2011, **480**, 326–327.

7 L. A. Joyce, S. H. Shabbir and E. V. Anslyn, The uses of supramolecular chemistry in synthetic methodology development: examples of anion and neutral molecular recognition, *Chem. Soc. Rev.*, 2010, **39**, 3621–3632.

8 S. I. Stupp and L. C. Palmer, Supramolecular chemistry and self-assembly in organic materials design, *Chem. Mater.*, 2014, **26**, 507–518.

9 R. C. Elgersma, T. Meijneke, R. de Jong, A. J. Brouwer, G. Posthuma, D. T. S. Rijkersa and R. M. J. Liskamp, Synthesis and structural investigations of N-alkylated β-peptidosulfonamide–peptide hybrids of the amyloidogenic amylin(20–29) sequence: implications of supramolecular folding for the design of peptide-based bionanomaterials, *Org. Biomol. Chem.*, 2006, **4**, 3587–3597.

10 E. Persch, O. Dumele and F. Diederich, Molecular recognition in chemical and biological systems, *Angew. Chem., Int. Ed.*, 2015, **54**, 3290–3327.

11 C. J. Bruns and J. F. Stoddart, Rotaxane-based molecular muscles, *Acc. Chem. Res.*, 2014, **47**, 2186–2199.

12 R. Dong, Y. Zhou, X. Huang, X. X. Zhu, Y. Lu and J. Shen, Functional supramolecular polymers for biomedical applications, *Adv. Mater.*, 2015, **27**, 498–526.

13 R. B. K. Siram, M. Stephen, F. Ali and S. Patil, Investigation of phase separation in bulk heterojunction solar cells via supramolecular chemistry, *J. Phys. Chem. C*, 2013, **117**, 9129–9136.

14 C. Bazzicalupi, A. Bianchi, E. Garcia-Espana and E. Delgado-Pinar, Metals in supramolecular chemistry, *Inorg. Chim. Acta*, 2014, **417**, 3–26.

15 D. J. Cram, S. Karbach, Y. H. Kim, L. Baczynskyj and G. W. Kalleymeyn, Shell closure of two cavitands forms carcerand complexes with components of the medium as permanent guests, *J. Am. Chem. Soc.*, 1985, **107**, 2575–2576.

16 R. Wyler, J. de Mendoza and J. Rebek Jr, A synthetic cavity assembles through self-complementary hydrogen bonds, *Angew. Chem., Int. Ed. Engl.*, 1993, **32**, 1699–1701.

17 M. Fujita, M. Tominaga, A. Hori and B. Therrien, Coordination assemblies from a Pd(II)-cornered square complex, *Acc. Chem. Res.*, 2005, **38**, 369–378.

18 M. Yoshizawa, J. K. Klosterman and M. Fujita, Functional molecular flasks: new properties and reactions within discrete, self-assembled hosts, *Angew. Chem., Int. Ed.*, 2009, **48**, 3418–3438.

19 B. H. Northrop, Y.-R. Zheng, K.-W. Chi and P. J. Stang, Self-organization in coordination-driven self-assembly, *Acc. Chem. Res.*, 2009, **42**, 1554–1563.

20 J. Rebek Jr, Molecular behavior in small spaces, *Acc. Chem. Res.*, 2009, **42**, 1660–1668.

21 B. Breiner, J. K. Clegg and J. R. Nitschke, Reactivity modulation in container molecules, *Chem. Sci.*, 2011, **2**, 51–56.

22 O. Mayzel and Y. Cohen, Diffusion coefficients of macrocyclic complexes using the PGSE NMR technique: determination of association constants, *J. Chem. Soc., Chem. Commun.*, 1994, 1901–1902.

23 O. Mayzel, O. Aleksiuk, F. Grynszpan, S. E. Biali and Y. Cohen, NMR diffusion coefficients of p-tert-butylcalix[n]arene systems, *J. Chem. Soc., Chem. Commun.*, 1995, 1183–1184.

24 O. Mayzel, A. Gafni and Y. Cohen, Water hydration of macrocyclic systems in organic solvents: an NMR diffusion and chemical shift study, *Chem. Commun.*, 1996, 911–912.

25 A. Gafni and Y. Cohen, Complexes of macrocycles with γ-cyclodextrin as deduced from NMR diffusion measurements, *J. Org. Chem.*, 1997, **62**, 120–125.

26 T. Parella, High-quality 1D spectra by implementing pulsed-field gradients as the coherence pathway selection procedure, *Magn. Reson. Chem.*, 1996, **34**, 329–347.

27 T. Parella, Pulsed field gradients: a new tool for routine NMR, *Magn. Reson. Chem.*, 1998, **36**, 467–495.

28 C. S. Johnson Jr, Diffusion ordered nuclear magnetic resonance spectroscopy: principles and applications, *Prog. Nucl. Magn. Reson. Spectrosc.*, 1999, **34**, 203–256.

29 A. Gafni, Y. Cohen, S. Palmer and D. Parker, Enantiomer discrimination using lipophilic cyclodextrins studied by electrode response, pulsed-gradient spin-echo (PGSE) NMR and relaxation rate measurements, *J. Chem. Soc., Perkin Trans. 2*, 1998, 19–24.

30 P. Timmerman, J. L. Weidmann, K. A. Jolliffe, L. J. Prins, D. N. Reinhoudt, S. Shinkai, L. Frish and Y. Cohen, NMR diffusion spectroscopy for the characterization of multicomponent hydrogen-bonded assemblies in solution, *J. Chem. Soc., Perkin Trans. 2*, 2000, 2077–2089.

31 L. Avram and Y. Cohen, Complexation in pseudorotaxanes based on α-cyclodextrin and different α,ω-diaminoalkanes by NMR diffusion measurements, *J. Org. Chem.*, 2002, **67**, 2639–2644.

32 L. Frish, F. Sansone, A. Casnati, R. Ungaro and Y. Cohen, Complexation of a peptidocalix[4]arene, a vancomycin mimic, with alanine-containing guests by NMR diffusion measurements, *J. Org. Chem.*, 2000, **65**, 5026–5030.

33 K. S. Cameron and L. Fielding, NMR diffusion spectroscopy as a measure of host–guest complex association constants and as a probe of complex size, *J. Org. Chem.*, 2001, **66**, 6891–6895.

34 L. Fielding, NMR methods for the determination of protein-ligand dissociation constants, *Curr. Top. Med. Chem.*, 2003, **3**, 39–53.

35 A. Pappalardo, M. E. Amato, F. P. Ballistreri, G. A. Tomaselli, R. M. Toscano and G. Trusso Sfrazzetto, Pair of diastereomeric uranyl salen cavitands displaying opposite enantiodiscrimination of α-amino acid ammonium salts, *J. Org. Chem.*, 2012, **77**, 7684–7687.

36 F. P. Ballistreri, A. Pappalardo, R. M. Toscano, G. A. Tomaselli and G. Trusso Sfrazzetto, Heteroditopic chiral uranyl–salen receptor for molecular recognition of amino acid ammonium salts, *Eur. J. Org. Chem.*, 2010, 3806–3810.

37 M. E. Amato, F. P. Ballistreri, S. D'Agata, A. Pappalardo, G. A. Tomaselli, R. M. Toscano and G. Trusso Sfrazzetto, Enantioselective molecular recognition of chiral organic

ammonium ions and amino acids using cavitand–salen-based receptors, *Eur. J. Org. Chem.*, 2011, 5674–5680.

38 A. Pappalardo, M. E. Amato, F. P. Ballistreri, A. Notti, G. A. Tomaselli, R. M. Toscano and G. Trusso Sfrazzetto, Synthesis and topology of [2 + 2] calix[4]resorcarene-based chiral cavitand-salen macrocycles, *Tetrahedron Lett.*, 2012, **53**, 7150–7153.

39 M. L. Giuffrida, E. Rizzarelli, G. A. Tomaselli, C. Satriano and G. Trusso Sfrazzetto, A novel fully water-soluble Cu(ı) probe for fluorescence live cell imaging, *Chem. Commun.*, 2014, 9835–9838.

40 P. S. Pregosin, P. G. A. Kumar and I. Fernandez, Pulsed gradient spin−echo (PGSE) diffusion and $^1$H,$^{19}$F heteronuclear overhauser spectroscopy (HOESY) NMR methods in inorganic and organometallic chemistry: something old and something new, *Chem. Rev.*, 2005, **105**, 2977–2998.

41 S. V. Kharlamov and S. V. Latypov, Modern diffusion-ordered NMR spectroscopy in chemistry of supramolecular systems: the scope and limitations, *Russ. Chem. Rev.*, 2010, **79**, 635–653.

42 A. Macchioni, G. Ciancaleoni, C. Zuccaccia and D. Zuccaccia, Determining accurate molecular sizes in solution through NMR diffusion spectroscopy, *Chem. Soc. Rev.*, 2008, **37**, 479–489.

43 G. M. Lombardo, A. L. Thompson, F. P. Ballistreri, A. Pappalardo, G. Trusso Sfrazzetto, G. A. Tomaselli, R. M. Toscano and F. Punzo, An integrated X-ray and molecular dynamics study of uranyl-salen structures and properties, *Dalton Trans.*, 2012, **41**, 1951–1960.

44 G. Brancatelli, A. Pappalardo, G. Trusso Sfrazzetto, A. Notti and S. Geremia, Mono- and dinuclear uranyl(VI) complexes with chiral Schiff base ligand, *Inorg. Chim. Acta*, 2013, **396**, 25–29.

45 L. Allouche, A. Marquis and J.-M. Lehn, Discrimination of metallosupramolecular architectures in solution by using diffusion ordered spectroscopy (DOSY) experiments: double-stranded helicates of different lengths, *Chem.–Eur. J.*, 2006, **12**, 7520–7525.

46 N. Giuseppone, J.-L. Schmitt, L. Allouche and J.-M. Lehn, DOSY NMR experiments as a tool for the analysis of constitutional and motional dynamic processes: implementation for the driven evolution of dynamic combinatorial libraries of helical strands, *Angew. Chem., Int. Ed.*, 2008, **47**, 2235–2239.

47 F. Gulion, R. Lauceri, L. Frish, T. Evan-Salem, Y. Cohen, R. De Zorzi, S. Geremia, L. Di Costanzo, L. Randaccio, D. Sciotto and R. Purrello, Noncovalent synthesis in aqueous solution and spectroscopic characterization of multi-porphyrin complexes, *Chem.–Eur. J.*, 2006, **12**, 2722–2729.

48 T. Evan-Salem, L. Frish, F. W. B. van Leeuwen, D. N. Reinhoudt, W. Verboom, M. S. Kaucher, J. T. Davis and Y. Cohen, Self-assembled ionophores from isoguanosine: diffusion NMR spectroscopy clarifies cation's and anion's influence on supramolecular structure, *Chem.–Eur. J.*, 2007, **13**, 1969–1977.

49 G. Gattuso, A. Notti, A. Pappalardo, S. Pappalardo and M. F. Parisi, A supramolecular amphiphile from a new water-soluble calix[5]arene and *n*-dodecylammonium chloride, *Tetrahedron Lett.*, 2013, **54**, 188–191.

50 S. Pappalardo, V. Villari, S. Slovak, Y. Cohen, G. Gattuso, A. Notti, A. Pappalardo, I. Pisagatti and M. F. Parisi, Counterion-dependent proton-driven self-assembly of linear supramolecular oligomers based on amino-calix[5] arene building blocks, *Chem.–Eur. J.*, 2007, **13**, 8164–8173.

51 J. M. Zayed, F. Biedermann, U. Rauwald and O. A. Scherman, Probing cucurbit[8]uril-mediated supramolecular block copolymer assembly in water using diffusion NMR, *Polym. Chem.*, 2010, **1**, 1434–1436.

52 Z. Zhang, Y. Luo, J. Chen, S. Dong, Y. Yu, Z. Ma and F. Huang, Formation of linear supramolecular polymers that is driven by C–H⋯π interactions in solution and in the solid state, *Angew. Chem., Int. Ed.*, 2011, **50**, 1397–1401.

53 A. Pappalardo, F. P. Ballistreri, G. Li Destri, P. G. Mineo, G. A. Tomaselli, R. M. Toscano and G. Trusso Sfrazzetto, Supramolecular polymer networks based on calix[5]arene tethered poly(p-phenyleneethynylene), *Macromolecules*, 2012, **45**, 7549–7556.

54 L. Avram and Y. Cohen, Diffusion NMR of molecular cages and capsules, *Chem. Soc. Rev.*, 2015, **44**, 586–602.

55 J. Braun, K. Renggli, J. Razumovitch and C. Vebert in *Dynamic Light Scattering in Supramolecular Materials Chemistry, Supramolecular Chemistry: From Molecules to Nanomaterials*, ed. P. Gale and J. Steed, Wiley-VCH, Weinheim, 2012.

56 D.-S. Gu and Y. Liu, Supramolecular chemistry of *p*-sulfonatocalix[n]arenes and its biological applications, *Acc. Chem. Res.*, 2014, **47**, 1925–1934.

57 F. Perret, A. N. Lazar and A. W. Coleman, Biochemistry of the para-sulfonato-calix[n]arenes, *Chem. Commun.*, 2006, 2425–2438.

58 A. Arduini, A. Pochini, S. Raverberi and R. Ungaro, *p-t*-Butyl-calix[4]arene tetracarboxylic acid. A water soluble calixarene in a cone structure, *J. Chem. Soc., Chem. Commun.*, 1984, 981–982.

59 P. Shahgaldian, A. W. Coleman and V. I. Kalchenko, NMR-studies on sugars and cyclanols - III on the configuration of C-methyl-branched sugars and cyclanols at the branching point, *Tetrahedron Lett.*, 2001, **42**, 577–582.

60 E.-H. Ryu and Y. Zhao, Efficient synthesis of water-soluble calixarenes using click chemistry, *Org. Lett.*, 2005, **7**, 1035–1037.

61 A. W. Coleman, S. Jebors, S. Cecillon, P. Perret, D. Garin, D. Marti-Battle and M. Moulin, Toxicity and biodistribution of para-sulfonato-calix[4]arene in mice, *New J. Chem.*, 2008, **32**, 780–782.

62 K. Yannakopoulou, Cationic cyclodextrins: cell penetrating agents and other diverse applications, *J. Drug Delivery Sci. Technol.*, 2012, **22**, 243–249.

63 I. Ghosh and W. M. Nau, The strategic use of supramolecular pK(a) shifts to enhance the bioavailability of drugs, *Adv. Drug Delivery Rev.*, 2012, **64**, 764–783.

64 C. J. Porter, N. L. Trevaskis and W. N. Charman, Lipids and lipid-based formulations: optimizing the oral delivery of lipophilic drugs, *Nat. Rev. Drug Discovery*, 2007, **6**, 231–248.

65 C. A. Lipinski, Drug-like properties and the causes of poor solubility and poor permeability, *J. Pharmacol. Toxicol. Methods*, 2000, **44**, 235–249.

66 R. Haag, Supramolecular drug-delivery systems based on polymeric core–shell architectures, *Angew. Chem., Int. Ed.*, 2004, **43**, 278–282.

67 F. Hirayama and K. Uekama, Cyclodextrin-based controlled drug release system, *Adv. Drug Delivery Rev.*, 1999, **36**, 125–141.

68 S. Menon, N. Modi, B. Mistry and K. Joshi, Improvement of some pharmaceutical properties of mycophenolate mofetil (MMF) by para sulphonatocalix[4]resorcinarene inclusion complex, *J. Inclusion Phenom. Mol. Recognit. Chem.*, 2011, **70**, 121–128.

69 S. Menon, B. Mistry, K. Joshi, N. Modi and D. Shashtri, Evaluation and solubility improvement of Carvedilol: PSC [n]arene inclusion complexes with acute oral toxicity studies, *J. Inclusion Phenom. Mol. Recognit. Chem.*, 2012, **73**, 295–303.

70 M. B. Patel, N. N. Valand, N. R. Modi, K. V. Joshi, U. Harikrishnan, S. P. Kumar, Y. T. Jasrai and S. Menon, Effect of p-sulfonatocalix[4]resorcinarene (PSC[4]R) on the solubility and bioavailability of a poorly water soluble drug lamotrigine (LMN) and computational investigation, *RSC Adv.*, 2013, **3**, 15971–15981.

71 Y. Xue, Y. Guan, A. Zheng and H. Xiao, Amphoteric calix[8] arene-based complex for pH-triggered drug delivery, *Colloids Surf., B*, 2013, **101**, 55–60.

72 Y.-R. Zheng, K. Suntharalingam, T. C. Johnstone and S. J. Lippard, Encapsulation of Pt(IV) prodrugs within a Pt(II) cage for drug delivery, *Chem. Sci.*, 2015, **6**, 1189–1193.

73 M. Fujita, D. Oguro, M. Mlyazawa, H. Oka, K. Yamaguchi and K. Ogura, Self-assembly of ten molecules into nanometre-sized organic host frameworks, *Nature*, 1995, **378**, 469–471.

74 S. Tashiro, M. Tominaga, M. Kawano, B. Therrien, T. Ozekiand and K. Fujita, Sequence-selective recognition of peptides within the single binding pocket of a self-assembled coordination cage, *J. Am. Chem. Soc.*, 2005, **127**, 4546–4547.

75 K. Nakabayashi, M. Kawano and M. Fujita, pH-Switchable through-space interaction of organic radicals within a self-assembled coordination cage, *Angew. Chem., Int. Ed.*, 2005, **44**, 5322–5325.

76 K. Nakabayashi, M. Kawano, T. Kato, K. Furukawa, S. I. Ohkoshi, T. Hozumi and M. Fujita, Manipulating the through-space spin–spin interaction of organic radicals in the confined cavity of a self-assembled cage, *Chem.–Asian J.*, 2007, **2**, 164–170.

77 K. Nakabayashi, Y. Ozaki, M. Kawano and M. Fujita, A self-assembled spin cage, *Angew. Chem., Int. Ed.*, 2008, **47**, 2046–2048.

78 Y. Nishioka, T. Yamaguchi, M. Kawano and M. Fujita, Asymmetric [2 + 2] olefin cross photoaddition in a self-

assembled host with remote chiral auxiliaries, *J. Am. Chem. Soc.*, 2008, **130**, 8160–8161.

79 Y. Nishioka, T. Yamaguchi, M. Yoshizawa and M. Fujita, Unusual [2+4] and [2+2] cycloadditions of arenes in the confined cavity of self-assembled cages, *J. Am. Chem. Soc.*, 2007, **129**, 7000–7001.

80 T. Yamaguchi and M. Fujita, Highly selective photomediated 1,4-radical addition to *o*-quinones controlled by a self-assembled cage, *Angew. Chem., Int. Ed.*, 2008, **47**, 2067–2069.

81 S. Karthikeyan and V. Ramamurthy, Templating photodimerization of trans-cinnamic acid esters with a water-soluble Pd nanocage, *J. Org. Chem.*, 2007, **72**, 452–458.

82 S. Karthikeyan and V. Ramamurthy, Templating Photodimerization of Coumarins within a Water-Soluble Nano Reaction Vessel, *J. Org. Chem.*, 2006, **71**, 6409–6413.

83 S. Karthikeyan and V. Ramamurthy, Self-assembled coordination cage as a reaction vessel: triplet sensitized [2+2] photodimerization of acenaphthylene, and [4+4] photodimerization of 9-anthraldehyde, *Tetrahedron Lett.*, 2005, **46**, 4495–4498.

84 A. V. Davis, D. Fiedler, F. E. Ziegler, A. Terpin and K. N. Raymond, Resolution of chiral, tetrahedral $M_4L_6$ metal−ligand hosts, *J. Am. Chem. Soc.*, 2007, **129**, 15354–15363.

85 S. M. Biros, R. G. Bergman and K. N. Raymond, The hydrophobic effect drives the recognition of hydrocarbons by an anionic metal−ligand cluster, *J. Am. Chem. Soc.*, 2007, **129**, 12094–12095.

86 C. J. Hastings, M. D. Pluth, S. M. Biros, R. G. Bergman and K. N. Raymond, Simultaneously bound guests and chiral recognition: a chiral self-assembled supramolecular host encapsulates hydrophobic guests, *Tetrahedron*, 2008, **64**, 8362–8367.

87 V. M. Dong, D. Fiedler, B. Carl, R. G. Bergman and K. N. Raymond, Molecular recognition and stabilization of iminium ions in water, *J. Am. Chem. Soc.*, 2006, **128**, 14464–14465.

88 D. Fiedler, R. G. Bergman and K. N. Raymond, Stabilization of reactive organometallic intermediates inside a self-assembled nanoscale host, *Angew. Chem., Int. Ed.*, 2006, **45**, 745–748.

89 D. H. Leung, R. G. Bergman and K. N. Raymond, Scope and mechanism of the C−H bond activation reactivity within a supramolecular host by an iridium guest: a stepwise ion pair guest dissociation mechanism, *J. Am. Chem. Soc.*, 2006, **128**, 9781–9797.

90 D. H. Leung, R. G. Bergman and K. N. Raymond, Highly selective supramolecular catalyzed allylic alcohol isomerization, *J. Am. Chem. Soc.*, 2007, **129**, 2746–2747.

91 C. J. Brown, G. M. Miller, M. W. Johnson, R. G. Bergman and K. N. Raymond, High-turnover supramolecular catalysis by a protected ruthenium(II) complex in aqueous solution, *J. Am. Chem. Soc.*, 2011, **133**, 11964–11966.

92 Z. J. Wang, K. N. Clary, R. G. Bergman, K. N. Raymond and F. D. Toste, A supramolecular approach to combining enzymatic and transition metal catalysis, *Nat. Chem.*, 2013, **5**, 100–105.

93 Z. J. Wang, C. J. Brown, R. G. Bergman, K. N. Raymond and F. D. Toste, Hydroalkoxylation catalyzed by a gold(I) complex encapsulated in a supramolecular host, *J. Am. Chem. Soc.*, 2011, **133**, 7358–7360.

94 W. M. Hart-Cooper, K. N. Clary, F. D. Toste, R. G. Bergman and K. N. Raymond, Selective monoterpene-like cyclization reactions achieved by water exclusion from reactive intermediates in a supramolecular catalyst, *J. Am. Chem. Soc.*, 2012, **134**, 17873–17876.

95 D. Fiedler, H. van Halbeek, R. G. Bergman and K. N. Raymond, Supramolecular catalysis of unimolecular rearrangements: substrate scope and mechanistic insights, *J. Am. Chem. Soc.*, 2006, **128**, 10240–10252.

96 C. J. Hastings, D. Fiedler, R. G. Bergman and K. N. Raymond, Aza cope rearrangement of propargyl enammonium cations catalyzed by a self-assembled "nanozyme", *J. Am. Chem. Soc.*, 2008, **130**, 10977–10983.

97 M. D. Pluth, R. G. Bergman and K. N. Raymond, Making amines strong bases: thermodynamic stabilization of protonated guests in a highly-charged supramolecular host, *J. Am. Chem. Soc.*, 2007, **129**, 11459–11467.

98 M. D. Pluth, R. G. Bergman and K. N. Raymond, Acid catalysis in basic solution: a supramolecular host promotes orthoformate hydrolysis, *Science*, 2007, **316**, 85–88.

99 M. D. Pluth, R. G. Bergman and K. N. Raymond, Catalytic deprotection of acetals in basic solution with a self-assembled supramolecular "nanozyme", *Angew. Chem., Int. Ed.*, 2007, **46**, 8587–8589.

100 M. D. Pluth, R. G. Bergman and K. N. Raymond, The acid hydrolysis mechanism of acetals catalyzed by a supramolecular assembly in basic solution, *J. Org. Chem.*, 2009, **74**, 58–63.

101 S. M. Biros and J. Rebek Jr, Structure and binding properties of water-soluble cavitands and capsules, *Chem. Soc. Rev.*, 2007, **36**, 93–104.

102 G. V. Oshovsky, D. N. Reinhoudt and W. Verboom, Supramolecular chemistry in water, *Angew. Chem., Int. Ed.*, 2007, **46**, 2366–2393.

103 C. L. D. Gibb and B. C. Gibb, Well-defined, organic nanoenvironments in water: the hydrophobic effect drives a capsular assembly, *J. Am. Chem. Soc.*, 2004, **126**, 11408–11409.

104 M. D. Giles, S. Liu, R. L. Emanuel, B. C. Gibb and S. M. Grayson, Dendronized supramolecular nanocapsules: pH independent, water-soluble, deep-cavity cavitands assemble *via* the hydrophobic effect, *J. Am. Chem. Soc.*, 2008, **130**, 14430–14431.

105 R. Kulasekharan and V. Ramamurthy, New water-soluble organic capsules are effective in controlling excited-state processes of guest molecules, *Org. Lett.*, 2011, **13**, 5092–5095.

106 H. Gan, C. J. Benjamin and B. C. Gibb, Nonmonotonic assembly of a deep-cavity cavitand, *J. Am. Chem. Soc.*, 2011, **133**, 4770–4773.

107 For a review on the complexation studies see: J. H. Jordan and B. C. Gibb, Molecular containers assembled through

the hydrophobic effect, *Chem. Soc. Rev.*, 2015, **44**, 547–585 and reference cited therein.

108 C. L. D. Gibb and B. C. Gibb, Templated assembly of water-soluble nano-capsules: inter-phase sequestration, storage, and separation of hydrocarbon gases, *J. Am. Chem. Soc.*, 2006, **128**, 16498–16499.

109 L. S. Kaanumalle, C. L. D. Gibb, B. C. Gibb and V. Ramamurthy, Controlling photochemistry with distinct hydrophobic nanoenvironments, *J. Am. Chem. Soc.*, 2004, **126**, 14366–14367.

110 A. Natarajan, L. S. Kaanumalle, S. Jockusch, C. L. D. Gibb, B. C. Gibb, N. J. Turro and V. Ramamurthy, Controlling photoreactions with restricted spaces and weak intermolecular forces: exquisite selectivity during oxidation of olefins by singlet oxygen, *J. Am. Chem. Soc.*, 2007, **129**, 4132–4133.

111 A. Greer, Organic chemistry: molecular cross-talk, *Nature*, 2007, **447**, 273–274.

112 L. S. Kaanumalle and V. Ramamurthy, Photodimerization of acenaphthylene within a nanocapsule: excited state lifetime dependent dimer selectivity, *Chem. Commun.*, 2007, 1062–1064.

113 A. K. Sundaresan and V. Ramamurthy, Consequences of controlling free space within a reaction cavity with a remote alkyl group: photochemistry of para-alkyl dibenzyl ketones within an organic capsule in water, *Photochem. Photobiol. Sci.*, 2008, **7**, 1555–1564.

114 C. L. D. Gibb, A. K. Sundaresan, V. Ramamurthy and B. C. Gibb, Templation of the excited-state chemistry of alpha-(n-alkyl) dibenzyl ketones: how guest packing within a nanoscale supramolecular capsule influences photochemistry, *J. Am. Chem. Soc.*, 2008, **130**, 4069–4080.

115 R. Kulasekharan, M. V. S. N. Maddipatla, A. Parthasarathy and V. Ramamurthy, Role of free space and conformational control on photoproduct selectivity of optically pure α-alkyldeoxybenzoins within a water-soluble organic capsule, *J. Org. Chem.*, 2013, **78**, 942–949.

116 A. Parthasarathy and V. Ramamurthy, Role of free space and weak interactions on geometric isomerization of stilbenes held in a molecular container, *Photochem. Photobiol. Sci.*, 2011, **10**, 1455–1462.

117 S. R. Samanta, A. Parthasarathy and V. Ramamurthy, Supramolecular control during triplet sensitized geometric isomerization of stilbenes encapsulated in a water soluble organic capsule, *Photochem. Photobiol. Sci.*, 2012, **11**, 1652–1660.

118 A. Parthasarathy, S. R. Samantha and V. Ramamurthy, Photodimerization of hydrophobic guests within a water-soluble nanocapsule, *Res. Chem. Intermed.*, 2013, **39**, 73–87.

119 R. Kulasekharan, R. Choudhury, R. Prabhakar and V. Ramamurthy, Restricted rotation due to the lack of free space within a capsule translates into product selectivity: photochemistry of cyclohexyl phenyl ketones within a water-soluble organic capsule, *Chem. Commun.*, 2011, **47**, 2841–2843.

120 S. Gupta, R. Choudhury, D. Krois, G. Wagner, U. H. Brinker and V. Ramamurthy, Photochemical generation and reactivity of carbenes within an organic cavitand and capsule: photochemistry of adamantanediazirines, *Org. Lett.*, 2011, **13**, 6074–6077.

121 L. S. Kaanumalle, C. L. D. Gibb, B. C. Gibb and V. Ramamurthy, Photo-Fries reaction in water made selective with a capsule, *Org. Biomol. Chem.*, 2007, **5**, 236–238.

122 S. Liu, H. Gan, A. T. Hermann, S. W. Rick and B. C. Gibb, Kinetic resolution of constitutional isomers controlled by selective protection inside a supramolecular nanocapsule, *Nat. Chem.*, 2010, **2**, 847–852.

123 A. K. Sundaresan, L. S. Kaanumalle, C. L. D. Gibb, B. G. Gibb and V. Ramamurthy, Chiral photochemistry within a confined space: diastereoselective photorearrangements of a tropolone and a cyclohexadienone included in a synthetic cavitand, *Dalton Trans.*, 2009, 4003–4011.

124 A. K. Sundaresan, C. L. D. Gibb, B. C. Gibb and V. Ramamurthy, Chiral photochemistry in a confined space: torquoselective photoelectrocyclization of pyridones within an achiral hydrophobic capsule, *Tetrahedron*, 2009, **65**, 7277–7288.

125 P. Jagadesan, B. Mondal, A. Parthasarathy, V. J. Rao and V. Ramamurthy, Photochemical reaction containers as energy and electron-transfer agents, *Org. Lett.*, 2013, **15**, 1326–1329.

126 V. Ramamurthy and A. Parthasarathy, Chemistry in restricted spaces: select photodimerizations in cages, cavities, and capsules, *Isr. J. Chem.*, 2011, **51**, 817–829.

127 N. Jayaraj, P. Jagadesan, S. R. Samanta, J. P. Da Silva and V. Ramamurthy, Release of guests from encapsulated masked hydrophobic precursors by a phototrigger, *Org. Lett.*, 2013, **15**, 4374–4377.

128 E. Ramasamy, N. Jayaraj, M. Porel and V. Ramamurthy, Excited state chemistry of capsular assemblies in aqueous solution and on silica surfaces, *Langmuir*, 2012, **28**, 10–16.

129 P. Jagadesan, J. P. Da Silva, R. S. Givens and V. Ramamurthy, Photorelease of incarcerated guests in aqueous solution with phenacyl esters as the trigger, *Org. Lett.*, 2015, **17**, 1276–1279.

130 L. R. MacGillivray and J. L. Atwood, A chiral spherical molecular assembly held together by 60 hydrogen bonds, *Nature*, 1997, **389**, 469–472.

131 S. Slovak, L. Avram and Y. Cohen, Encapsulated or not encapsulated? Mapping alcohol sites in hexameric capsules of resorcin[4]arenes in solution by diffusion NMR spectroscopy, *Angew. Chem., Int. Ed.*, 2010, **49**, 428–431.

132 L. Avram and Y. Cohen, The role of water molecules in a resorcinarene capsule as probed by NMR diffusion measurements, *Org. Lett.*, 2002, **4**, 4365–4368.

133 A. Shivanyuk and J. Rebek Jr, Reversible encapsulation by self-assembling resorcinarene subunits, *Proc. Natl. Acad. Sci. U. S. A.*, 2001, **98**, 7662–7665.

134 A. Shivanyuk and J. Rebek Jr, Reversible encapsulation of multiple, neutral guests in hexameric resorcinarene hosts, *Chem. Commun.*, 2001, 2424–2425.

135 L. C. Palmer, A. Shivanyuk, M. Yamanaka and J. Rebek Jr, Resorcinarene assemblies as synthetic receptors, *Chem. Commun.*, 2005, 857–858.

136 T. Evan-Salem, I. Baruch, L. Avram, Y. Cohen, L. C. Palmer and J. Rebek Jr, Resorcinarenes are hexameric capsules in solution, *Proc. Natl. Acad. Sci. U. S. A.*, 2006, **103**, 12296–12300.

137 L. Avram and Y. Cohen, Discrimination of guests encapsulation in large hexameric molecular capsules in solution: pyrogallol[4]arene *versus* resorcin[4]arene capsules, *J. Am. Chem. Soc.*, 2003, **125**, 16180–16181.

138 S. Slovak and Y. Cohen, In-out interactions of different guests with the hexameric capsule of resorcin[4]arene, *Supramol. Chem.*, 2010, **22**, 803–807.

139 I. E. Philip and A. E. Kaifer, Electrochemically driven formation of a molecular capsule around the ferrocenium ion, *J. Am. Chem. Soc.*, 2002, **124**, 12678–12679.

140 I. Philip and A. E. Kaifer, Noncovalent encapsulation of cobaltocenium inside resorcinarene molecular capsules, *J. Org. Chem.*, 2005, **70**, 1558–1564.

141 G. Bianchini, A. Scarso, G. L. Sorella and G. Strukul, Switching the activity of a photoredox catalyst through reversible encapsulation and release, *Chem. Commun.*, 2012, 12082–12084.

142 L. Avram, Y. Cohen and J. Rebek Jr, Recent advances in hydrogen-bonded hexameric encapsulation complexes, *Chem. Commun.*, 2011, 5368–5375.

143 Q. Zhang and K. Tiefenbacher, Hexameric resorcinarene capsule is a Bronsted acid: investigation and application to synthesis and catalysis, *J. Am. Chem. Soc.*, 2013, **135**, 16213–16219.

144 A. Cavarzan, A. Scarso, P. Sgarbossa, G. Strukul and J. N. H. Reek, Supramolecular control on chemo- and regioselectivity *via* encapsulation of (NHC)-Au catalyst within a hexameric self-assembled host, *J. Am. Chem. Soc.*, 2011, **133**, 2848–2851.

145 A. Cavarzan, J. N. H. Reek, F. Trentin, A. Scarso and G. Strukul, Substrate selectivity in the alkyne hydration mediated by NHC-Au(I) controlled by encapsulation of the catalyst within a hydrogen bonded hexameric host, *Catal. Sci. Technol.*, 2013, **3**, 2898–2901.

146 S. Giust, G. La Sorella, L. Sperni, G. Strukul and A. Scarso, Substrate selective amide coupling driven by encapsulation of a coupling agent within a self-assembled hexameric capsule, *Chem. Commun.*, 2015, **51**, 1658–1661.

147 B. Drake, C. B. Prater, A. L. Weisenhorn, S. A. Gould, T. R. Albrecht, C. F. Quate, D. S. Cannell, H. G. Hansma and P. K. Hansma, Imaging crystals, polymers, and processes in water with the atomic force microscope, *Science*, 1989, **243**, 1586–1589.

148 A. Janshoff, M. Neitzert, Y. Oberdcrfer and H. Fuchs, Force spectroscopy of molecular systems - single molecule spectroscopy of polymers and biomolecules, *Angew. Chem., Int. Ed.*, 2000, **39**, 3212–3237.

149 F. Kienberger, A. Ebner, H. J. Gruber and P. Hinterdorfer, Molecular recognition imaging and force spectroscopy of single biomolecules, *Acc. Chem. Res.*, 2006, **39**, 29–36.

150 D. J. Müller and Y. Dufrêne, Atomic force microscopy as a multifunctional molecular toolbox in nanobiotechnology, *Nat. Nanotechnol.*, 2008, **3**, 261–269.

151 M. Beyer and H. Clausen-Schaumann, Mechanochemistry: the mechanical activation of covalent bonds, *Chem. Rev.*, 2005, **105**, 2921–2948.

152 E. U. T. van Velzen, J. F. J. Engbersen, P. J. de Lange, J. W. G. Mahy and D. N. Reinhoudt, Self-assembled monolayers of resorcin[4]arene tetrasulfides on gold, *J. Am. Chem. Soc.*, 1995, **117**, 6853–6862.

153 H. Schcnherr, G. J. Vancso, B.-H. Huisman, F. C. J. M. van Veggel and D. N. Reinhoudt, Lattice structure of self-assembled monolayers of dialkyl sulfides and calix[4]arene sulfide adsorbates on Au(111) revealed by atomic force microscopy, *Langmuir*, 1999, **15**, 5541–5546.

154 P. Hinterdorfer, W. Baumgartner, H. J. Gruber, K. Schilcher and H. Schindler, Detection and localization of individual antibody-antigen recognition events by atomic force microscopy, *Proc. Natl. Acad. Sci. U. S. A.*, 1996, **93**, 3477–3481.

155 T. Schrcder, T. Geisler, B. Schnatwinkel, D. Anselmetti and J. Mattay, Single-molecule force spectroscopy of supramolecular heterodimeric capsules, *Phys. Chem. Chem. Phys.*, 2010, **12**, 10981–10987.

156 R. Eckel, R. Ros, B. Decker, J. Mattay and D. Anselmetti, Supramolecular chemistry at the single-molecule level, *Angew. Chem., Int. Ed.*, 2005, **44**, 484–488.

157 Y. Gilbert, M. Deghorain, L. Wang, B. Xu, P. D. Pollheimer, H. J. Gruber, J. Errington, B. Hallet, X. Haulot, C. Verbelen, P. Hols and Y. F. Dufrene, Single-molecule force spectroscopy and imaging of the vancomycin/D-Ala-D-Ala interaction, *Nano Lett.*, 2007, **7**, 796–801.

158 R. Prasanth, G. Nair and C. M. Girish, Enhanced endocytosis of nano-curcumin in nasopharyngeal cancer cells: An atomic force microscopy study, *Appl. Phys. Lett.*, 2011, **99**, 163706.

159 K. J. V. Vliet and P. Hinterdorfer, Probing drug-cell interactions, *Nano Today*, 2006, **1**, 18–25.

## LETTER

CrossMark
click for updates

# Hierarchically controlled protonation/aggregation of a porphyrin–spermine derivative†

Chiara Maria Antonietta Gangemi, Rosalba Randazzo, Maria Elena Fragalà, Gaetano Andrea Tomaselli, Francesco Paolo Ballistreri, Andrea Pappalardo, Rosa Maria Toscano, Giuseppe Trusso Sfrazzetto, Roberto Purrello* and Alessandro D'Urso*

We designed and synthesized a new porphyrin–spermine derivative that self-assembles under hierarchical control. Its aggregation processes depend on the protonation of both the spermine units and central core nitrogen atoms. Therefore, the time duration of pH titrations and/or the direct protonation of a specific site allow for choosing the desired aggregation state of the system.

Self-assembly processes in chemistry are important to obtain supramolecular architectures with the desired properties.[1] Yet, if not under control, they might just lead to a mixture of aggregated species with unknown molecular parameters (such as sequence, stoichiometry, tridimensional shape, *etc.*). In recent years, two different approaches have been exploited to drive the non-covalent syntheses. One of them foresees a step by step approach that, thanks to the hierarchical addition of rationally designed molecular units, leads to ordered supramolecular architectures with a given sequence, stoichiometry, dimensionality and chirality.[2] On the other hand, by exploiting the sergeant–soldier principle it is possible to drive the system to a predetermined desired final state without the need of proceeding by a step by step process.[3] The knowledge of the rules governing these processes allows us to control the self-assembly and to find the ways to synthesize more complex structures with specific functionality (molecular wires, switches, *etc.*).[4]

Water-soluble porphyrins are excellent building blocks for supramolecular architectures,[5] first of all because, in spite of their solubility in an aqueous environment, they maintain their hydrophobic character. This aspect is fundamental because it allows for easy driving of their self-assembly and/or specific aggregation with other similar molecules.[6] In addition, they have unique spectroscopic features (extremely high extinction coefficients, tunability of absorption maximum and emission intensity by simple introduction of specific metal ions in the core, *etc.*) and their periphery can be functionalized, allowing for choosing substituents that might impart designed properties to the new porphyrin derivatives.[7] The self-assembly of porphyrins can be simply modulated by pH as, for example, for a well-known class of *meso*-benzylsulfonated derivatives, which form H- and J-aggregates, following full core protonation at pH $\approx$ 2 ($pK_a \approx 4.8$).[8] In these examples, the only path for self-aggregation is the protonation of the porphyrin core.

In a previous paper we demonstrated that it is possible to open new self-aggregation pathways, independent from core protonation.[3e] This was feasible by designing the porphyrin derivative with specific *meso*-substituents whose partial protonation induces self-aggregation fostered by the formation of hydrogen bonds between protonated (H-bond donor) and unprotonated (H-bond acceptor) sites. In this case, the phosphonated groups present in the *meso*-tetrakis(4-phosphonatophenyl)porphine ($H_2TPPP$), in principle, were able to activate different aggregation processes. Yet, also in this case we observed only one protonation step responsible for porphyrin self-aggregation;[3d] the only difference with respect to the $H_2TPPS$ case is that the key aggregation step is not at the end of the thermodynamic protonation pathways but was shifted in the middle of it.

Inspired by this fascinating scenario, we decided to create a more complex supramolecular system by applying the concept of hierarchical self-assembly. The present work stems from previous data, but here we show that the nature of the side chains allows the title porphyrin to broaden the pH range for hierarchically controlled porphyrin self-aggregation processes. In particular, the introduction of four spermine units in the *meso*-positions of the porphyrin ring activates the self-aggregation processes, which in turn depend on both the protonation of the spermine units and central core nitrogen atoms.

Starting from this idea, we synthesized *meso*-tetrakis-(4-carboxyspermineyphenyl)porphine **1** ($H_2TCPPSpm4$, Scheme 1). Functionalization of *meso*-tetrakis(4-carboxyphenyl)porphine

*Department of Chemical Science, University of Catania, Viale A. Doria 6, 95125 Catania, Italy. E-mail: adurso@unict.it*

† Electronic supplementary information (ESI) available: All synthetic compounds were characterised by ¹H NMR, APT, 1D-zTOCSY, ESI-MS and UV-vis spectroscopy. See DOI: 10.1039/c5nj01264c

**Scheme 1** Schematic representation of the synthetic procedure to obtain **1** (H$_2$TCPPSpm4).

(TCPP) with four spermine arms was performed by a one-pot reaction using HATU as a carbonyl activating agent. In particular, reaction between TCPP and tri-BOC-Spm **2**, in the presence of HATU and DIPEA in DMF, leads to tetra(tri-BOC-spermine) derivative **3**, which after treatment with an excess of trifluoro-acetic acid in dichloromethane affords the desired product **1** (Scheme 1, all compounds were characterized by ^{1}H NMR, ^{13}C NMR-APT, and mass spectrometry, see ESI†).

The presence of four spermine arms, each having three protonable nitrogen atoms, permits us to obtain a different and pH-tunable number of positive charges. This property should allow for modulating the number of H-bond acceptor (deprotonated amine groups) and donor (protonated amines) sites, which are expected to promote the formation of self-assembled aggregates. In particular, most of the partially protonated forms of H$_2$TCPPSpm4 are potentially able to spontaneously self-assemble, prompted by the formation of H-bonds between protonated and unprotonated amino groups.

Four protonation processes are expected for H$_2$TCPPSpm4: one for the porphyrin inner core and three for each nitrogen atom of spermine arms.‡ The p$K_a$ values of spermine have been reported in the literature and range from 11 to 7.[9] However, the p$K_a$ values of the spermine arms linked to the porphyrin macrocycle are expected to be different from that of the free molecule. In fact, each protonation step of spermine causes an increase of four positive charges on the whole molecule, causing a shift towards lower pH values of the successive protonation steps. A comparison between the p$K_a$ values of inner core protonation of cationic porphyrins§ (close to **1**) and those of spermine strongly suggests that core protonation should follow amine protonation. As a consequence, it is possible to envisage that self-aggregation of the porphyrin having the protonated core should be highly disfavored by electrostatic repulsions.

In order to understand and manage the aggregation state of H$_2$TCPPSpm4, we have performed a thorough characterization of the protonation equilibria. It is worth recalling that aggregation processes can be analyzed not only under a thermodynamic point of view (*i.e.* interactions involved, binding constant value...), but also the kinetic aspects need special attention. It is known, in fact, that aggregation processes strongly depend on time and start after a very variable, initial time lag. This means that for our system, by using the classic continuous titration

procedure, it would be possible, in principle, to observe aggregation at pH quite different from that at which aggregate seeds are formed. It is worth underlining that, aggregation is a kind of sergeant-soldier process because it is self-catalytic and starts from low concentrations of specific seeds.

Therefore, the study of the protonation equilibria has to be performed very carefully, using due precautions. To avoid or minimize interference by aggregation in the determination of p$K_a$ values it is possible: (i) to prepare independent solutions at different pH values, or (ii) to perform a very fast continuous titration.

The advantage of the first method (independent solutions) is that self-aggregation is completely avoided because measurements are performed soon after porphyrin dissolution at a given pH; the main disadvantage is that a thorough experiment is very lengthy. The second approach (fast continuous titration) is faster than the first one, but can be affected by aggregation processes that have very short time lags. The third possibility combines the two previous ones and consists in overlapping few points of the independent solution experiment with a complete continuous titration curve, to catch and evaluate the possible differences.

Thus, we performed both type of titrations by monitoring the UV-vis spectrum of H$_2$TCPPSpm4 (2 μM) (see ESI†). The data are reported in Fig. 1 and show the Soret band intensity at 414 nm *vs.* the pH values. The comparison between the two types of titration shows some differences (*e.g.* absorption of the continuous titration is hypochromic by about 15% reporting some aggregation, but no pH shift of the curve) that in our opinion are not particularly relevant for the determination of the p$K_a$ values. Yet, they do evidence the formation of porphyrin assemblies.

From the continuous titrations it is possible to derive three different protonation processes: (i) the first one (p$K_{a1}$) is



**Fig. 1** Absorbance *vs.* pH, for the continuous titration at 414 nm (solid black square) and at 435 nm (red square), of 2 μM H$_2$TCPPSpm4 solution. Absorbance at 414 nm of the independent solution experiment at different pH is shown as comparison (open black circle). The inset shows a zoom of the UV titration at 435 nm in the 4.3–6.5 pH range.

observed at pH $\sim$ 8 and refers to the protonation of the most external spermine nitrogen atoms; (ii) at pH $\sim$ 5.8 the protonation of the second amino groups ($pK_{a2}$) of the spermine arms occurs; (iii) the third protonation process ($pK_{a3}$) at pH 3.5 corresponds to the porphyrin core protonation, confirmed by the color change of the solution from purple to green (typically observed for this process). The same $pK_a$ values have been obtained performing the fluorescence spectra of an $H_2TCPPSpm4$ solution by continuous titration methods (see ESI†).

Different from the $pK_a$ determined at pH 3.5 and 8, which are easy to detect owing to very drastic changes in absorbance, the intermediate $pK_a$ at pH 5.8 is not very evident and its presence will also be confirmed from the experiments presented hereafter.

In order to study the dependence of the self-assembly processes by pH, we performed UV-vis spectra of solutions prepared by dissolving $H_2TCPPSpm4$ at pH close to the $pK_a$ (5.0, 6.5 and 8.0) and under conditions in which $H_2TCPPSpm4$ is fully protonated (pH = 1.5). To take into account the kinetic aspect of aggregation we recorded the spectra immediately after porphyrin dissolution and 24 h later (Fig. 2).

As foreseen, inner core protonation of the macrocycles together with the positive charges in the side arms disfavors self-aggregation. This is well evidenced by the equality of the absorption spectra at pH 1.5 of the solutions just prepared ($t$ = 0 h) and after 24 h. On the contrary, for porphyrins left for 24 h in aqueous solutions at pH 8 it is possible to observe the spectroscopic changes typical of aggregation, i.e. hypochromicity and broadening of the Soret absorption band (Fig. 2). From these data it turns out that the protonation steps at pH = 8 of the porphyrin macrocycle are crucial for the formation of aggregates.

The data concerning the pH range between 5 and 6.5 are quite interesting and help in delineating the delicate dependence of the aggregation processes from the pH-tuned hydrogen bond scheme. In particular, at pH = 5 (that is under conditions in which pH $\approx$ $pK_{a2}$), after 24 h, $H_2TCPPSpm4$ is aggregated as shown by the hypochromic effect. On the contrary, the data of the solution obtained by dissolving $H_2TCPPSpm4$ at pH 6.5 show that the title porphyrin remains monomeric even after 24 h. This behavior does suggest that by skipping the protonation step at pH 5, it is

possible to avoid the aggregation of porphyrins and maintain it in the monomeric form up to pH 8 (Fig. 2). Even scanning electron microscopy experiments confirm the presence of porphyrin aggregates depending on pH (see ESI†). Working at pH 1.5 the substrate surface does not reveal the presence of any aggregates, while a more structured surface is well evident upon increasing the pH value. In particular, small spherical nanostructures are visible at pH 5, while at pH 8 a high density of particles is well detectable.

Further proofs of the relevance of the hierarchical sequence of protonation steps in the pH range 5–7 is given by fluorescence and RLS[10] measurements performed by monitoring: (i) a solution obtained by dissolving $H_2TCPPSpm4$ (2 μM) at pH 6.5, and (ii) a solution at pH 6.5 as a result of a continuous slow pH-metric titration. RLS data show the absence of the aggregated form of $H_2TCPPSpm4$ at pH 6.5, in the case of the solution prepared directly by dissolving the porphyrin at this pH. In contrast an enhancement of the signal is detected as a consequence of slow titration (Fig. 3)¶ that can be easily explained by recalling that this approach leads to porphyrin assemblies formed during the time of measurements. The presence of aggregates is also suggested by the quenching of the fluorescence in the solution obtained by slow titration, with respect to the fluorescence spectrum recorded for solution prepared directly at pH 6.5 (Fig. 3). This difference confirms the presence of an alternative, time dependent kinetic aggregation path that is "parallel" with respect to the thermodynamic protonation pathway and can be rationally chosen and designed.

In conclusion we demonstrate that it is possible to design and synthesize porphyrins that self-assemble under hierarchical control. The introduction of peripheral groups with protonation steps at pH higher than the inner core protonation process allows for discriminating between the two pathways – kinetic (aggregation) and thermodynamic (protonation) – to obtain the desired aggregation state in solution. For example, at pH 6.5 it is possible to have porphyrins in the monomeric or in the aggregated state by simply choosing the path to reach the wanted pH value.



Fig. 2 UV spectra of 2 μM $H_2TCPPSpm4$ solutions at different pH values (from left 1.5, 5, 6.5 and 8) as soon as prepared (black curves) and after 24 h (red curves).



Fig. 3 RLS (left) and fluorescence (right) spectra of 2 μM $H_2TCPPSpm4$ solutions at pH 6.5 prepared directly by dissolving at desired pH (black curve) and by slow pH titration (red curve).

In addition, these results show that the experiments with water-soluble but not hydrophilic molecules (like the title one) do begin with the preparation of the stock solution. This means that it is very relevant to know the self-assembly processes involved in such systems, in order to be able to obtain the desired final state. In the present case preparation of the stock solution a bit more acidic or basic with respect to 6.5 would lead to aggregated porphyrins and, consequently, to misleading results.

## Experimental

All stock solutions of $H_2TCPPSpm4$ were prepared by dissolving the solid in ultrapure water obtained from the Elga Purelab Flex system by Veolia, at pH 1 for HCl, in order to achieve concentrations ranging from $2 \times 10^{-4}$ M to $3 \times 10^{-4}$ M. The concentration of these stock solutions was checked by spectrophotometric experiments using $\varepsilon_{\lambda 435nm} = 338\,000$ $M^{-1}$ $cm^{-1}$ at pH = 1. To prepare independent solutions we dilute in several cuvettes at different pH, the right calculated amount of $H_2TCPPSpm4$ stock solution to obtain in each cuvette 2 μM working solutions. As soon as we prepared the solution, we recorded the spectrum. For the continuous titration we dilute the right calculated amount of stock solution to obtain 2 μM working solution, at pH 1. Then, for every 15 minutes, we added small amounts of NaOH to increase the pH of the solution and performed the spectrum. A JASCO V-560 UV-vis spectrophotometer equipped with a 1 cm path-length cell was used for the UV-vis measurements. For RLS and fluorescence data, a fluorolog FL-11 Jobin-Yvon Horiba was used.

SEM analysis of $H_2TCPPSpm4$ drop casted on silicon substrates at different pH has been performed by using a Field Emission Scanning Electron Microscope (Zeiss Supra 55VP). The EDS analysis has been performed using an Oxford x-Act 10 $mm^2$ SSD detector.

The NMR experiments were carried out at 27 °C on a Varian UNITY Inova 500 MHz spectrometer (¹H at 499.88 MHz, ¹³C-NMR at 125.7 MHz) equipped with pulse field gradient module (Z axis) and a tuneable 5 mm Varian inverse detection probe (ID-PFG). ESI mass spectra were acquired on an ES-MS Thermo-Finnigan LCQ-DECA using MeOH (positive ion mode). Positive MALDI-TOF mass spectra were acquired by a Voyager DE (PerSeptive Biosystem) equipped with a nitrogen laser (emission at 337 nm for 3 ns) and a flash AD converter (time base 2 ns).

## Acknowledgements

## Notes and references

‡ One of the protonation steps of spermine is, in fact, missing owing to the involvement of one of the terminal amino groups in the formation of amido groups, which serves to anchor the spermines to the carboxyphenyl peripheral groups of the porphyrin macrocycle (see Scheme 1).
§ The p$K_a$ of the nitrogen atoms is, in turn, modulated by the nature of the peripheral *meso* substituents: porphyrins functionalised with cationic groups show p$K_a$ values lower than those measured for the anionic substituted porphyrins. In the latter case porphyrins become zwitterionic, opening the way to very interesting and exploitable aggregation processes.
¶ The low intensity of the RLS signal, and the shape of the absorption band of the aggregated species, which shows only hypochromicity and slight broadening, indicate that self-aggregation of the studied porphyrin leads to formation of small aggregates.

1 J.-M. Lehn, *Angew. Chem., Int. Ed. Engl.*, 1988, **27**, 89.
2 (*a*) A. D'Urso, M. E. Fragalà and R. Purrello, *Chem. Commun.*, 2012, **48**, 8165; (*b*) D.-S. Guo, K. Chen, H.-Q. Zhang and Y. Liu, *Chem. – Asian J.*, 2009, **4**, 436.
3 (*a*) J.-M. Lehn, *Supramolecular Chemistry Concepts and Perspective*, VCH, Weinheim, Germany, 1995; (*b*) J. A. A. E. Elemans, A. E. Rowan and R. J. M. Nolte, *J. Mater. Chem.*, 2003, **13**, 2661; (*c*) M. M. J. Smulders, A. P. H. J. Schenning and E. W. Meijer, *J. Am. Chem. Soc.*, 2008, **130**, 606; (*d*) I. Destoop, H. Xu, C. Oliveras-Gonzalez, E. Ghijsens, D. B. Amabilino and S. De Feyter, *Chem. Commun.*, 2013, **49**, 7477; (*e*) M. De Napoli, S. Nardis, R. Paolesse, M. G. H. Vicente, R. Lauceri and R. Purrello, *J. Am. Chem. Soc.*, 2004, **126**, 5934.
4 (*a*) N. P. M. Huck, W. F. Jager, B. de Lange and B. L. Feringa, *Science*, 1996, **273**, 1686; (*b*) A. R. Pease, J. O. Jeppesen, J. F. Stoddart, Y. Luo, C. P. Collier and J. R. Heath, *Acc. Chem. Res.*, 2001, **34**, 433.
5 (*a*) C. J. Medforth, Z. Wang, K. E. Martin, Y. Song, J. L. Jacobsen and J. A. Shelnutt, *Chem. Commun.*, 2009, 7261; (*b*) C. M. Drain, A. Varotto and I. Radivojevic, *Chem. Rev.*, 2009, **109**, 1630.
6 A. D'Urso, P. Francesco Nicotra, G. Centonze, M. E. Fragalà, G. Gattuso, A. Notti, A. Pappalardo, S. Pappalardo, M. F. Parisi and R. Purrello, *Chem. Commun.*, 2012, **48**, 4046.
7 (*a*) T. E. O. Screen, K. B. Lawton, G. S. Wilson, N. Dolney, R. Ispasoiu, T. Goodson III, S. J. Martin, D. D. C. Bradley and H. L. Anderson, *J. Mater. Chem.*, 2001, **11**, 312; (*b*) B. Sun, Z. Ou, D. Meng, Y. Fang, Y. Song, W. Zhu, P. V. Solntsev, V. N. Nemykin and K. M. Kadish, *Inorg. Chem.*, 2014, **53**, 8600; (*c*) J. M. M. Rodrigues, A. S. F. Farinha, P. V. Muteto, S. M. Woranovicz-Barreira, F. A. A. Paz, M. G. P. M. S. Neves, J. A. S. Cavaleiro, A. C. Tomè, M. T. S. R. Gomes, J. L. Sessler and J. P. C. Tomè, *Chem. Commun.*, 2014, **50**, 1359; (*d*) J. S. Lindsey and D. F. Bocian, *Acc. Chem. Res.*, 2011, **44**, 638.
8 (*a*) D. L. Akins, H.-R. Zhu and C. Guo, *J. Phys. Chem.*, 1996, **100**, 5420; (*b*) N. Micali, F. Mallamace, A. Romeo, R. Purrello and L. Monsù Scolaro, *J. Phys. Chem. B*, 2000, **104**, 5897; (*c*) A. S. R. Koti, J. Taneja and N. Periasamy, *Chem. Phys. Lett.*, 2003, **375**, 171; (*d*) R. Rubires, J. Crusats, Z. El-Hachemi, T. Jaramillo, M. Lopez, E. Valls, J.-A. Farrera and J. M. Ribò, *New J. Chem.*, 1999, 189; (*e*) O. Ohno, Y. Kaizu and H. Kobayashi, *J. Chem. Phys.*, 1993, **99**, 4128; (*f*) J. M. Short, J. A. Berriman, C. Kübel, Z. El-Hachemi, J.-V. Naubron and T. S. Balaban, *ChemPhysChem*, 2013, **14**, 3209.
9 M. L. Antonelli, S. Balzano, V. Carunchio, E. Cernia and R. Purrello, *J. Inorg. Biochem.*, 1988, **32**, 153.
10 It is a spectroscopic technique suitable for detecting the formation of aggregates. For more details see: (*a*) R. F. Pasternack and P. J. Collings, *Science*, 1995, **269**, 935; (*b*) P. J. Collings, E. J. Gibbs, T. E. Starr, O. Vafek, C. Yee, L. A. Pomerance and R. F. Pasternack, *J. Phys. Chem. B*, 1999, **103**, 8474.

# Assembling of Supramolecular Capsules with Resorcin[4]arene and Calix[n]arene Building Blocks

Chiara M. A. Gangemi[a], Andrea Pappalardo[a,b,*] and Giuseppe Trusso Sfrazzetto[*a]

**Andrea Pappalardo**

**G. Trusso Sfrazzetto**

[a]*Department of Chemical Sciences, University of Catania, Viale A. Doria 6, 95125 Catania, Italy;* [b]*I.N.S.T.M. UdR of Catania, Viale A. Doria 6, 95125 Catania, Italy*

**Abstract:** Molecular capsules are containers endowed with isolated nanometer-sized cavities. In particular, supramolecular capsules −generated by exploiting hydrogen bonds, metal-coordination bonds and/or hydrophobic effects− represent an intriguing version of these fascinating molecules, and an impressive challenge for synthetic chemists. Resorcin[4]arene-based cavitands and conformationally preorganized calixarenes are two classes of receptors largely used as building blocks for the construction of these assemblies. This review focuses on the capsular self-assembly of suitably functionalized building blocks, analyzing from time to time the main driving force(s) involved for their formation.

## 1. INTRODUCTION

Covalently assembled molecular capsules, also called molecular containers or molecular cages, were firstly introduced by Cram and co-workers in 1985 [1]. Due to their ability to accommodate inside their internal cavity a wide range of guest molecules, "molecular capsules have attracted considerable attention for their potential applications, including stabilization and detection of reactive intermediates, encapsulation of precursors and labile chemical species, inclusion of drug molecules for drug delivery, and nanoreactors as well" [2]. In his early papers, Cram described the formation of molecular capsules (*i.e.*, carcerands Fig. **1**), through the covalent linking of two resorcin[4]arene subunits. The main advantage of this system is the high stability of the capsules, due to the presence of covalent bonds. "However, the low yield of the capsule formation and the strenuous conditions for the encapsulation and release of guests" led to the development of a new typology of molecular containers based on the concept of "self-assembly": the supramolecular capsules [2n]. Self-assembly is a thermodynamically favourable process in which a disordered system, constituted by two or more molecules, forms a more organized structure exploiting specific interactions among the starting molecules. By exploiting non-covalent interactions (*e.g.* hydrogen bonds and van der Waals forces) it was possible to achieve, under thermodynamic control and in high yields, self-assembled molecular containers which are able to include and release guest molecules under mild conditions.

Rebek reported for the first time the formation of a similar capsule, called "tennis-ball", by developing hydrogen bonds between two bis-glycoluril derivatives (Fig. **2**) [3]. One of the goals of the supramolecular approach to molecular containers is the "dynamic self-assembly", where host-guest interactions lead to a supramolecular assembly with unique properties, which are not shown by the individual components [2a, 2c, 2g, 2k, 2m, 4].



**Fig. (1).** Schematic representation of Cram's molecular capsules.

As a consequence, the physicochemical properties of a guest included inside a container are different from those of the free molecule in solution.



**Fig. (2).** Rebek's tennis ball structure. Bridgehead phenyl groups omitted for clarity. Reproduced in part from Ref. 3 with permission of The Royal Society of Chemistry.

*Address correspondence to this author at the Department of Chemical Science, University of Catania, 95125, Catania, Italy; Tel/Fax: ++39-095-7385010, ++39-095-580138; E-mails: andrea.pappalardo@unict.it; giuseppe.trusso@unict.it

**Scheme 1.** Formation of supramolecular capsule **2** in presence of pyrazine and DBU.

A recent definition states that a molecular container is *i*) qualitatively, a host that fully prevents "guest exchange, unless the container is opened; and *ii*) quantitatively, it envelops at least 83% of a smaller guest" [5]. When 100% of a guest is included, there is no possibility for the guest to be released outside the host, without the opening of the container. In general, molecular capsules are subject to an irreversible opening, thus their reuse is precluded. By contrast, supramolecular capsules can open and re-close in response to an external stimulus or to environmental factors.

Recognition studies were initially conducted in organic solvents for several reasons, mainly because of the low solubility of the hosts in water and the scarce control of non-covalent interactions in aqueous media. In fact, due to their low dielectric constants, organic media allow a facile control of weak forces. However recently, supramolecular chemists moved their interest to water [6]. In biological systems Nature exploits these non-covalent interactions to build up complex architectures, like DNA, RNA, membranes, proteins, cells, ensuring the life. The development of organic synthesis has allowed the realization of water-soluble synthetic hosts able to self-assembly in aqueous media exploiting hydrophobic effects, metal-ligand coordination and hydrogen bonds.

An important progress in the study and characterization of supramolecular capsules was made by the development of NMR techniques, specifically diffusion NMR [7]. Its success is due to the upgrade of NMR instruments "with reliable gradient systems for performing gradient enhanced multi-dimensional NMR" [8]. Therefore, diffusion ordered spectroscopy (DOSY) [9] is currently used to characterize and to determine dimension and structure of several host-guest systems [10], organometallic complexes [11], supramolecular systems [12], supramolecular polymers [13].

A recent review on the applications of the diffusion NMR to study cages and container molecules, describing "some methodological and practical aspects concerning diffusion NMR", was reported by Cohen and Avram [14].

This review looks over recent developments concerning resorcinarene and calixarene receptors that completely surround their guests leading to the formation of supramolecular capsules. We have tried to be exhaustive in this literature investigation, but in the omitted cases an attempt has been made to drive the reader to the most important publications and references.

## 2. RESORCIN[4]ARENE CAPSULES

Resorcin[4]arene cavitands are defined as synthetic organic compounds that form a hydrophobic cavity with an internal volume up to $350Å^3$, that can accommodate organic molecules [15]. The resorcin[4]arene scaffold can be easily functionalized at both lower and upper rims. In general, these molecules are synthesized starting from 1,3-dihydroxyphenol or 1,2,3-trihydroxyphenol and an appropriate aldehyde, which addresses the features of the lower rim [16], and the solubility of these compounds. Resorcin[4]arene units possess a hemispherical structure with a diameter of ca. 10 Å at the upper rim. The presence of eight hydroxyl groups on the upper rim paves the way to a wide functionalization range, thus obtaining deep cavities or the possibility to build supramolecular capsules exploiting hydrogen bonds [17a]. In non-polar solvents, "the roots of synthetic self-assemblies are dominated by two strategies: hydrogen bonding and metal coordination. These are powerful approaches that utilize relatively strong and highly directional non-covalent interactions to drive product formation" [17b].

### 2.1. Capsules *via* Hydrogen Bond

Despite the relatively weak energy of a single hydrogen bond (ca. 10-30 kJ/mol), the possibility to form a network of multiple interactions leads to the formation of thermodynamically stable capsules. Chapman and co-workers obtained supramolecular capsule **2** by treating tetrahydroxy cavitand **1** with pyrazine and 1,8-diazabicyclo[5.4.0]undec-7-ene (DBU) as a base (Scheme **1**) [18].

The establishment of a network of hydrogen bonds is responsible for the formation of cylindrical capsule **2** (Scheme **1**), possessing an internal cavity volume of ca. $425Å^3$ [19]. The inclusion of the guest in this confined space is associated with particular phenomena, for example amplification and acceleration of chemical reactions inside **2** [4g, 20]. The absence of conformational mobility of the guests inside the cavity leads to novel products, different by the normal reaction condition [21], and particular conformations, when the guests are alkanes that are longer than the length of the cavity", called "isomeric constellations" and "social isomers [20c, 22]. Rebek functionalized the resorcinarene platform with four pyrazine-2,3-dicarboxylic acid imide moieties, thus enlarging the volume of the inner-space of the cavitand (Fig. **3**) [23]. A recent review highlighted significant examples of photo switching and photophysics applied on resorcinarene-based cavitands and hydrogen-bonded capsule **4** based on cavitand **3** (Fig. **3**) [2b].

**Fig. (3).** Rebek's cylindrical capsule **4** . Adapted from *Chem. Soc. Rev.,* **2015**, *44*, 449**,** with permission of The Royal Society of Chemistry.

To increase the volume of the hydrophobic cavity, glycoluril moieties have been inserted between the imides of the capsule which subsequently allowed inclusion of larger guests (linear aliphatic hydrocarbons, from $C_{14}$ to $C_{19}$), (Scheme **2**) [17, 24]. The capsule **5** is formed in the presence of long hydrocarbons, and contains four molecules of glycoluril as linkers between the cavitand units (Fig. **4**).

By addition of an excess of glycoluril units, the NMR spectra of the guests longer than the capsule length, reveal signals suggestive of the formation of further expanded capsules, containing more glycoluril linkers, as shown in Figure (**4**) [25]. The length of these capsular systems depends on the size of the guests as well as on the number of glycoluril units present. The largest of them observed has a length and inner volume of ca. 35 Å and 980 Å$^3$, respectively.

Recently, Paek *et al.* reported on the synthesis of a new benzamido-iminocavitand **8**, which in the presence of 4-methylanisole,



**Scheme 2.** Formation of extended capsule **5** by insertion of glycoluril between the imides groups of the capsule **4**.



**Fig. (4).** Supramolecular capsules **5**, **6** and **7**, incorporating 4, 8 and 16 molecules of glycoluril, respectively.

**Scheme 3.** Formation of capsule **9** based on the benzamido-iminocavitand **8**.



**Scheme 4.** Tetracarboxylcavitands **10** and **13**, and their relative supramolecular capsules **11,12** and **14,15**, respectively.

forms capsule **9** exploiting multiple peptide-like hydrogen bonds (Scheme **3**) [26].

Kobayashi and co-workers developed an alternative resor-carene-based capsule, consisting of two different molecules of hemispherical cavitand and four molecules of a hydrogen-bonding linker [27]. Tetracarboxylcavitand **10**, in the presence of 2-amino-pyrimidine or tetrahydro-2-pyrimidinone, leads to capsules **11** and **12**, respectively, developing 16 hydrogen bonds (Scheme **4**). Capsule **11** can include 2,6-dimethoxynaphtalene and 2,6-dibromonaphtalene, while capsule **12** can include small guests, due to a shorter length of the cavity. The introduction of phenyl groups in compound **13** provides larger cavities (capsules **14** and **15**, Scheme **4**), that can include more sized guests, *e.g.* hexakis-(4-methoxyphenyl-benzene) and hexakis-(4-iodophenyl)benzene.

Unsymmetrical nanocapsules can be achieved using two different cavitands, containing appropriate donor and acceptor hydrogen-bonding groups, respectively.

Kobayashi and co-workers reported also on a heterodimeric capsule **17**, assembled by tetracarboxylcavitand **10** and tetra(3-pyridyl) cavitand **16** in the presence of 1,4-disubstituted benzenes (Scheme **5**) [28].

The presence of four phenolic groups on the upper rim of the resorcinarene scaffold leads to cavitand **18**, which combined with the pyridyl cavitand **19** forms, through four hydrogen bonds, the self-assembled capsule **20** (Scheme **6**) [29].

This capsule is assembled without specific guests. Capsule **20** can also include 1,4-diacetoxy-2,5-dialkoxybenzenes, "wherein the acetoxy groups are oriented toward both aromatic cavity ends, while the dialkoxy groups are located on the equatorial level of **20**" [30, 2n]. Recently, capsule **20** was used to include 1,4-bis-(1-propynyl)benzene derivatives, due to the ability of the supramolecular capsule to modify its cavity dimensions, depending on the guest size. Moreover, the inclusion of these guests increases the stability of hydrogen bonds [31].

**Scheme 5.** Assembly of heterodimeric capsule **17**.



**Scheme 6.** Self-assembly of heterodimeric capsule **20**.

**Scheme 7.** Self-assembly of heterodimeric capsule **22**.



**Scheme 8.** Rebek's homo and heterodimeric capsules.

Naruta and co-workers employed tetracarboxyl cavitands **10** and meso-tetra-(2-pyridyl)porphyrin **21**, to self-assemble a heterodimeric capsule **22** through the formation of quadruple hydrogen bond (Scheme **7**) [32]. Capsule **22** can encapsulate small molecules whose dimensions range from methane to cyclopentane.

Rebek and co-workers proposed an elegant example of dynamic heterodimeric capsule [33]. The resorcin[4]arene **23** easily forms hexameric capsule **24** (Scheme **8**), which was reported for the first time by Atwood in 1997 [34]. This capsule is spontaneously formed "in apolar solvents from six resorcin[4]arene units **23**, which are readily prepared in multigram quantities in a single step.

**Scheme 9.** Tetracyano cavitands and relative metal-induced capsules.

With an internal volume of approximately 1400 Å³ it also represents one of the largest hydrogen-bonded molecular capsules. In addition to the six resorcin[4]arene units, eight water molecules are essential and participate to its formation in solution" [35]. The construction of the capsule and the encapsulation of different guests have been extensively investigated in solution [36]. A recent review reported on the application of these hexameric capsules [4j]. Moreover, cavitands **3** with an appropriate guest affords hybrid capsule **25** and homomeric capsule **4** in chloroform solution. The dynamic nature of these hybrid systems was fully demonstrated through ¹H NMR titration of the capsular assembly with a specific guest able to change the nature of the heterodimeric capsule. Both homodimeric and heterodimeric capsules were assembled in the presence of para-substituited azobenzenes and 1,1'-dimethyl-ferrocene [37]. The formation of homodimeric capsule **4** is also

driven by the encapsulation of *trans*-azobenzene. After irradiation at 360 nm, *trans*-azobenzene is converted into the *cis*-isomer, breaking the capsule and releasing the corresponding monomers, which in the presence of ferrocenyl derivatives in solution, self-assembled into heterodimeric capsule **25**.

## 2.2. Capsules *via* Metal Coordination

Metal-ligand coordination possesses higher energy (ca. 100-300 kJ/mol) compared to the hydrogen bond, thus the presence on the upper rim of a cavitand having functional groups able to coordinate a metal ion leads to more stable supramolecular capsules. Tetracyanocavitands **26** and **29**, and relative metal-induced capsules **27-28** and **30-31** respectively, were synthesized by Dalcanale and co-workers (Scheme **9**) [38]. Supramolecular capsules **27** and **28** self-assembled from **26** in the presence of four equivalents of square-

**Scheme 10.** Tetrapicolyl cavitand **32** and relative metal-induced capsules **33** and **34**.



**Scheme 11.** Iminodiacetate cavitand **35** and relative metal-capsules.

planar metal complexes (Pd and Pt, respectively), including inside the cavity one molecule of triflate countercation. The presence of cyanophenyl groups in cavitands **29** allows the formation of capsules with a larger inner space able to include more sized guests.

Subsequently, Dalcanale developed an alternative synthetic approach to obtain metal-assisted cages. Bridging the corresponding resorcinarenes with an aldehyde bearing pycolil derivatives, the cavitand **32** and supramolecular capsules **33** and **34** were obtained (Scheme **10**) [39]. Computer simulations estimated an internal volume of the cavity of ca. 1800 Å³. The introduction of alkyl thioether groups at the lower rim of cavitand **32** permits to anchor the host on an Au(111) surface [40]. As observed in solution, the

cage "can be reversibly assembled and disassembled on the gold surface. AFM can distinguish between single cavitand and cage molecules of 2.5 nm and 5.8 nm heights, respectively" [40]. Furthermore, the presence of four terminal double bonds at the lower rim allows the grafting of cavitand **32** on silicon wafer [41]. The self-assembling of the capsule in presence of a complementary cavitand bearing a pyrenyl group at the lower rim was monitored by using AFM, XPS, and fluorescence spectroscopy. Hong and co-workers developed a similar approach, based on the interaction of pyridyl-substituted cavitands and Pd/Pt metal ions [42].

Harrison and co-workers synthesized a water-soluble cavitand **35**, bearing four imino-diacetate groups, able to form supramolecu-

**Scheme 12.** Terpyridyl cavitand **38** and relative hexameric capsule **39**. Reprinted from Ref. [45], with permission from Elsevier.



**Scheme 13.** Bipyridyl cavitand **40** and relative capsule **41**.

lar capsules in the presence of $Co^{2+}$ and $Fe^{2+}$ (Scheme **11**) [43], and evaluated their host properties towards several guest molecules (*e.g.*, hydrocarbons, aromatic compounds, alcohols, ketones and haloalkanes).

Beer *et al.* prepared high ordered supramolecular capsules using a cavitand with dithiocarbamate moieties on the upper rim [44]. The geometry and the stoichiometry of the final cage can be tuned by the fine selection of the metal ion: in particular, zinc and cadmium ions afford a trimeric assembly, able to include in the inner space $C_{60}$ and $C_{70}$ fullerenes, while with Ni, Cu, Pd and Au tetrameric capsules are formed.

The introduction of four terpyridyl groups on the resorcinarene scaffold leads to cavitand **38** that is able to form, in the presence of zinc ion, a hexameric capsule **39**, with a spherical cavity diameter of approximately 3 nm (Scheme **12**) [45].

Replacement of terpyridyl groups with 2-2′-bipyridyl moieties leads to cavitand **40**, which self-assembles into cage **41** by addition of silver cations (Scheme **13**) [46].

The capsule can include different aliphatic and aromatic guests. Recently, Haino and co-workers employed capsule **41** to recognize chiral guests: due to the dissymmetric nature of the capsule, in the presence of a chiral guest inside the cavity, a diastereomeric supramolecular complex is formed [47]. This phenomenon was detected by CD measurements, obtaining diastereomeric excesses in the range 50-98%. Notably, "the π-π stacking of the flat bipyridyl rings in cavitand **40** induces the formation of a dimeric capsule" in the solid state, which encapsulates two molecules of nitromethane [48]. Furthermore, supramolecular capsules based on cavitand **40** are assembled into chiral capsules with *P*- or *M*- helical structures.

The heterocavitand capsules belong to a particular class of supramolecular capsules formed in the presence of a specific metal ion, in which two different cavitands self-assemble into a cage. The main difficulty in the construction of this kind of architecture is the precise control of the simultaneous coordination of two or more cavitand ligands with a metal ion. In general, homocavitand capsules are more stable in solution, while heterocavitand capsules are

**Fig. (5).** Tetrahedral M$_6$L$_4$ coordination cage **42**.

rare [49]. Kobayashi and co-workers reported on hybrid capsules exploiting simultaneously hydrogen bond and metal-ligand coordination [50]. This construction presents the advantage to control the encapsulation process, since is possible to selectively break the hydrogen bonds (*i.e.*, by addition of DMSO), maintaining the capsular structure by the metal-ligand interactions.

### 2.3. Water-Soluble Capsules

In non-polar solvents the roots of synthetic self-assembled capsules are the formation of hydrogen bonds and the metal coordination, "two highly directional non-covalent interactions. In water, due to its polar nature and strong hydrogen bonding ability" [17b], these interactions undergo to a considerable reshaping. The hydrogen-bond-based capsules are less numerous than in organic media, and "metal ion coordination is by far the most common approach to self-assembly capsules in water" [17b]. Indeed, the fine tuning of the strength of coordination, for example by "increasing the electrostatic component of the coordination bond by a careful choice of metal and ligand, has allowed the formation of supramolecular capsules in water. However, there is a third approach to obtain molecular containers in water, using assembly motifs that are either enthalpically or entropically strong and directional: the hydrophobic effect" [51, 17b]. Recently, Gibb and co-workers published an overview of self-assembled capsules by exploiting this approach [5].

### 2.3.1. Capsules via Metal Coordination

One of the first capsular systems based on the metal-coordination was proposed by Fujita and co-workers. Tetrahedral M$_6$L$_4$ coordination cage **42** is assembled from four tridentate nitrogen-based ligands, six palladium ions, and six ethylendiamine ligands (Fig. **5**) [52]. This cage is able to recognize tripeptides *via* a

series of π-π and CH-π interactions, and intramolecular guest-guest interactions [53]. "Many of these non-covalent interactions involve charge transfer, and as a consequence, a color variation of the solutions in the presence of the guest is observed" [17b]. Host **42** is also able to accommodate aminic radicals providing a device responsive to the external environment due to its electronic configuration [54].

In addition, Fujita and co-workers used metallo-cage **42** to catalyze reactions with species normally unreactive, or to induce asymmetric reactions inside the cavity of a cage possessing a chiral element attached to the metal center [55]. Recently, Lippard reported on an innovative application of tetrahedral cage **42** (M = Pt) as nanocontainer of a *cis*-platinum prodrug able to exhibit high cellular uptake [56]. Ramamurthy and co-workers reported also on the photodimerization of *trans*-cinnamic acid esters into the capsular system **42** [57], producing the monomeric *cis*-isomer in considerably reduced yield with respect to the reaction in absence of the cage **42**, along with dimeric products in a range of 21-63% yield.

Fujita's group developed several water-soluble hosts **43a-f** shown in Figure (**6**). The dimensions of the inner space, and consequently the recognition properties of the corresponding cage, can be controlled by choosing appropriate ligands (X) and metal ions (M) [58]. Aromatic guests, azaporphines [59], as well as unsubstituted porphyrins [60] can be included using pyrazine as a linker, while two or more coronene molecules can be twisted using longer spacers. These examples demonstrate that hosts **43** are able to interact with guest molecules in a supramolecular stack.

While "mono-, di-, and tri-nucleotides are not involved in duplex formation in water because of hydrogen bonding with solvent molecules (largely prevaling over hydrogen bonding between nucleotides)" [17b], interestingly hosts **43a** and **43b** are able to form 1:2 supramolecular complexes in water with 5′-adenosine mono-

**Fig. (6).** Second generation of cages **43a-f** developed by Fujita (M = Pd or Pt).

phosphate, 5′-uridine monophosphate and di-nucleotide thymidylyl-(3′-5′)-2′-deoxyadenosine, respectively [61]. In these complexes, purine and pyrimidine bases are included within the host, while the sugar and phosphate moieties remain outside the cavity.

Fujita and co-workers employed host **43e**, having Cu(II), Pd(II) or Co(II) metal ions, to contain porphyrin-like guests [62]. "In particular, hetero-guest complexes formed between host **43e**, porphines, and azaporphines were isolated by mixing the components in the correct stoichiometry. Furthermore, they demonstrated that Ni(II) and Co(II) complexes contained within hosts **43a**, **43c** and **43e** exhibit a phenomenon of spin crossover, in which the transition metal ion switches between high and low spin states as a result of external stimuli [63]. Fujita's group has also demonstrated that this type of hosts can assemble in an interpenetrating manner to form assemblies composed of up to nine planar aromatic rings [64]. In fact, cage **43e** can assemble twenty-five components to form a complex containing three triphenylene guests sandwiched between four triazine panels.

In the first generation of hosts, the three pyridine nitrogen atoms are in *para* position with respect to the central triazine ring. Fujita's group has also developed the assembly of a second generation of tridentate triazine ligands, in which the pyridine nitrogens are in *meta* position to the triazine ring" (host **44**, Fig. **7**) [17b].



**Fig. (7).** Second generation of Fujita's water-soluble hosts.

The cavity of **44** is able to include a wide range of guests. Notably, **44** induces an enantiomeric enrichment (81%) by encapsulation of the homo-chiral pair of 1,1′-bi-2-naphthol (BINOL) from *n*-hexane solutions [65]. This is one of the most efficient examples of enantiomeric extraction so far reported in the literature [10i]. Host **44** has been also used in the recognition of polypeptides [66].

Raymond has developed a series of tetrahedral capsules **45** constituted by four metal ions (*e.g.* Ga(III), Al(III), In(III), Ti(IV) and Ge(IV)), and six catecholamide-based ligands (Fig. **8**). The nature of the metal cation tunes the kinetic parameters in the construction of the capsules. Due to the negative charge of this assembly, the preference is for hydrophobic and positively charged guests, although some neutral hydrophobic guests can be included. The hosts are inherently chiral, and only homochiral assemblies have been observed (ΔΔΔΔ and ΛΛΛΛ). In the synthesis, a racemate of the two enantiomers is obtained, however, with Ga(III), Al(III) and Fe(III) assemblies, these mixtures can be readily resolved using (*S*)-*N*-methyl-nicotinium as the chiral guest [67].



**Fig. (8).** Tetrahedral capsule **45** of Raymond's group.

These capsules are able to efficiently recognize a wide range of guests, including saturated organic compounds such as linear and cyclic alkanes, polycyclics, [68] benzene derivatives, diterpenoids [69] and iminium ions [70]. With respect to Fujita's capsules, these tetrahedral hosts possess a restricted access into the cavity. Computational studies have shown that the host must deform his structure, opening a face of the tetrahedron in order to encapsulate a guest [71]. Recent studies have demonstrated that, before encapsulation

into the cavity, a guest is stabilized outside the host *via* weak binding forces (*e.g.* Coulombic, cation-π and van der Waals interactions) [72]. The thermodynamic parameters of the recognition event between the Ga(III) complex of **45** and a series of mono-cationic iridium complexes were determined in water and methanol, using $^1$H NMR experiments at different temperatures [73]. The significant differences observed between water and methanol suggest that solvent reorganization upon guest complexation, rather than specific host-guest interactions, play a dominant role in these binding events. In addition, the possibility to partially include ruthenocenyl guests having different length inside **45**-Ga(III) complex was also examined [74].

Gallium complex **45** is able to encapsulate in water media CpRuCl(cod) (Cp = cylopentadiene, cod = 1,5-cyclooctadiene), a catalyst used for the formation of C-C bond [75]. $^1$H NMR spectra show a duplication of all the signals upon inclusion of a chiral guest (CpRu(cis-1,3,7-octatriene)) inside the tetrahedral capsule, due to the presence of **45** in a racemic form. Capsule **45** can also recognize basic amines, phosphines, and (super basic) azaphosphatranes, since these guests are internalized in the protonated state [76]. This phenomenon is to ascribed to a shift of the p$K_a$ values of the guests into the host environment. Raymond and co-workers also investigated the modification of physicochemical properties of a guest into a confined space. They showed how encapsulation effects the rotation barrier of amide bonds into Ga(III) complex of **45**, demonstrating that the hydrophobic cavity stabilizes the (hydrophobic) transition state of rotation [77]. Moreover, Raymond's group studied the applications of tetrahedral metallo-cage **45** as nanoscale reactor. In particular, reactivity of a series of encapsulated mono-cationic half-sandwich iridium guests was analyzed. In addition, the catalytic properties of other metal transition complexes inside the supramolecular cage **45** were tested [78].



**Fig. (9).** Tetra-anionic capsule **46** reported by Nitschke.

Nitschke proposed an alternative tetrahedral complex able to act as a supramolecular capsule. Host **46** is a tetra-anionic host (Fig. **9**), easy to synthesize and able to include hydrophobic guests such as cyclopentane and cyclohexane [79]. Capsule **46** can be disassembled irreversibly or reversibly by the addition of *tris*(2-ethylamino)amine or *p*-toluenesulfonic acid, respectively. Interestingly, **46** can bind and stabilize white phosphorus (P$_4$), both in water solution and in the solid state [80].

Very recently, Telkki *et al.* reported on the ability of metallo-cage **46** (M = Fe) to include xenon gas in water [81]. In detail, when 4.9 bar of Xe gas atmosphere was added to the solution, $^{129}$Xe NMR spectrum shows the encapsulation of Xe due to hydrophobic effects, with a binding constant of 16 M$^{-1}$. Furthermore, exchange spectroscopy spectrum (EXSY) reveals that the Xe in **46** undergoes

chemical exchange with the Xe in the bulk solution, with a rate constant of 10 Hz. The potential applications of this system might include recognition of rare gases and, due to the wide use of this element as inert probe in magnetic resonance imaging, in $^{129}$Xe NMR-based biosensing.

Aoki proposed an alternative concept of metal-induced supramolecular capsule, formed by trimeric Zn$^{2+}$-cyclen complex and the trianion of trithiocyanuric acid assembled in a 4:4 ratio to form a cuboctahedral supramolecular complex [82]. They evaluated the molecular recognition properties in water solution of linear (C$_1$-C$_{12}$) and cyclic hydrocarbons. This molecular cage is able to recognize guests larger than the inner volume of the capsule (160 Å$^3$), suggesting that the internal space of the host is flexible. The authors also demonstrated the capacity of this host to store propane and *n*-butane both in aqueous solution and in the solid state.



**Fig. (10).** Water soluble cavitands **47** and **48** reported by Gibb and co-workers. Adapted from *Chem. Soc. Rev.,* 2011, *40*, 363 with permission of The Royal Society of Chemistry.

### 2.3.2. Capsules via Hydrophobic Effect

In addition to metal coordination, also hydrophobic effect can drive the formation of supramolecular capsules, determined by the desolvation of hydrophobic surfaces of the single molecules [2d, 6]. The synthesis of macrocyclic hosts able to form supramolecular capsules by hydrophobic effect is more expensive with respect to the metal coordination complexes. As a consequence, few examples of self-assembled capsules driven by the hydrophobic effect have been reported in the Literature. The first example reported by Gibb and co-workers is a water soluble deep cavitand based on a resorcin[4]arene scaffold **47**, bearing eight hydrophilic functionalities (carboxylic acids), both on the upper and lower rim (Fig. **10**) [51, 83]. The "octa-acid" cavitand **47** is self-assembled in water in presence of several guests [5]. Notably, **47** can include propane and butane with a 2:2 stoichiometry from the gas phase and into the aqueous phase [84]. Since the binding constant for propane is one order of magnitude weaker than butane, capsule **47** can selectively extract butane from a propane/butane mixture.

Very recently, Gibb and Sullivan reported on the binding between **47** and some constitutional isomers of hexane and chloropentane by extensive NMR studies [85]. Octa-acid **47** exhibits a preference for branched and spherical guests rather than highly flexible

and unbranched derivatives, demonstrating that **47** is capable of differentiating these small molecules. Furthermore, other *n*-alkanes are also recognized by octa-acid **47** [86]. "Guests longer than decane cannot adopt a fully extended conformation in the nanocapsule, and, therefore, must fold" [17b]. An extensive study on the folding of a wide range of guests inside the capsular system of **47** in water solution was recently reported by Ramamurthy [87].

Ramamurthy reported on the binding of amphiphiles, such as adamantane carboxylic acid that forms a 1:1 supramolecular complex with **47**, which aggregates at higher concentrations [88]. This result was further confirmed by using fluorescent dyes of different size [89]. Notably, the fluorescent guests preserve all emission properties of the dyes in dry aromatic solvents. It suggests that the inner space of these capsules is essentially dry. In another contribution, Gibb analyzed the binding properties of **47** toward several isosteric guests, differing for their hydrophilicity [90]. In general, guests with low and medium hydrophilicity form a capsular system with **47**, while guests with high affinity for water form a 1:1 complex. Tolbert observed that a series of benzylidene-3-methylimidazolidinones form 2:1 host-guest complexes with octa-acid **47** [91]. Measuring the *cis-trans* ratio of each guest and the emission properties after irradiation of the corresponding supramolecular complex, the authors observed a different *cis-trans* ratio with respect to the uncomplexed guests. Bohne and co-workers, using fluorescence measurements and stopped-flow experiments, estimated in real time the kinetics of the formation of 1:1 (less than 1 ms) and 2:1 host−guest (lifetime of 2.7 s) complexes formed between octa-acid **47** and pyrene [92].

Combining NMR and EPR (steady-state and time-resolved) experiments, Turro and Ramamurthy investigated the ability of guests encapsulated into **47** to 'communicate' *via* orbital interactions, through the walls of the hosts, with guests in bulk solution [93]. Recently, Ramamurthy demonstrated an electron transfer across the wall of the dimeric capsule formed by **47**, using 4,4'-dimethylstilbene and an *N*-methyl pyridinium guest, by NMR, fluorescence and laser flash photolysis experiments [94]. Moreover, he functionalized gold nanoparticles (2−5 nm) with two cavitands based on octa-acid **47**, possessing four thiol groups at the lower rim and differing for the presence of the four carboxylic groups on the upper rim [95]. These functionalized AuNPs, can be assembled in different supramolecular architectures with the appropriate guest.

Gibb and Grayson reported on the synthesis of dendritic nonionic water-soluble cavitand **48**, functionalized with sixty-four hydroxyl groups, necessary for the solubilization in pure water (Fig. **10**) [96]. The properties of the dendritic host **48** are very similar to octa-acid **47**. Rick and co-workers described an interesting study to evaluate the binding properties of **47** toward water molecules, revealing that its cavity can contain 0-7 water molecules [97]. Kaifer demonstrated that the encapsulation of a redox-active guest, such as a ferrocene derivative, influences the electrochemical properties of the guest itself [98]. In a similar manner, suitable charged guests can mediate electrochemical oxidation of encapsulated ferrocene [99].

Recently, Ramamurthy and co-workers obtained a new water soluble cavitand **49** (Fig. **11**) bearing cationic groups due to the presence of eight diethyl ammonium groups. Complexation and photochemical studies suggest properties similar to the OA capsule **47** [100]. A further modification of the host **47** leads to cavitand **50** (Fig. **12**) [101].



**Fig. (11).** Octa-triethyl ammonium cavitand [49]. Adapted from Ref. [5] with permission of The Royal Society of Chemistry.



**Fig. (12).** Tetra-methyl-octa-acid cavitand **50**. Adapted from Ref. [5] with permission of The Royal Society of Chemistry.

The presence of four methyl groups on the upper rim of the host generates a deeper cavity, with different complexation properties with respect to **47**. In fact, host **50** forms 1:1 complexes with methane, ethane, *n*-heptane and *n*-octane, a mixture of 1:1 and 2:2 complexes with propane, *n*-butane, and *n*-hexane, a 2:2 capsular system with *n*-pentane, and 2:1 capsules with longer chain alkanes ($C_9$-$C_{14}$). The presence of the methyl groups disrupts the formation of the capsular system, thus other complexation pathways occur with host **50**. Whereas host **47** leads exclusively to dimeric systems, host **50** can form dimeric, tetrameric and hexameric capsules by function on the size of the guest [102]. At last, a hetero-capsule constituted by **47** and **50** was recently reported [103]. In this study, a mixing of homo- and hetero-dimeric capsules was observed depending on the guests.

The covalent bond between two units of octa-acid cavitand **47**, using a long aliphatic chain, affords dimeric cavitand **51** (Scheme **14**, up) [104]. With the appropriate guest, four different assemblies can be obtained (Scheme **14**, *vide infra*). The 1:1 capsule is formed with short *n*-alkanes ($C_6$, $C_8$ and $C_{10}$), and *n*-hexadecane ($C_{16}$). With longer alkanes ($C_{18}$-$C_{23}$), NMR experiments revealed the presence of two 2:2 capsule complexes (a and b in Scheme **14**).

### 2.3.1. Capsules via Hydrogen Bonds

Rebek's group developed efficient water-soluble supramolecular capsules, self-assembled in water by the formation of hydrogen bonds. By modification of the starting tetra-benzimidazolone cavitand proposed by de Mendoza [105], Rebek synthesized cavitand **52** (Fig. **13**), a water-soluble version of this host [106].

The "vase conformation of host **52** is stabilized by water molecules, which bridge adjacent benzimidazolones through hydrogen bonds, and one or more water molecules at each corner could be involved" [107]. Host **52** forms a dimeric capsule in the presence of

**Scheme 14.** Dimeric host **51** and relative supramolecular complexes. Adapted from Ref. [5] with permission of The Royal Society of Chemistry.



**Fig. (13).** Rebek's water-soluble cavitand **52**. Reproduced from *Chem. Commun.*, 2014, *50*, 4895 with permission of The Royal Society of Chemistry.

*n*-undecane and longer alkanes (up to *n*-tetradecane), exploiting the formation of a network of **16** hydrogen bonds. The guest *n*-undecane in an extended conformation comfortably fits the inner space of the capsule, while longer alkanes adopt *gauche* conformations. In general, longer *n*-alkanes (C$_{10}$-C$_{14}$), stilbenes and benzanilides induce the capsule formation, while α,ω-amino acids are taken up in the monomeric cavitand **52**, with the polar head-groups exposed to solvent. "In either container, the guests must assume folded shapes to be accommodated [108]. Typical α-amino acids did not give kinetically stable complexes with **52**, but zwitterionic 11-amino-undecanoic acid was an excellent guest in D$_2$O". The capsules increase their size to accommodate folded alkanes by a minimal arrangement of the hydrogen bond network, using the molecules of water as mobile linkers between the benzimidazolone

units. The inclusion of a guest is accomplished by the releasing of water molecules to the bulk of the solvent, leading to an entropy stabilization. Rebek's group also demonstrated the ability of cavitand **52** to recognize the lipopeptide ghrelin, an amino acid peptide which bears an octanoyl ester on serine **3**, supporting by ITC measurements a 1:1 host/guest stoichiometry, as well as for ibuprofen [107].

## 3. CALIX[N]ARENE CAPSULES

Calix[n]arenes are probably the most studied macrocyclic hosts in supramolecular chemistry. Since the pioneering work by Gutsche's group, the structural versatility combined with their wide functionalization and structural robustness, has led to the availability of a number of derivatives, which have found applications in several fields. The dimensions of the cavity, as well as the conformational mobility and the structural rigidity of the macrocycles are dependent on the number of constituent phenol units and their chemical manipulation at both the upper and lower rims. The smallest members of this family (calix[4,5]arenes) are the most common scaffolds used, because of well-established derivatization procedures and facile control of the conformation during chemical transformations at both rims.

### 3.1. Homodicapsules

"The self-assembly process can be induced by exploiting hydrogen bonding [109], ion pairing [110], metal-coordination [38b] and solvophobic forces [111]. Among the hydrogen-bonded systems, calixarene tetraurea derivatives **53** have been particularly studied, since in apolar organic solvents they give rise to the formation of dimeric self-assembled capsules **54** (Scheme **15**), able to complex, in a reversible fashion, neutral organic molecules and organic cations [112]. The driving force is the formation of a seam of intermolecular hydrogen bonds between urea substituents in a cyclic ''head-to-tail'' arrangement" [112e].

Small guest molecules of appropriate size and shape (*e.g.*, benzene, camphor or tetra-alkyl ammonium) are reversibly encapsulated inside the inner space of these capsular assemblies (Fig. **14**) [113]. Furthermore, "the concave surface cavity bears a substantial negative partial charge due to the entangled π-systems of the aromatic rings. Consequently, the cavity provides optimal conditions to accommodate cationic guests" [114].



**Scheme 15.** Dimeric self-assembled capsules **54** based on tetraurea calix[4]arenes 53. Adapted from Ref. [112b] with permission of The Royal Society of Chemistry.

Böhmer reported on a combination of resorcarene **3** and tetraurea calix[4]arene **53** with Et$_4$N$^+$PF$_6^-$ salt, that lead to an unprecedented arrangement of ion pairs by simultaneous but separated encapsulation of the ions into two distinct homodicapsules **4** and **54**, respectively (Scheme **16**) [115].

In 2004, Ungaro described the formation of "chiral dimeric capsules from *N,C*-linked peptidocalix[4]arenes, exploiting the simultaneous presence of a *N*-linked and a *C*-linked amide group on the diametral positions of a cone calix[4]arene (Fig. **15**) [116]. This hydrogen-bonding motif for the self-assembly of calix[4]arene dimeric capsules is intriguing since the robustness of the capsules can be controlled by changing length, nature, and number of the peptide chains".



**45%**    **78%**    **58%**    **67%**    **48%**    **57%**

**146%**    **103%**



**56** R= L-AlaNHCbz, R'=L-AlaOMe
**57** R= L-AlaNHCbz, R'=D-AlaOMe
**58** R= L-AlaNHCbz, R'= L-PheOMe
**59** R= (dl)-LeuNHAc, R'= GlyOMe
**60** R= L-Ala-L-AlaNHCbz, R'= L-AlaOMe
**61** R= L-Ala-L-AlaNHCbz, R'= L-Ala-L-AlaOME
**62** R= Lile-L-LeuNHCbz, R'= L-Val-L-PheOME
**63** R= L-Ala-L-Ala-L-AlaNHCbz,
     R'=L-Ala-L-Ala-L-AlaOME
**64** R=C(O)Et, R'= NH-*n*Bu

**Fig. (15).** *N,C*-Linked peptidocalix[4]arenes **55-64** used to obtain chiral dimeric capsules.

**Fig. (14).** Tetraurea calixarene monomer and typical guest cations. Percentages are packing coefficients of the guest inside the cavity.



**3**                    **54**

**PF₆⁻ NEt₄⁺**
**CDCl₃**

**4·[CHCl₃-PF₆]**        **55·Et₃N⁺**

**Scheme 16.** Separated encapsulation of ion pair. Adapted from *Chem. Soc. Rev.,* 2010, *39*, 3810 with permission of The Royal Society of Chemistry.

**Scheme 17.** Formation of supramolecular capsules **66** upon encapsulation of α,ω-diamines.



**Scheme 18.** Guest induced formation of bis-capsules **68**, **70** and **72**.

Parisi *et al.* reported on some capsules based on calix[5]arenes [117a-d]. Among these, they presented an interesting study on the ability of "carboxylcalix[5]arene receptor **65** to encapsulate α,ω-diamines of appropriate length ($C_{10}$-$C_{12}$), by means of a proton-transfer-mediated recognition process followed by salt-bridge-assisted bis-*endo*-complexation" (Scheme **17**) [117e].

An interesting guest-induced formation of capsules was presented by Liu, by using *p*-sulfonato[4,5]arenes **67** and **71** or sulfonatothiacalix[4]arenes **69** with 1,10-phenantrolinium ion or its derivatives [118]. The relative bis-capsules **68**, **72** and **70**, respectively, possessing different degrees of compactness depending on the types of calix used, were prepared (Scheme **18**).

**Scheme 19.** Formation of supramolecular capsules **74** and **75**, based on *p*-phosphonic acid calix[5]arene **73**.

An interesting nanocapsule, stable in water and able to carry drugs, is based on *p*-phosphonic acid calix[5]arene **73** (Scheme **19**) [119].

Raston and co-workers demonstrated that supramolecular capsule **74** is able to load carboplatin, an anti-cancer, "with 85% encapsulation reported (complex **75**). The spontaneous release of carboplatin is realized through the removal of water from the system, which results in either amorphous calix[5]arene. These stable molecular capsules offer further potential in improving the efficacy of drug delivery, while reducing side effects" [119].

"As reported before, the most common examples of calixarene-based capsules are stabilized by hydrogen bonding, or constructed with metal-ligand or covalent bonds. In contrast, nanocapsules formed from components that strictly interact by van der Waals forces have received less attention. However, the weak nature of these forces is likely to give the system the flexibility to allow guest capture and release in particular conditions, without disrupting the capsules. Guest exchange in such solid matrices would be very advantageous for applications in separations and clean organic syntheses" [120].

An example of this class was reported by Coleman *et al.*, and is represented by supramolecular capsule **77**, based on *p*-hexanoyl-calix[4]arene **76** (Scheme **20**) [120]. The same research group demonstrated that *p*-octanoylcalix[4]arene leads to a more stable supramolecular capsule [121]. These capsular calixarene-based solids are "good adsorbent for saturated and unsaturated hydrocarbons, polarizable inert gases, and for carbon dioxide" [122].



**Scheme 20.** *p*-Hexanoyl-calix[4]arene **76** and relative capsule **77**.

### 3.2 Heterodimeric Capsules

Several examples of heterodimeric capsules, built up with complementary H-donor/H-acceptor or positively/negatively charged groups in the calixarene scaffold have been reported. Li *et al.* studied the ability of tetra-arylureacalix[4]arene and *tetra*-tosylureacalix[4]arene to encapsulate cyclo-ketons [123]. Reinhoudt exploited ionic interactions between anionic calix[4]arenes **78** and **79**, bearing at the upper rim four amino acid moieties, and cationic tetra-amidiniumcalix[4]arene **80**, to achieve water-soluble molecular capsules **81** and **82**, able to trap quaternary ammonium cations such as *N*-methylquinolidinium cation (Scheme **21**) [124]. "The strength of the ionic interactions allows the formation of stable molecular assemblies in pure water, with association constants $K_a \sim 10^5$ $M^{-1}$. The length of the side chain of the different amino acid moieties strongly influences the thermodynamic parameters of binding" [124].

A molecular capsule based on ionic interactions between two oppositely charged *tetra*-sulfonatocalix[4]arene **83** and *tetra*-guanidinium calix[4]arene **84** was assembled by Reinhoudt (Scheme **22**) [125]. In this case a β-cyclodextrin self-assembled monolayer on gold (β-CD SAM) was used as a molecular print-board to anchor the *tetra*-guanidinium calix[4]arene and to build the supramolecular capsule on the surface.

Ballester prepared the heterodimeric capsule **88**, formed through a network of hydrogen bonds between the ureido groups of calix[4]arene **86** and calix[4]pyrrole **87**, in the presence of trimethylamine-*N*-oxide and dichloromethane (Scheme **23**) [126].

### 3.3. Capsules *via* Metal Coordination

Hybrid metal-organic capsules can be obtained taking advantage of metal-directed assembly of conveniently functionalized calix[n]arenes, as reported by Cholewa and Dalgarno in 2014 [127]. Calix[4]arene **89**, containing carboxylate groups at the *para*-position, is used as building block with a pre-organised Rh(II) complex to assemble dimeric capsule **90**, with four dirhodium centres (Scheme **24**) [128].

Supramolecular capsules based on the gadolinium cation were also obtained through bis-imidazolium ion and two subunits of *p*-sulfonatocalix[4]arene, in a "head-to-tail" manner, with the metal ion acting as a bridge [129]. A larger cavity was obtained by Neri and co-workers with *p*-sulfonatocalix[7]arenes and $Ba^{2+}$ cations, to create capsules containing diquat guest molecules [130].

**78** X = CH$_3$
R= OCH$_2$CH$_2$OEt

**79** X = (CH$_2$)$_4$NHCOOC(CH$_3$)$_3$
R= OCH$_2$CH$_2$OEt

**80** R = OCH$_2$CH$_2$OEt
R' = CH$_2$CH$_2$CH$_3$

**81** X = CH$_3$,
R = OCH$_2$CH$_2$OEt,
R' = CH$_2$CH$_2$CH$_3$

**82** X = (CH$_2$)$_4$NHCOOC(CH$_3$)$_3$,
R = OCH$_2$CH$_2$OEt,
R' = CH$_2$CH$_2$CH$_3$

**Scheme 21.** Complementary *tetra*-amidinium- and *tetra*-carboxy calix[4]arene capsules.



**Scheme 22.** Self-assembled supramolecular capsule **85** on gold β-cyclodextrin self-assembled monolayer. Reprinted with permission from Ref 125.American Chemical Society.



**Scheme 23.** Hetero-dicapsule **88** based on calix[4]arene **86** and calix[4]pyrrole **87** containing trimethyl-*N*-oxide guest.

**Scheme 24.** Capsule **90** assembled with rhodium metal cation.

The "directional bonding" approach, privileged by the presence of a metal centre, can be used to construct different "Platonic solids". This approach was used by De Mendoza and co-workers in 2012 to obtain a metal organic capsule, following an octahedral topology, through the interaction of uranyl ions and calix[4]arenes (Fig. **16**, A). Moreover, icosahedral topology was obtained using larger calix[5]arenes and $UO_2^{2+}$ ions (Fig. **16**, B) [131].



**Fig. (16).** "Platonic solid" realized using calix[5]arenes and $UO_2^{2+}$ ions. Reproduced from *CrystEngComm,* 2014, *16*, 3655 with permission of The Royal Society of Chemistry.

Dalgarno and co-workers reported on the assembly of di-*p*-carboxyl-calix[4]arene **91**, Cd(II) ions and 1,10-phenanthroline leading to the tilted capsule **92**, consisting of two metal centres, two calixarenes and two chelating moieties (Scheme **25**) [132].

In particular, substituted 1,10-phenanthrolines "play an important role in determining the shape of the capsules. When 2-methyl-1,10-phenanthroline or 3,4,7,8-tetramethyl-1,10-phenanthroline are used as a co-ligand, the resulting dimeric capsules are orientated in a "head-to-head" fashion" [133].

Toupet *et al.* proposed a metal-coordinated capsule based on mono-phosphinecalix[4]arene **93** and platinum cation, attaining the *trans*-capsule **94** *via* metal coordination (Scheme **26**) [134].

### 3.4. Molecular Boxes

The self-assembly of dimelamine calix[4]arenes **95** with barbituric acid (BA) and cyanuric acid (CYA) derivatives gives molecular boxes **96** consisting of two rosette motifs, top and bottom ones, which are connected by three calixarene units (Scheme **27**). Each rosette plane is formed by hydrogen bonding between melamine moieties of **95** and barbituric or cyanuric acid, and contains 18 H-bonds. Each box, formed upon mixing **95** with 2 equivalents of BA or CYA in apolar solvent, contains a total of **36** H-bonds. Consequently, they are thermodynamically stable in apolar solvents (*e.g.* benzene, toluene and chloroform), while their stability decreases with the increasing of the solvent polarity.

Capsules **96** were used by Reinhoudt *et al.* for the encapsulation of anthraquinone derivatives [135], (*e.g.*, alizarin) which form hydrogen bonded trimers inside the capsule [136]. "The encapsulation process imposes large structural changes in the assembly, resulting in a complete change of symmetry from *staggered* to



**Scheme 25.** Capsule **92** assembled from calix **91**, Cd(II) ions and 1,10-phenantroline.

**Scheme 26.** Formation of the *trans*-capsule **94**.



**Fig. (17).** Graphical representation of the symmetry groups for the assembly of capsule **96** (top and side view). Reprinted with permission from Ref. [135]. American Chemical Society.

*eclipsed*, and in an enlargement of the cavity of the molecular box in the solid state as well as in solution" (Fig. **17**) [137].

To mimic structural diversity of natural antibodies, different moieties (such as ureido, pyridyl, carbohydrate, amino acid, di- and tri-peptides) were introduced in the melamine groups. However, one of the main problems on bio-recognition systems is the low stability of hydrogen bonded supramolecular assemblies in polar solvents. For this reason, Reinhoudt studied the stability of these assemblies in competitive polar solvents [138], or in bilayer membranes in which the double rosette structures are more stable [139].

As reported by Reinhoudt and co-workers, tetra-rosette assemblies are spontaneously and selectively formed in apolar solvents [140]. When three equivalents of tetramelamine derivatives **97** are mixed with twelve equivalents of 5,5-diethyl-barbiturate (DEB) at room temperature, **72** hydrogen bonds are established, instead of **36** H-bonds that are formed in the double rosette boxes. Moreover, the introduction of a chiral center in the cyanurate molecules affords chiral assemblies, in which the free energy is different for the two diastereomers, depending on the rigidity of the spacer in **97** (Scheme **28**).

Using self-organized calixarene "rosette-like" capsules, Reinhoudt and co-workers reported the "first example of liquid crystalline material. The dimelamine-calix[4]arene was functionalized with octadecyl chains to promote the self-organization into a liquid-crystalline phase" [141].

### 3.5. Russian Dolls

An interesting class of capsules is the so-called "Russian Doll Capsules". These systems are made up of two water soluble *p*-sulfonatocalix[4]arenes **99** and a Na-[18]crown-6, forming a super-anionic capsule **100** that is capable of selectively crystallizing polynuclear metal cations from solution (Scheme **29**). In 2000, Raston assembled a solid state molecular capsule based on a combination of hydrogen bonds and metal coordination of Yttrium(III) or Europium(III) [142].



**Scheme 27.** General scheme for the formation of rosette motif molecular boxes **96**. Reprinted with permission from Ref. [135]. American Chemical Society.

**98** only **P** diastereomer

**97**

X= R Barbituric Acid (BA)
X= NH, NR Cyanuric Acid (CYA)

X= R Barbituric Acid (BA)
X= NH, NR Cyanuric Acid (CYA)

**98** only **P** and **M** diastereomer

**Scheme 28.** General scheme for the formation of double and tetrarosette assemblies. Reprinted with permission from Ref. [135]. American Chemical Society.



**99**

$= [M(H_2O)_7]^{3+}$

**100**

**Scheme 29.** Assembly of superanionic capsule [100].

In the same year, Raston's group created a Russian doll-like crystalline complex formed by the self-assembled superanionic capsule $[\{Na^+ \subset (18\text{-crown-6})(OH_2)_2\} \subset \{(p\text{-sulfonatocalix[4]arene}^{4-})_2\}]^{7-}$ and dinuclear $[Rh_2(\mu\text{-OH}_2)(H_2O)_8]^{4+}$ [143]. They addressed the way to form capsules using bulky cations to avoid the electrostatic repulsion between the two negatively charged calixarenes, and underlined the possibility to use a large array of different inorganic and organic substrates. The replacement of the 18-crown-6 with the [2.2.2] cryptand in the inner part of the assembly, and the use of lanthanide ions (e.g. Ce, Nd, Sm, Eu) led to a 2D coordination ion polymer, are at the basis of "Russian doll" capsule **101** (Scheme **30**) [144].

A very rapid crystallization of lanthanide-based molecular capsules is achieved using diaza[18]crown-6 at pH < 3 [143b, 144, 145]. Raston and coworkers established by DOSY NMR studies that a pre-association in solution occurs between crown ethers and *p*-sulfonatocalix[4]arene **99** [146]. A partial "Russian doll" is formed by using the diaza-crown ether at low pH or Na-18-crown-6, but only once the entire superanion is constructed, the assembly is able to selective crystallize aqueous-metal cations from the mixture.

The use of 18-crown-6 and praseodymium triflate constrain the calixarenes to assemble into an "upper rim to upper rim" organization. In the solid state, this system presents an extended structure

**Scheme 30.** Assembly of the "Russian doll" **101**.



**Scheme 31.** Schematic formation of nanometer scale spheroids based on *p*-sulfonatocalix[4]arene **99**. Reproduced from Ref. [147] with permission of The Royal Society of Chemistry.

based on these capsules that have twelve *p*-sulfonatocalix[4]arenes at the vertices of a cuboctahedron (Scheme **31**) [147].

Examples of bis-molecular capsule arrangements formed with *p*-sulfonatocalix[5]arene [148] or *p*-sulfonatocalix[6]arene [149] have been reported by Atwood and Raston (Fig. **18**), although the formation of supramolecular complexes with *p*-sulfonato-calix[5,6]arenes remains more difficult because of low yielding synthesis and the higher degree of conformational flexibility.

**4. CONCLUSION**

In this review we have encompassed self-assembled capsules based on resorcin[4]arene cavitands and calix[n]arenes. Since these

macrocycles possess a hemispherical shape, they are perfect building blocks to build up capsular assemblies. These supramolecular assemblies are constructed exploiting non-covalent interactions such as hydrogen bonds, metal-coordination bonds, hydrophobic effect, as well as CH-π interactions originating from the size complementarity between the guest and the space inside the capsules. Guest molecules inside this self-assembled space show unique chemical and physical features that are different from the bulk solution. Every day novel strategies for supramolecular self-assembly emerge. Furthermore, researchers are spending considerable effort to prepare hydrophilic and water-soluble hosts able to form self-assembled capsules directed to drug delivery. Nowadays, several self-assembled capsules find practical applications such as capsular

**Fig. (18).** Bis-molecular capsule arrangements formed with (A) *p*-sulfonatocalix[5]arene, and (B,C) *p*-sulfonatocalix[6]arene, respectively. Reproduced from Ref. [147] with permission of The Royal Society of Chemistry.

devices, photoswitchable capsules for biomedical purposes and supramolecular capsule polymers. It is expected, in this burgeoning field, that new self-assembled capsules will disclose further attractive phenomena in host-guest chemistry, physical organic chemistry and materials science.

## CONFLICT OF INTEREST

The authors confirm that this article content has no conflict of interest.

## ACKNOWLEDGEMENTS

## REFERENCES

[1]     (a) Cram, D.J.; Karbach, S.; Kim, Y.H.; Baczynskyj L.; Kalleymeyn, G.W. Shell closure of two cavitands forms carcerand complexes with components of the medium as permanent guests. *J. Am. Chem. Soc.*, **1985**, *107*, 2575-2576; (b) Tanner, M.E.; Knobler, C.B.; Cram, D.J. Hemicarcerands permit entrance to and egress from their inside phases with high structural recognition and activation free energies. *J. Am. Chem. Soc.*, **1990**, *112*, 1659-1660; (c) Cram, D.J. Molecular container compounds. *Nature*, **1992**, *356*, 29-36; (d) Jasat, A.; Sherman, J.C. Carceplexes and hemicarceplexes. *Chem. Rev.*, **1999**, *99*, 931-967; (e) Warmuth, R.; Yoon, J. Recent highlights in hemicarcerand chemistry. *Acc. Chem. Res.*, **2001**, *34*, 95-105.

[2]     (a) Hof, F.; Craig, S.L.; Nuckolls, C.; Rebek Jr, J. Molecular encapsulation. *Angew. Chem.*, *Int. Ed.*, **2002**, *41*, 1488-1508; (b) Berryman, O.B.; Dube, H.; Rebek Jr., J. Photophysics applied to cavitands and capsules. *Isr. J. Chem.*, **2011**, *51*, 700-709; (c) Rebek Jr., J. Simultaneous encapsulation: Molecules held at close range. *Angew. Chem.*, *Int. Ed.*, **2005**, *44*, 2068-2078; (d) Biros, S.M.; Rebek Jr., J. Structure and binding properties of water-soluble cavitands and capsules. *Chem. Soc. Rev.*, **2007**, *36*, 93-104; (e) Schröder, T.; Sahu, S.N.; Anselmetti, D.; Mattay, J. Supramolecular capsules derived from Resorcin[4]arenes by H-bonding and metal coordination: Synthesis, characterization, and Single-molecule force spectroscopy. *Isr. J. Chem.*, **2011**, *51*, 725-742; (f) Inokuma, Y.; Kawano, M.; Fujita, M. Crystalline molecular flasks. *Nat. Chem.*, **2011**, *3*, 349-358; (g) Yoshizawa, M.; Klosterman, J.K.; Fujita, M. Functional molecular flasks: New properties and reactions within discrete, self-assembled hosts. *Angew. Chem.*, *Int. Ed.*, **2009**, *48*, 3418-3438; (h) Klosterman, J.K.; Yamauchi, Y.; Fujita, M. Functional molecular flasks: New properties and reactions within discrete, self-assembled hosts. *Chem. Soc. Rev.*, **2009**, *38*, 1714-1725; (i) Fiedler, D.; Leung, D.H.; Bergman, R.G.; Raymond, K.N. Selective molecular recognition, C−H bond activation, and catalysis in nanoscale reaction vessels. *Acc. Chem. Res.*, **2005**, *38*, 349-358;

(j) Raymond, K.N.; Brown, C.J. Inner and outer beauty. *Top. Curr. Chem.*, **2012**, *323*, 1-18; (k) Pluth, M.D.; Bergman, R.G.; Raymond, K.N. Proton-mediated chemistry and catalysis in a self-assembled supramolecular host. *Acc. Chem. Res.*, **2009**, *42*, 1650-1659; (l) Adriaenssens, L.; Ballester, P. Hydrogen bonded supramolecular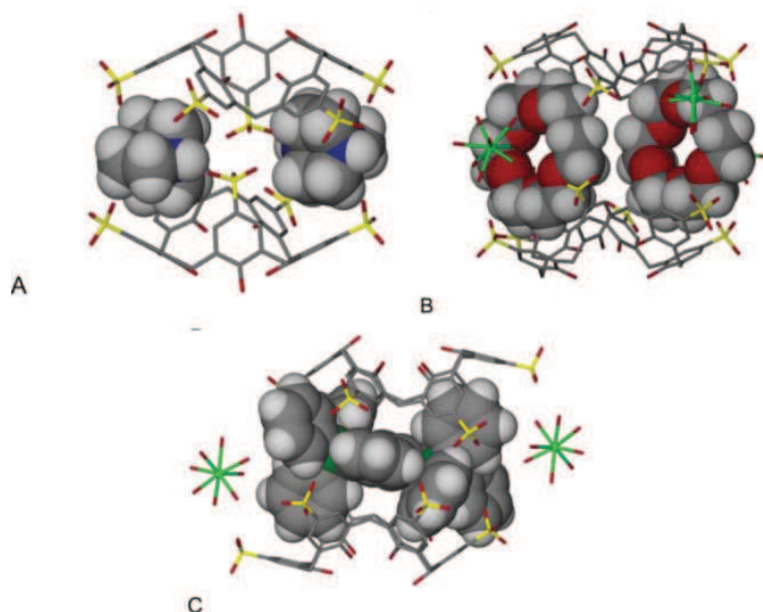 capsules with functionalized interiors: The controlled orientation of included guests. *Chem. Soc. Rev.*, **2013**, *42*, 3261-3277; (m) Breiner, B.; Clegg, J.K.; Nitschke, J.R. Reactivity modulation in container molecules. *Chem. Sci.*, **2011**, *2*, 51-56; (n) Kobayashi, K.; Yamanaka, M. Self-assembled capsules based on tetrafunctionalized calix[4]resorcinarene cavitands. *Chem. Soc. Rev.*, **2015**, *44*, 449-466

[3]     Wyler, R.; de Mendoza, J.; Rebek Jr., J. A synthetic cavity assembles through self-complementary hydrogen bonds. *Angew. Chem.*, *Int. Ed. Engl.*, **1993**, *32*, 1699-1701.

[4]     (a) Fujita, M.; Tominaga, M.; Hori, A.; Therrien, B. Coordination assemblies from a Pd(II)-cornered square complex. *Acc. Chem. Res.*, **2005**, *38*, 369-378; (b) Northrop, B.H.; Zheng, Y.R.; Chi, K.W.; Stang, P.J. Self-organization in coordination-driven self-assembly. *Acc. Chem. Res.*, **2009**, *42*, 1554-1563; (c) Rebek Jr., J. Molecular behavior in small spaces. *Acc. Chem. Res.*, **2009**, *42*, 1660-1668; (d) Mastalerz, M. Shape-persistent organic cage compounds by dynamic covalent bond formation. *Angew. Chem.*, *Int. Ed.*, **2010**, *49*, 5042-5053; (e) Avram, L.; Cohen, Y.; Rebek Jr., J. Recent advances in hydrogen-bonded hexameric encapsulation complexes. *Chem. Commun.*, **2011**, *47*, 5368-5375.

[5]     Jordan, J.H.; Gibb, B.C. Molecular containers assembled through the hydrophobic effect. *Chem. Soc. Rev.*, **2015**, *44*, 547-585.

[6]     Oshovsky, G.V.; Reinhoudt, D.N.; Verboom, W. Supramolecular chemistry in water. *Angew. Chem. Int. Ed.*, **2007**, *46*, 2366-2393.

[7]     (a) Mayzel, O.; Cohen, Y. Diffusion coefficients of macrocyclic complexes using the PGSE NMR technique: Determination of association constants. *J. Chem. Soc.*, *Chem. Commun.*, **1994**, (16), 1901-1902; (b) Mayzel, O.; Aleksiuk, O.; Grynszpan, F.; Biali, S.E.; Cohen, Y. NMR diffusion coefficients of p-tert-butylcalix[n]arene systems. *J. Chem. Soc.*, *Chem. Commun.*, **1995**, (11), 1183-1184; (c) Mayzel, O.; Gafni, A.; Cohen, Y. Water hydration of macrocyclic systems in organic solvents: An NMR diffusion and chemical shift study. *J. Chem. Soc.*, *Chem. Commun.*, **1996**, (8), 911-912; (d) Gafni, A.; Cohen, Y. Complexes of macrocycles with γ-Cyclodextrin as deduced from NMR diffusion measurements *J. Org. Chem.*, **1997**, *62*, 120-125.

[8]     (a) Parella, T. High-quality 1D spectra by implementing pulsed-field gradients as the coherence pathway selection procedure. *Magn. Reson. Chem.*, **1996**, *34*, 329-347; (b) Parella, T. Pulsed field gradients: A new tool for routine NMR. *Magn. Reson. Chem.*, **1998**, *36*, 467-495.

[9]     Johnson Jr., C.S. Diffusion ordered nuclear magnetic resonance spectroscopy: Principles and applications. *Prog. Nucl. Magn. Reson. Spectrosc.*, **1999**, *34*, 203-256.

[10]    (a) Gafni, A.; Cohen, Y.; Palmer, S.; Parker, D. Enantiomer discrimination using lipophilic cyclodextrins studied by electrode response, pulsed-gradient spin-echo (PGSE) NMR and relaxation rate measurements. *J. Chem. Soc.*, *Perkin Trans. 2*, **1998**, (1), 19-24; (b) Timmerman, P.; Weidmann, J.L.; Jolliffe, K.A.; Prins, L.J.; Reinhoudt, D.N.; Shinkai, S.; Frish, L.; Cohen, Y. NMR diffusion spectroscopy for the characterization of multicomponent hydrogen-bonded assemblies in solution. *J. Chem. Soc.*, *Perkin Trans. 2*, **2000**,

(10), 2077-2089; (c) Avram, L.; Cohen, Y. Complexation in pseudorotaxanes based on α-cyclodextrin and different α,ω-diaminoalkanes by NMR diffusion measurements. *J. Org. Chem.*, **2002**, *67*, 2639-2644; (d) Frish, L.; Sansone, F.; Casnati, A.; Ungaro, R.; Cohen, Y. Complexation of a peptido-calix[4]arene, a vancomycin mimic, with alanine-containing guests by NMR diffusion measurements. *J. Org. Chem.*, **2000**, *65*, 5026-5030; (e) Cameron, K.S.; Fielding, L. NMR diffusion spectroscopy as a measure of host–guest complex association constants and as a probe of complex size. *J. Org. Chem.*, **2001**, *66*, 6891-6895; (f) Fielding, L. NMR methods for the determination of protein-ligand dissociation constants. *Curr. Top. Med. Chem.*, **2003**, *3*, 39-53; (g) Pappalardo, A.; Amato, M.E.; Ballistreri, F.P.; Tomaselli, G.A.; Toscano, R.M.; Trusso Sfrazzetto, G. Pair of diastereomeric uranyl salen cavitands displaying opposite enantiodiscrimination of α-amino acid ammonium salts. *J. Org. Chem.*, **2012**, *77*, 7684-7687; (h) Ballistreri, F.P.; Pappalardo, A.; Toscano, R.M.; Tomaselli, G.A.; Trusso Sfrazzetto, G. A new heteroditopic chiral uranyl-salen receptor for molecular recognition of amino acid ammonium salts. *Eur. J. Org. Chem.*, **2010**, *20*, 3806-3810; (i) Amato, M.E.; Ballistreri, F.P.; D'Agata, S.; Pappalardo, A.; Tomaselli, G.A.; Toscano, R.M.; Trusso Sfrazzetto, G. Enantioselective molecular recognition of chiral organic ammonium ions and amino acids using cavitand-salen-based receptors. *Eur. J. Org. Chem.*, **2011**, *(28)*, 5674-5680; (j) Pappalardo, A.; Amato, M.E.; Ballistreri, F.P.; Notti, A.; Tomaselli, G.A.; Toscano, R.M.; Trusso Sfrazzetto, G. Synthesis and topology of [2+2] calix[4]resorcarene-based chiral cavitand-salen macrocycles. *Tetrahedron Lett.*, **2012**, *53*, 7150-7153; (k) Giuffrida, M.L.; Rizzarelli, E.; Tomaselli, G.A.; Satriano, C.; Trusso Sfrazzetto, G. Enantioselective extraction mediated by a chiral cavitand-salen covalently assembled on a porous silicon surface. *Chem. Commun.*, **2014**, 9835-9838.

[11]    (a) Pregosin, P.S.; Kumar, P.G.A.; Fernandez, I. Pulsed gradient spin–echo (PGSE) diffusion and 1H-19F heteronuclear overhauser spectroscopy (HOESY) NMR methods in inorganic and organometallic chemistry: Something old and something new. *Chem. Rev.*, **2005**, *105*, 2977-2998; (b) Kharlamov, S.V.; Latypov, S.V. Modern diffusion-ordered NMR spectroscopy in chemistry of supramolecular systems: The scope and limitations. *Russ. Chem. Rev.*, **2010**, *79*, 635-653; (c) Macchioni, A.; Ciancaleoni, G.; Zuccaccia, C.; Zuccaccia, D. Determining accurate molecular sizes in solution through NMR diffusion spectroscopy. *Chem. Soc. Rev.*, **2008**, *37*, 479-489; (d) Lombardo, G.M.; Thompson, A.L.; Ballistreri, F.P.; Pappalardo, A.; Trusso Sfrazzetto, G.; Tomaselli, G.A.; Toscano, R.M.; Punzo, F. An integrated X-ray and molecular dynamics study of uranyl-salen structures and properties. *Dalton Trans.*, **2012**, *41*, 1951-1960; (e) Brancatelli, G.; Pappalardo, A.; Trusso Sfrazzetto, G.; Notti, A.; Geremia, S. Mono- and dinuclear uranyl(VI) complexes with chiral Schiff base ligand. *Inorg. Chim. Acta*, **2013**, *396*, 25-29.

[12]    (a) Allouche, L.; Marquis, A.; Lehn, J.M. Discrimination of metallo supramolecular architectures in solution by using diffusion ordered spectroscopy (DOSY) experiments: Double-stranded helicates of different lengths. *Chem. - Eur. J.*, **2006**, *12*, 7520-7525; (b) Giuseppone, N.; Schmitt, J.L.; Allouche, L.; Lehn, J.M. DOSY NMR experiments as a tool for the analysis of constitutional and motional dynamic processes: Implementation for the driven evolution of dynamic combinatorial libraries of helical strands. *Angew. Chem., Int. Ed.*, **2008**, *47*, 2235-2239; (c) Gulion, F.; Lauceri, R.; Frish, L.; Evan-Salem, T.; Cohen, Y.; De Zorzi, R.; Geremia, S.; Di Costanzo, L.; Randaccio, L.; Sciotto, D.; Purrello, R. Noncovalent synthesis in aqueous solution and spectroscopic characterization of multi-porphyrin complexes. *Chem. - Eur. J.*, **2006**, *12*, 2722-2729; (d) Evan-Salem, T.; Frish, L.; van Leeuwen, F.W.B.; Reinhoudt, D.N.; Verboom, W.; Kaucher, M.S.; Davis, J.T.; Cohen, Y. Self-assembled ionophores from isoguanosine: Diffusion NMR spectroscopy clarifies cation's and anion's influence on supramolecular structure *Chem. - Eur. J.*, **2007**, *13*, 1969-1977; (e) Gattuso, G.; Notti, A.; Pappalardo, A.; Pappalardo, S.; Parisi, M.F. A supramolecular amphiphile from a new water-soluble calix[5]arene and n-dodecylammonium chloride. *Tetrahedron Lett.*, **2013**, *54*, 188-191; (f) Hori, A.; Kumazawa, K.; Kusukawa, T.; Chand, D.K.; Fujita, M.; Sakamoto, S.; Yamaguchi, K. DOSY Study on dynamic catenation: Self-assembly of a [3]catenane as a meta-stable compound from twelve simple components. *Chem. - Eur. J.*, **2001**, *7*, 4142-4149.

[13]    (a) Pappalardo, S.; Villari, V.; Slovak, S.; Cohen, Y.; Gattuso, G.; Notti, A.; Pappalardo, A.; Pisagatti, I.; Parisi, M.F. Counterion-dependent proton-driven self-assembly of linear supramolecular oligomers based on amino-calix[5]arene building blocks. *Chem. - Eur. J.*, **2007**, *13*, 8164-8173; (b) Zayed, J.M.; Biedermann, F.; Rauwald, U.; Scherman, O.A. Probing cucurbit[8]uril-mediated supramolecular block copolymer assembly in water using diffusion NMR. *Polym. Chem.*, **2010**, *1*, 1434-1436; (c) Zhang, Z.; Luo, Y.; Chen, J.; Dong, S.; Yu, Y.; Ma, Z.; Huang, F. Formation of linear supramolecular polymers that is driven by C-H···π interactions in solution and in the solid state. *Angew. Chem., Int. Ed.*, **2011**, *50*, 1397-1401; (d) Pappalardo, A.; Ballistreri, F.P.; Li Destri, G.; Mineo, P.G.; Tomaselli, G.A.; Toscano, R.M.; Trusso Sfrazzetto, G. Supramolecular polymer networks based on Calix[5]arene tethered poly(p-phenyleneethynylene). *Macromolecules*, **2012**, *45*, 7549-7556.

[14]    Avram, L.; Cohen, Y. Diffusion NMR of molecular cages and capsules. *Chem. Soc. Rev.*, **2015**, *44*, 586-602.

[15]    (a) Moran, J.R.; Karbach, S.; Cram, D.J. Cavitands: Synthetic molecular vessels. *J. Am. Chem. Soc.*, **1982**, *104*, 5826-5828; (b) Cram, D.J. Cavitands: Organic hosts with enforced cavities. *Science*, **1983**, *219*, 1177-1183.

[16]    Weinelt, F.; Schneider, H. Mechanisms of macrocycle genesis. The condensation of resorcinol with aldehydes. *J. Org. Chem.*, **1991**, *56*, 5527-5535.

[17]    (a) Ajami, D.; Rebek Jr, J. Expanding capsules. *Supramol. Chem.*, **2009**, *21*, 103-106; (b) Laughreya, Z.; Gibb, B.C. Water-soluble, self-assembling container molecules: an update. *Chem. Soc. Rev.*, **2011**, *40*, 363-386.

[18]    (a) Chapman, R.G.; Sherman, J.C. Study of templation and molecular encapsulation using highly stable and guest-selective self-assembling structures. *J. Am. Chem. Soc.*, **1995**, *117*, 9081-9082; (b) Chapman, R.G.; Olovsson, G.; Trotter, J.; Sherman, J.C. Crystal structure and thermodynamics of reversible molecular capsules. *J. Am. Chem. Soc.*, **1998**, *120*, 6252-6260; (c) Chapman, R.G.; Sherman, J.C. Reversible molecular capsules composed of two cavitands linked via an assortment of charged-hydrogen bonds and covalent bonds. *J. Am. Chem. Soc.*, **1998**, *120*, 9818-9826.

[19]    Heinz, T.; Rudkevich, D.M.; Rebek Jr. J. Pairwise selection of guests in a cylindrical molecular capsule of nanometre dimensions. *Nature*, **1998**, *394*, 764-766.

[20]    (a) Rebek Jr. J. Simultaneous encapsulation: molecules held at close range. *Angew. Chem. Int. Ed.*, **2005**, *44*, 2068-2078; (b) Rebek Jr., J. Contortions of encapsulated alkyl groups. *Chem. Commun.*, **2007**, *(27)*, 2777-2789; (c) Shivanyuk, A.; Rebek, J., Jr. Isomeric constellations of encapsulation complexes store information on the nanometer scale. *Angew. Chem. Int. Ed. Engl.*, **2003**, *42*, 684-686.

[21]    (a) Chen, J.; Korner, S.; Craig, S.L.; Rudkevich, D.M.; Rebek Jr., J. Chemistry: Amplification by compartmentalization. *Nature*, **2002**, *415*, 385-386; (b) Chen, J.; Korner, S.; Craig, S.L.; Lin, S.; Rudkevich, D.M.; Rebek Jr., J. Chemical amplification with encapsulated reagents. *Proc. Natl. Acad. Sci. USA*, **2002**, *99*, 2593-2596; (c) Chen, J.; Rebek Jr. J. Selectivity in an encapsulated cycloaddition reaction. *Org. Lett.*, **2002**, *4*, 327-329; (d) Iswasawa, T.; Mann, E.; Rebek Jr., J. A reversible reaction inside a self-assembled capsule. *J. Am. Chem. Soc.*, **2006**, *128*, 9308-9309.

[22]    (a) Shivanyuk, A.; Rebek Jr., J. Social isomers in encapsulation complexes. *J. Am. Chem. Soc.*, **2002**, *124*, 12074-12075; (b) Yamanaka, M.; Shivanyuk, A.; Rebek Jr., J. Experimental and computational probes of the space in a self-assembled capsule. *Proc. Natl. Acad. Sci. USA*, **2004**, *101*, 2669-2672; (c) Yamanaka, M.; Rebek Jr., J. Constellational diastereomers in encapsulation complexes. *Chem. Commun.*, **2004**, *(15)*, 1690-1691; (d) Yamanaka, M.; Kobayashi, K. Capsular assemblies of calix[4]resorcinarene-based cavitands. *Asian J. Org. Chem.* **2013**, *2*, 276-289.

[23]    Scarso, A.; Tremblau, L.; Rebek Jr., J. Helical folding of alkanes in a self-assembled, cylindrical capsule. *J. Am. Chem. Soc.*, **2004**, *126*, 13512-13518.

[24]    (a) Heinz, T.; Rudkevich, D.M.; Rebek, J., Jr. Molecular recognition with in a self-assembled cylindrical host. *Angew. Chem. Int. Ed.*, **1999**, *38*, 1136-1139; (b) Ajami, D.; Rebek, J., Jr. Expanded capsules with reversibly added spacers. *J. Am. Chem. Soc.*, **2006**, *128*, 5314-5315; (c) Ajami, D.; Rebek, J., Jr. Adaptations of guest and host in expanded self-assembled capsules. *Proc. Natl Acad. Sci. USA*, **2007**, *104*, 16000-16003.

[25]    (a) Corbett, P.T.; Sanders, J.K.M.; Otto, S. Systems chemistry: Pattern formation in random dynamic combinatorial libraries. *Angew. Chem. Int. Ed.*, **2007**, *46*, 8858-8861; (b) Corbett, P.T.; Leclaire, J.; Vial, L.; West, K.R.; Wietor, J.L.; Sanders, J.K.M.; Otto, S. Dynamic combinatorial chemistry. *Chem. Rev.*, **2006**, *106*, 3652-3711.

[26]    Park, Y.S.; Park, J.; Paek, K. Versatile self-assembled molecular capsule formation of a resorcin[4]arene-based benzamidoimino cavitand. *Chem. Commun.*, **2013**, *49*, 6316-6318.

[27]    (a) Kobayashi, K.; Shirasaka, T.; Yamaguchi, K.; Sakamoto, S.; Horn, E.; Furukawa, N. Molecular capsule constructed by multiple hydrogen bonds: Self-assembly of cavitand tetracarboxylic acid with 2-aminopyrimidine. *Chem. Commun.*, **2000**, *(1)*, 41-42; (b) Yamanaka, M.; Ishii, K.; Yamada, Y.; Kobayashi, K. Tunable capsule space: self-assembly of hemispherical cavitands with hydrogen-bonding linkers. *J. Org. Chem.*, **2006**, *71*, 8800-8806.

[28]    (a) Kobayashi, K.; Ishii, K.; Sakamoto, S.; Shirasaka, T.; Yamaguchi, K. Guest-induced assembly of tetracarboxyl-cavitand and tetra(3-pyridyl)-cavitand into a heterodimeric capsule *via* hydrogen bonds and CH−halogen and/or CH−π interaction. *J. Am. Chem. Soc.*, **2003**, *125*, 10615-10624; (b) Kobayashi, K.; Ishii, K.; Yamanaka, M. Orientational isomerism and binding ability of nonsymmetrical guests encapsulated in a self-assembling heterodimeric capsule, *Chem. Eur. J.*, **2005**, *11*, 4725-4734.

[29]    (a) Kobayashi, K.; Kitagawa, R.; Yamada, Y.; Yamanaka, M.; Suematsu, T.; Sei, Y.; Yamaguchi, K. Orientational isomerism controlled by the difference in electronic environments of a self-assembling heterodimeric capsule. *J. Org. Chem.*, **2007**, *72*, 3242-3246; (b) Kitagawa, H.; Kawahata, M.; Kitagawa, R.; Yamada, Y.; Yamanaka, M.; Yamaguchi, K.; Kobayashi, K. Guest-encapsulation behavior in a self-assembled heterodimeric capsule. *Tetrahedron*, **2009**, *65*, 7234-7239.

[30]    Kitagawa, H.; Kobori, Y.; Yamanaka, M.; Yamaguchi, K.; Kobayashi, K. Encapsulated-guest rotation in a self-assembled heterocapsule directed toward a supramolecular gyroscope. *Proc. Natl. Acad. Sci. USA*, **2009**, *106*, 10444-10448.

[31]    Ichihara, K.; Kawai, H.; Togari, Y.; Kikuta, E.; Kitagawa, H.; Tsuzuki, S.; Yoza, K.; Yamanaka, M.; Kobayashi, K. Encapsulation-induced remarkable

stability of a hydrogen-bonded heterocapsule. *Chem. - Eur. J.*, **2013**, *19*, 3685-3692.

[32] Nakazawa, J.; Mizuki, M.; Shimazaki, Y.; Tani, F.; Naruta, Y. Encapsulation of small molecules by a cavitand porphyrin self-assembled *via* quadruple hydrogen bonds. *Org. Lett.*, **2006**, *8*, 4275-4278.

[33] Ajami, D.; Schramm, M.P.; Volonterio, A.; Rebek Jr, J. Assembly of hybrid synthetic capsules. *Angew. Chem. Int. Ed.*, **2007**, *46*, 242-244.

[34] (a) MacGillivray, L.R.; Atwood, J.L. A chiral spherical molecular assembly held together by 60 hydrogen bonds. *Nature*, **1997**, *389*, 469-472; (b) Slovak, S.; Avram, L.; Cohen, Y. Encapsulated or not encapsulated? Mapping alcohol sites in hexameric capsules of resorcin[4]arenes in solution by diffusion nmr spectroscopy. *Angew. Chem. Int. Ed.*, **2010**, *49*, 428-431.

[35] (a) Avram, L.; Cohen, Y. The role of water molecules in a resorcinarene capsule as probed by NMR diffusion measurements. *Org. Lett.*, **2002**, *4*, 4365-4368; (b) Zhang, Q.; Tiefenbacher, K. Hexameric resorcinarene capsule is a Brønsted acid: Investigation and application to synthesis and catalysis. *J. Am. Chem. Soc.*, **2013**, *135*, 16213-16219.

[36] (a) Shivanyuk, A.; Rebek, J. Recognition of guests in solution by self-assembling resorcinarene subunits. *Proc. Natl. Acad. Sci. U. S. A.*, **2001**, *98*, 7662-7665; (b) Shivanyuk, A.; Rebek, J.J. Reversible encapsulation of multiple, neutral guests in hexameric resorcinarene hosts. *Chem. Commun.*, **2001**, (23), 2424-2425; (c) Palmer, L.C.; Shivanyuk, A.; Yamanaka, M.; Rebek, J., Jr. Resorcinarene assemblies as synthetic receptors. *Chem. Commun.*, **2005**, (7), 857-858; (d) Evan-Salem, T.; Baruch, I.; Avram, L.; Cohen, Y.; Palmer, L.C.; Rebek, J., Jr. Resorcinarenes are hexameric capsules in solution. *Proc. Natl. Acad. Sci. U. S. A.*, **2006**, *103*, 12296-12300; (e) Avram, L.; Cohen, Y. Discrimination of guests encapsulation in large hexameric molecular capsules in solution: Pyrogallol[4]arene versus resorcin[4]arene capsules. *J. Am. Chem. Soc.*, **2003**, *125*, 16180-16181; (f) Slovak, S.; Cohen, Y. In-out interactions of different guests with the hexameric capsule of resorcin[4]arene. *Supramol. Chem.*, **2010**, *22*, 803-807; (g) Philip, I.E.; Kaifer, A.E. Electrochemically driven formation of a molecular capsule around the ferrocenium ion. *J. Am. Chem. Soc.*, **2002**, *124*, 12678-12679; (h) Philip, I.; Kaifer, A.E. Noncovalent encapsulation of cobaltocenium inside resorcinarene molecular capsules. *J. Org. Chem.*, **2005**, *70*, 1558-1564; (i) Bianchini, G.; Scarso, A.; Sorella, G.L.; Strukul, G. Switching the activity of a photoredox catalyst through reversible encapsulation and release. *Chem. Commun.*, **2012**, (99), 12082-12084.

[37] Lux, J.; Rebek Jr., J. Reversible switching between self-assembled homomeric and hybrid capsules. *Chem. Commun.*, **2013**, *49*, 2127-2129.

[38] (a) Jacopozzi, P.; Dalcanale, E. Metal-induced self-assembly of cavitand-based cage molecules. *Angew. Chem. Int. Ed.*, **1997**, *36*, 613-615; (b) Fochi, F.; Jacopozzi, P.; Wegelius, E.; Rissanen, K.; Cozzini, P.; Marastoni, E.; Fisicaro, E.; Mannini, P.; Fokkens, R.; Dalcanale, E. Self-assembly and anion encapsulation properties of cavitand-based coordination cages. *J. Am. Chem. Soc.*, **2001**, *123*, 7539-7552; (c) Zuccaccia, D.; Pirondini, L.; Pinali, R.; Dalcanale, E.; Macchioni, A. Dynamic and structural NMR studies of cavitand-based coordination cages. *J. Am. Chem. Soc.*, **2005**, *127*, 7025-7032; (d) Cuminetti, N.; Ebbing, M.H.K.; Prados, P.; de Mendoza, J.; Dalcanale, E. Enlarged cavitand-based coordination cages. *Tetrahedron Lett.*, **2001**, *42*, 527-530.

[39] Pinalli, R.; Cristini, V.; Sottili, V.; Geremia, S.; Campagnolo, M.; Caneschi, A.; Dalcanale, E. Cavitand-based nanoscale coordination cages. *J. Am. Chem. Soc.*, **2004**, *126*, 6516-6517.

[40] Menozzi, E.; Pinalli, R.; Speets, E. A.; Ravoo, B.J.; Dalcanale, E.; Reinhoudt, D.N. Surface-confined single-molecules: Assembly and disassembly of nanosize coordination cages on Gold (111). *Chem. Eur. J.*, **2004**, *10*, 2199-2206.

[41] Busi, M.; Laurenti, M.; Condorelli, G.G.; Motta, A.; Favazza, M.; Fragalà, I.L.; Montalti, M.; Prodi, L.; Dalcanale, E. Self-assembly of nanosize coordination cages on Si(100) surfaces. *Chem. Eur. J.*, **2007**, *13*, 6891-6898.

[42] (a) Park, S.J.; Hong, J.I. Self-assembled nanoscale capsules between resorcin[4]arene derivatives and Pd(II) or Pt(II) complexes. *Chem. Commun.*, **2001**, (17), 1554-1555; (b) Park, S.J.; Shin, D.M.; Sakamoto, S.; Yamaguchi, K.; Chung, Y.K.; Lah, M.S.; Hong, J.I. Dynamic equilibrium between a supramolecular capsule and bowl generated by inter- and intramolecular metal clipping. *Chem. Eur. J.*, **2005**, *11*, 235-241.

[43] (a) Fox, O.D.; Dalley, N.K.; Harrison, R.G. A metal-assembled, pH-dependent, resorcinarene-based cage molecule. *J. Am. Chem. Soc.*, **1998**, *120*, 7111-7112; (b) Fox, O.D.; Dalley, N.K.; Harrison, R.G. Structure and small molecule binding of a tetranuclear Iron(II) Resorc[4]arene-based cage complex. *Inorg. Chem.*, **1999**, *38*, 5860-5863; (c) Fox, O.D.; Leung, J.F.Y.; Hunter, J.M.; Dalley, N.K.; Harrison, R.G. Metal-assembled Cobalt(II) Resorc[4]arene-based cage molecules that reversibly capture organic molecules from water and act as NMR shift reagents. *Inorg. Chem.*, **2000**, *39*, 783-790.

[44] (a) Fox, O.D.; Drew, M.G.B.; Beer, P.D. Resorcarene-based nanoarchitectures: Metal-directed assembly of a molecular loop and tetrahedron. *Angew. Chem. Int. Ed.*, **2000**, *39*, 135-140; (b) Fox, O.D.; Cookson, J.; Wilkinson, E.J.S.; Drew, M.G.B.; MacLean, E.J.; Teat, S.J.; Beer, P.D. Nanosized polymetallic resorcinarene-based host assemblies that strongly bind fullerenes. *J. Am. Chem. Soc.*, **2006**, *128*, 6990-7002.

[45] Schröder, T.; Brodbeck, R.; Letzel, M.C.; Mix, A.; Schnatwinkel, B.; Tonigold, M.; Volkmer, D.; Mattay, J. A self-assembling metallosupramolecular cage based on cavitand-terpyridine subunits. *Tetrahedron Lett.*, **2008**, *49*, 5939-5942.

[46] (a) Haino, T.; Kobayashi, M.; Chikaraishi, M.; Fukazawa, Y. A new self-assembling capsule *via* metal coordination. *Chem. Commun.*, **2005**, (18), 2321-2323; (b) Haino, T.; Kobayashi, M.; Fukazawa, Y. Guest encapsulation and self-assembly of a cavitand-based coordination capsule. *Chem. Eur. J.*, **2006**, *12*, 3310-3319; (c) Haino, T.; Fukuta, K.; Iwamoto, H.; Iwata, S. Non-covalent isotope effect for guest encapsulation in self-assembled molecular capsules. *Chem. Eur. J.*, **2009**, *15*, 13286-13290.

[47] Tsunoda, Y.; Fukuta, K.; Imamura, T.; Sekiya, R.; Furuyama, T.; Kobayashi, N.; Haino, T. High diastereoselection of a dissymmetric capsule by chiral guest complexation. *Angew. Chem. Int. Ed.*, **2014**, *53*, 7243-7247.

[48] Kobayashi, M.; Takatsuka, M.; Sekiya, R.; Haino, T. Molecular recognition of upper rim functionalized cavitand and its unique dimeric capsule in the solid state. *Org. Biomol. Chem.*, **2015**, *13*, 1647-1653.

[49] (a) Kobayashi, K.; Yamada, Y.; Yamanaka, M.; Sei, Y.; Yamaguchi, K. Complete selection of a self-assembling homo- or hetero-cavitand cage *via* metal coordination based on ligand tuning. *J. Am. Chem. Soc.*, **2004**, *126*, 13896-13897; (b) Yamanaka, M.; Yamada, Y.; Sei, Y.; Yamaguchi, K.; Kobayashi, K. Selective formation of a self-assembling Homo or Hetero cavitand cage *via* metal coordination based on thermodynamic or kinetic control. *J. Am. Chem. Soc.*, **2006**, *128*, 1531-1539.

[50] (a) Yamanaka, M.; Toyoda, N.; Kobayashi, K. Hybrid cavitand capsule with hydrogen bonds and metal−ligand coordination bonds: Guest encapsulation with anion assistance. *J. Am. Chem. Soc.*, **2009**, *131*, 9880-9881; (b) Yamanaka, M.; Kawaharada, M.; Nito, Y.; Takaya, H.; Kobayashi, K. Structural alteration of hybrid supramolecular capsule induced by guest encapsulation. *J. Am. Chem. Soc.*, **2011**, *133*, 16650-16656.

[51] Gibb, C.L.D.; Gibb, B.C. Well-defined, organic nanoenvironments in water: The hydrophobic effect drives a capsular assembly. *J. Am. Chem. Soc.*, **2004**, *126*, 11408-11409.

[52] Fujita, M.; Oguro, D.; Mlyazawa, M.; Oka, H.; Yamaguchi, K.; Ogura, K. Self-assembly of ten molecules into nanometre-sized organic host frameworks. *Nature*, **1995**, *378*, 469-471.

[53] Tashiro, S.; Tominaga, M.; Kawano, M.; Therrien, B.; Ozekiand, T.; Fujita, K. Sequence-selective recognition of peptides within the single binding pocket of a self-assembled coordination cage. *J. Am. Chem. Soc.*, **2005**, *127*, 4546-4547.

[54] (a) Nakabayashi, K.; Kawano, M.; Fujita, M. pH-Switchable through-space interaction of organic radicals within a self-assembled coordination cage. *Angew. Chem., Int. Ed.*, **2005**, *44*, 5322-5325; (b) Nakabayashi, K.; Kawano, M.; Kato, T.; Furukawa, K.; Ohkoshi, S.I.; Hozumi, T.; Fujita, M. Manipulating the through-space spin-spin interaction of organic radicals in the confined cavity of a self-assembled cage. *Chem.-Asian J.*, **2007**, *2*, 164-170; (c) Nakabayashi, K.; Ozaki, Y.; Kawano, M.; Fujita, M. A self-assembled spin cage. *Angew. Chem., Int. Ed.*, **2008**, *47*, 2046-2048.

[55] Nishioka, Y.; Yamaguchi, T.; Kawano, M.; Fujita, M. Asymmetric [2 + 2] olefin cross photoaddition in a self-assembled host with remote chiral auxiliaries. *J. Am. Chem. Soc.*, **2008**, *130*, 8160-8161.

[56] Zheng, Y.R.; Suntharalingam, K.; Johnstone, T.C.; Lippard, S.J. Encapsulation of Pt(IV) prodrugs within a Pt(II) cage for drug delivery. *Chem. Sci.*, **2015**, *6*, 1189-1193.

[57] Karthikeyan, S.; Ramamurthy, V. Templating photodimerization of trans-cinnamic acid esters with a water-soluble Pd nanocage. *J. Org. Chem.*, **2007**, *72*, 452-458.

[58] Yoshizawa, M.; Nakagawa, J.; Kumazawa, K.; Nagao, M.; Kawano, M.; Ozeki, T.; Fujita, M. Discrete stacking of large aromatic molecules within organic-pillared coordination cages. *Angew. Chem., Int. Ed.*, **2005**, *44*, 1810-1813.

[59] Ono, K.; Klosterman, J.K.; Yoshizawa, M.; Sekiguchi, K.; Tahara, T.; Fujita, M. ON/OFF red emission from azaporphine in a coordination cage in water. *J. Am. Chem. Soc.*, **2009**, *131*, 12526-12527.

[60] Ono, K.; Yoshizawa, M.; Kato, T.; Watanabe, K.; Fujita, M. Porphine dimeric assemblies in organic-pillared coordination cages. *Angew. Chem., Int. Ed.*, **2007**, *46*, 1803-1806.

[61] Sawada, T.; Yoshizawa, M.; Sato, S.; Fujita, M. Minimal nucleotide duplex formation in water through enclathration in self-assembled hosts. *Nat. Chem.*, **2009**, *1*, 53-56.

[62] Ono, K.; Yoshizawa, M.; Kato, T.; Fujita, M. Three-metal-center spin interactions through the intercalation of metal azaporphines and porphines into an organic pillared coordination box. *Chem. Commun.*, **2008**, (20), 2328-2330.

[63] Ono, K.; Yoshizawa, M.; Akita, M.; Kato, T.; Tsunobuchi, Y.; Ohkoshi, S.I.; Fujita, M. Spin crossover by encapsulation. *J. Am. Chem. Soc.*, **2009**, *131*, 2782-2783.

[64] Yamauchi, Y.; Yoshizawa, M.; Fujita, M. Engineering stacks of aromatic rings by the interpenetration of self-assembled coordination cages. *J. Am. Chem. Soc.*, **2008**, *130*, 5832-5833.

[65] (a) Tashiro, S.; Tominaga, M.; Yamaguchi, Y.; Kato, K.; Fujita, M. Folding a de novo designed peptide into an α-helix through hydrophobic binding by a bowl-shaped host. *Angew. Chem., Int. Ed.*, **2006**, *45*, 241-244; (b) Yoshizawa, M.; Tamura, M.; Fujita, M. Chirality enrichment through the heterorecognition of enantiomers in an achiral coordination host. *Angew. Chem., Int. Ed.*, **2007**, *46*, 3874-3876.

[66] Tashiro, S.; Tominaga, M.; Yamaguchi, Y.; Kato, K.; Fujita, M. Peptide Recognition: Encapsulation and α-helical folding of a nine-residue peptide within a hydrophobic dimeric capsule of a bowl-shaped host. *Chem.-Eur. J.*, **2006**, *12*, 3211-3217.

[67]   Davis, A.V.; Fiedler, D.; Ziegler, F.E.; Terpin, A.; Raymond, K.N. Resolution of chiral, tetrahedral M4L6 metal–ligand hosts. *J. Am. Chem. Soc.*, **2007**, *129*, 15354-15363.

[68]   Biros, S.M.; Bergman, R.G.; Raymond, K.N. The hydrophobic effect drives the recognition of hydrocarbons by an anionic metal–ligand cluster. *J. Am. Chem. Soc.*, **2007**, *129*, 12094-12095.

[69]   Hastings, C.J.; Pluth, M.D.; Biros, S.M.; Bergman, R.G.; Raymond, K.N. A chiral self-assembled supramolecular host encapsulates hydrophobic guests. *Tetrahedron*, **2008**, *64*, 8362-8367.

[70]   Dong, V.M.; Fiedler, D.; Carl, B.; Bergman, R.G.; Raymond, K.N. Molecular recognition and stabilization of iminium ions in water. *J. Am. Chem. Soc.*, **2006**, *128*, 14464-14465.

[71]   Cram, D.J.; Tanner, M.E.; Knobler, C.B. Guest release and capture by hemicarcerands introduces the phenomenon of constrictive binding. *J. Am. Chem. Soc.*, **1991**, *113*, 7717-7727.

[72]   Pluth, M.D.; Tiedemann, B.E.F.; van Halbeek, H.; Nunlist, R.; Raymond, K.N. Diffusion of a highly charged supramolecular assembly: Direct observation of ion association in water. *Inorg. Chem.*, **2008**, *47*, 1411-1413.

[73]   Leung, D.H.; Bergman, R.G.; Raymond, K.N. Enthalpy–entropy compensation reveals solvent reorganization as a driving force for supramolecular encapsulation in water. *J. Am. Chem. Soc.*, **2008**, *130*, 2798-2805.

[74]   Tiedemann, B.E.F.; Raymond, K.N. Second-order Jahn-Teller effect in a host-guest complex. *Angew. Chem., Int. Ed.*, **2007**, *46*, 4976-4978.

[75]   Fiedler, D.; Bergman, R.G.; Raymond, KN. Stabilization of reactive organometallic intermediates inside a self-assembled nanoscale host. *Angew. Chem., Int. Ed.*, **2006**, *45*, 745-748.

[76]   Pluth, M.D.; Bergman, R.G.; Raymond, K.N. Making amines strong bases: Thermodynamic stabilization of protonated guests in a highly-charged supramolecular host. *J. Am. Chem. Soc.*, **2007**, *129*, 11459-11467.

[77]   Pluth, M.D.; Bergman, R.G.; Raymond, K.N. Acceleration of amide bond rotation by encapsulation in the hydrophobic interior of a water-soluble supramolecular assembly. *J. Org. Chem.*, **2008**, *73*, 7132-7136.

[78]   (a) Leung, D.H.; Bergman, R.G.; Raymond, K.N. Scope and mechanism of the C–H bond activation reactivity within a supramolecular host by an iridium guest: A stepwise ion pair guest dissociation mechanism. *J. Am. Chem. Soc.*, **2006**, *128*, 9781-9797; (b) Leung, D.H.; Bergman, R.G.; Raymond, K.N. Highly selective supramolecular catalyzed allylic alcohol isomerization. *J. Am. Chem. Soc.*, **2007**, *129*, 2746-2747; (c) Brown, C.J.; Miller, G.M.; Johnson, M.W.; Bergman, R.G.; Raymond, K.N. High-turnover supramolecular catalysis by a protected ruthenium(II) complex in aqueous solution. *J. Am. Chem. Soc.*, **2011**, *133*, 11964-11966; (d) Wang, Z.J.; Clary, K.N.; Bergman, R.G.; Raymond, K.N.; Toste, F.D. A supramolecular approach to combining enzymatic and transition metal catalysis. *Nat. Chem.*, **2013**, *5*, 100-103; (e) Wang, Z.J.; Brown, C.J.; Bergman, R.G.; Raymond, K.N.; Toste, F.D. Hydroalkoxylation catalyzed by a Gold(I) complex encapsulated in a supramolecular host. *J. Am. Chem. Soc.*, **2011**, *133*, 7358-7360; (f) Hart-Cooper, W.M.; Clary, K.N.; Toste, F.D.; Bergman, R.G.; Raymond, K.N. Selective monoterpene-like cyclization reactions achieved by water exclusion from reactive intermediates in a supramolecular catalyst. *J. Am. Chem. Soc.*, **2012**, *134*, 17873-17876; (g) Fiedler, D.; van Halbeek, H.; Bergman, R.G.; Raymond, K.N. Supramolecular catalysis of unimolecular rearrangements: Substrate scope and mechanistic insights. *J. Am. Chem. Soc.*, **2006**, *128*, 10240-10252; (h) Hastings, C.J.; Fiedler, D.; Bergman, R.G.; Raymond, K.N. Aza cope rearrangement of propargyl enammonium cations catalyzed by a self-assembled "Nanozyme". *J. Am. Chem. Soc.*, **2008**, *130*, 10977-10983; (i) Pluth, M.D.; Bergman, R.G.; Raymond, K.N. Acid catalysis in basic solution: A supramolecular host promotes orthoformate hydrolysis. *Science*, **2007**, *316*, 85-88; (j) Pluth, M.D.; Bergman, R.G.; Raymond, K.N. Catalytic deprotection of acetals in basic solution with a self-assembled supramolecular "Nanozyme". *Angew. Chem., Int. Ed.*, **2007**, *46*, 8587-8589; (k) Pluth, M.D.; Bergman, R.G.; Raymond, K.N. The acid hydrolysis mechanism of acetals catalyzed by a supramolecular assembly in basic solution. *J. Org. Chem.*, **2009**, *74*, 58-63.

[79]   Mal, P.; Schultz, D.; Beyeh, K.; Rissanen, K.; Nitschke, J.R. An unlockable-relockable iron cage by subcomponent self-assembly. *Angew. Chem., Int. Ed.*, **2008**, *47*, 8297-8301.

[80]   Mal, P.; Breiner, B.; Rissanen, K.; Nitschke, J.R. White phosphorus is air-stable within a self-assembled tetrahedral capsule. *Science*, **2009**, *324*, 1697-1699.

[81]   Roukala, J.; Zhu, J.; Giri, C.; Rissanen, K.; Lantto, P.; Telkki, V.V. Encapsulation of Xenon by a self-assembled Fe4L6 metallosupramolecular cage. *J. Am. Chem. Soc.*, **2015**, *137*, 2464-2467.

[82]   Aoki, S.; Suzuki, S.; Kitamura, M.; Haino, T.; Shiro, M.; Zulkefeli, M.; Kimura, E. Molecular recognition of hydrocarbon guests by a supramolecular capsule formed by the 4:4 self-assembly of tris(Zn2+-Cyclen) and trithiocyanurate in aqueous solution. *Chem. Asian J.*, **2012**, *7*, 944-956.

[83]   Liu, S.; Whisenhunt-Ioup, S.E.; Gibb, C.L.D.; Gibb, B.C. An improved synthesis of "octa-acid" deep-cavity cavitand. *Supramol. Chem.*, **2011**, *23*, 480-485.

[84]   Gibb, C.L.D.; Gibb, B.C. Templated assembly of water-soluble nano-capsules: inter-phase sequestration, storage, and separation of hydrocarbon gases. *J. Am. Chem. Soc.*, **2006**, *128*, 16498-16499.

[85]   Sullivan, M.R.; Gibb, B.C. Differentiation of small alkane and alkyl halide constitutional isomers *via* encapsulation *Org. Biomol. Chem.*, **2015**, *13*, 1869-1877.

[86]   Gibb, C.L.D.; Gibb, B.C. Straight-chain alkanes template the assembly of water-soluble nano-capsules. *Chem. Commun.*, **2007**, (16), 1635-1637.

[87]   Choudhury, R.; Barman, A.; Prabhakar, R.; Ramamurthy, V. Hydrocarbons depending on the chain length and head group adopt different conformations within a water-soluble nanocapsule: 1H NMR and molecular dynamics studies. *J. Phys. Chem. B*, **2013**, *117*, 398-407.

[88]   (a) Jayaraj, N.; Zhao, Y.; Parthasarathy, A.; Porel, M.; Liu, R.S.H.; Ramamurthy, V. Nature of supramolecular complexes controlled by the structure of the guest molecules: Formation of octa-acid based capsuleplex and cavitandplex. *Langmuir*, **2009**, *25*, 10575-10586; (b) Sun, H.; Gibb, C.L.D.; Gibb, B.C. Calorimetric analysis of the 1:1 complexes formed between a water-soluble deep-cavity cavitand, and cyclic and acyclic carboxylic acids. *Supramol. Chem.*, **2008**, *20*, 141-147.

[89]   Porel, M.; Jayaraj, N.; Kaanumalle, L.S.; Maddipatla, M.V.S.N.; Parthasarathy, A.; Ramamurthy, V. Sulfonatocalix[8]arene as a potential reaction cavity: photo- and electro-active dicationic guests arrest conformational equilibrium. *Langmuir*, **2009**, *25*, 3473-3481.

[90]   Gibb, C.L.D.; Gibb, B.C. Guests of differing polarities provide insight into structural requirements for templates of water-soluble nano-capsules. *Tetrahedron*, **2009**, *65*, 7240-7248.

[91]   Baldridge, A.; Samanta, S.R.; Jayaraj, N.; Ramamurthy, V.; Tolbert, L.M. Activation of fluorescent protein chromophores by encapsulation. *J. Am. Chem. Soc.*, **2010**, *132*, 1498-1499.

[92]   Tang, H.; de Oliveira, C.S.; Sonntag, G.; Gibb, C.L.D.; Gibb, B.C.; Bohne, C. Dynamics of a supramolecular capsule assembly with pyrene. *J. Am. Chem. Soc.*, **2012**, *134*, 5544-5547.

[93]   (a) Chen, J.Y.C.; Jayaraj, N.; Jockusch, S.; Ottaviani, M.F.; Ramamurthy, V.; Turro, N.J. An EPR and NMR study of supramolecular effects on paramagnetic interaction between a nitroxide incarcerated within a nanocapsule with a nitroxide in bulk aqueous media. *J. Am. Chem. Soc.*, **2008**, *130*, 7206-7207; (b) Jockusch, S.; Zeika, O.; Jayaraj, N.; Ramamurthy, V.; Turro, N.J. An electron spin polarization study of the interaction of photoexcited triplet molecules with mono- and polynitroxyl stable free radicals. *J. Phys. Chem. Lett.*, **2010**, *1*, 2628-2632.

[94]   Porel, M.; Jockusch, S.; Parthasarathy, A.; Rao, V.J.; Turro, N.J.; Ramamurthy, V. Photoinduced electron transfer between a donor and an acceptor separated by a capsular wall *Chem. Commun.*, **2012**, *48*, 2710-2712.

[95]   Samanta, S.R.; Kulasekharan, R.; Choudhury, R.; Jagadesan, P.; Jayaraj, N.; Ramamurthy, V. Interaction between encapsulated excited organic molecules and free nitroxides: communication across a molecular wall. *Langmuir*, **2012**, *28*, 11920-11928.

[96]   (a) Giles, M.D.; Liu, S.; Emanuel, R.L.; Gibb, B.C.; Grayson, S.M. Dendronized supramolecular nanocapsules: pH independent, water-soluble, deep-cavity cavitands assemble *via* the hydrophobic effect. *J. Am. Chem. Soc.*, **2008**, *130*, 14430-14431; (b) Grayson, S.M.; Gibb, B.C. Dendronized cavitands: A step towards a synthetic viral capsid? *Soft Matter*, **2010**, *6*, 1377-1382.

[97]   Ewell, J.; Gibb, B.C.; Rick, S.W. Water inside a hydrophobic cavitand molecule. *J. Phys. Chem. B*, **2008**, *112*, 10272-10279.

[98]   Podkoscielny, D.; Gibb, C.L.D.; Gibb, B.C.; Kaifer, A.E. Encapsulation of ferrocene and peripheral electrostatic attachment of viologens to dimeric molecular capsules formed by an octa-acid, deep-cavity cavitand. *Chem.-Eur. J.*, **2008**, *14*, 4704-4710.

[99]   Podkoscielny, D.; Gadde, S.; Kaifer, A.E. Mediated electrochemical oxidation of a fully encapsulated redox active center. *J. Am. Chem. Soc.*, **2009**, *131*, 12876-12877.

[100]  (a) Kulasekharan, R.; Ramamurthy, V. New water-soluble organic capsules are effective in controlling excited-state processes of guest molecules. *Org. Lett.*, **2011**, *13*, 5092-5095; (b) Ishida, Y.; Kulasekharan, R.; Shimada, T.; Takagi, S.; Ramamurthy, V. Efficient singlet-singlet energy transfer in a novel host-guest assembly composed of an organic cavitand, aromatic molecules, and a clay nanosheet. *Langmuir*, **2013**, *29*, 1748-1753; (c) Ishida, Y.; Kulasekharan, R.; Shimada, T.; Ramamurthy, V.; Takagi, S. Supramolecular-surface photochemistry: Supramolecular assembly organized on a clay surface facilitates energy transfer between an encapsulated donor and a free acceptor *J. Phys. Chem. C*, **2014**, *118*, 10198-10203.

[101]  Gan, H.; Benjamin, C.J.; Gibb, B.C. Nonmonotonic assembly of a deep-cavity cavitand. *J. Am. Chem. Soc.*, **2011**, *133*, 4770-4773.

[102]  Gan, H.; Gibb, B.C. Guest-mediated switching of the assembly state of a water-soluble deep-cavity cavitand. *Chem. Commun.*, **2013**, *49*, 1395-1397.

[103]  Gan, H.; Gibb, B.C. Guest-controlled self-sorting in assemblies driven by the hydrophobic effect. *Chem. Commun.*, **2012**, *48*, 1656-1658.

[104]  Liu, S.; Russell, D.H.; Zinnel, N.F.; Gibb, B.C. Guest packing motifs within a supramolecular nano-capsule and a covalent analogue. *J. Am. Chem. Soc.*, **2013**, *135*, 4314-4324.

[105]  Ebbing, M.H.K.; Villa, M.J.; Valpuesta, J.M.; Prados, P.; de Mendoza, J. Resorcinarenes with 2-benzimidazolone bridges: self-aggregation, self-assembled dimeric capsules, and guest encapsulation. *Proc. Natl. Acad. Sci. U.S.A*, **2002**, *99*, 4962-4966.

[106]  Zhang, K.D.; Ajami, D.; Rebek Jr., J. Hydrogen-bonded capsules in water. *J. Am. Chem. Soc.*, **2013**, *135*, 18064-18066.

[107]  Zhang, K.D.; Ajami, D.; Gavette, J.V.; Rebek Jr., J. Complexation of alkyl groups and ghrelin in a deep, water-soluble cavitand. *Chem. Commun.*, **2014**, *50*, 4895-4897.

[108]   Gavette, J.V.; Zhang, K.D.; Ajami, D.; Rebek Jr., J. Folded alkyl chains in water-soluble capsules and cavitands. *Org. Biomol. Chem.*, **2014**, *12*, 6561-6563.

[109]   (a) Shimizu, K.D.; Rebek Jr., J. Synthesis and assembly of self-complementary calix[4]arenes. *Proc. Natl. Acad. Sci. U.S.A*, **1995**, *92*, 12403-12407; (b) Vysotsky, M.O.; Thondorf, I.; Bohmer, V. Self-assembled hydrogen-bonded dimeric capsules with high kinetic stability. *Angew. Chem., Int. Ed.*, **2000**, *39*, 1264-1267.

[110]   Corbellini, F.; Di Costanzo, L.; Crego-Calama, M.; Geremia, S.; Reinhoudt, D.N. Guest encapsulation in a water-soluble molecular capsule based on ionic interactions. *J. Am. Chem. Soc.*, **2003**, *125*, 9946-9947.

[111]   Cram, D.J.; Choi, H.J.; Bryant, J.A.; Knobler, C.B. Solvophobic and entropic driving forces for forming velcraplexes, which are 4-fold, lock-key dimers in organic media. *J. Am. Chem. Soc.*, **1992**, *114*, 7748-7765.

[112]   (a) Hamann, B.C.; Shimizu, K.D.; Rebek Jr., J. Reversible encapsulation of guest molecules in a calixarene dimer. *Angew. Chem., Int. Ed. Engl.*, **1996**, *35*, 1326-1329; (b) Palmer, L.C.; Rebek Jr., J. The ins and outs of molecular encapsulation. *Org. Biomol. Chem.*, **2004**, *2*, 3051-3059; (c) Moon, C.; Brunklaus, G.; Sebastiani, D.; Rudzevich, Y.; Bohmer, V.; Spiess, H.W. Solid-state NMR and computational studies of tetratolyl urea calix[4]arene inclusion compounds. *Phys.Chem.Chem.Phys.*, **2009**, *11*, 9241-9249; (d) Sansone, F.; Baldini, L.; Casnati, A.; Chierici, E.; Faimani, G.; Ugozzoli, F.; Ungaro, R. Chiral dimeric capsules from *N, C*-linked peptidocalix[4]arenes self-assembled through an antiparallel β-sheetlike motif. *J. Am. Chem. Soc.*, **2004**, *126*, 6204-6205; (e) Castellano, R.K.; Rebek, J., Jr. Formation of discrete, functional assemblies and informational polymers through the hydrogen-bonding preferences of calixarene aryl and sulfonyl tetraureas. *J. Am. Chem. Soc.*, **1998**, *120*, 3657-3663.

[113]   Weimann, D.P.; Schalley, C.A. Host-guest chemistry of self-assembling supramolecular capsules in the gas phase. *Supramol. Chem.*, **2008**, *20*, 117-128.

[114]   (a) Frish, L.; Vysotsky, M.O.; Matthews, S.E.; Bohmer, V.; Cohen, Y. Tropylium cation capsule of hydrogen-bonded tetraurea calix[4]arene dimers. *J. Chem. Soc., Perkin Trans*, **2002**, *2*, 88-93; (b) Frish, L.; Vysotsky, M.O.; Bohmer, V.; Cohen, Y. Compensation of steric demand by cation-π interactions, cobaltocenium cations as guests in tetraurea calix[4]arene dimers. *Org. Biomol. Chem.*, **2003**, *1*, 2011-2014.

[115]   Vysotsky, M.O.; Pop, A.; Broda, F.; Thondorf, I.; Bohmer, V. Molecular motions within self-assembled dimeric capsules with tetraethylammonium cations as guest. *Chem.-Eur. J.*, **2001**, *7*, 4403-4410.

[116]   Baldini, L.; Sansone, F.; Faimani, G.; Massera, C.; Casnati, A.; Ungaro, R. Self-assembled chiral dimeric capsules from difunctionalized *N,C*-linked peptidocalix[4]arenes: scope and limitations. *Eur. J. Org. Chem.*, **2008**, (5), 869-886.

[117]   (a) Garozzo, D.; Gattuso, G.; Kohnke, F.H.; Malvagna, P.; Notti, A; Occhipinti, S; Pappalardo, S.; Parisi, M.F.; Pisagatti, I. Guest-induced capsular assembly of calix[5]arenes. *Tetrahedron Lett.*, **2002**, *43*, 7663-7667; (b) Garozzo, D.; Gattuso, G.; Kohnke, F.H.; Notti, A.; Pappalardo, S.; Parisi, M.F.; Pisagatti, I.; White, A.J.P.; Williams, D.J. Inclusion networks of a calix[5]arene-based exoditopic receptor and long-chain alkyldiammonium ions. *Org. Lett.*, **2003**, *5*, 4025-4028; (c) Gattuso, G.; Notti, A.; Pappalardo, A.; Parisi, M.F.; Pisagatti, I.; Pappalardo, S.; Garozzo, D.; Messina, A.; Cohen, Y.; Slovak, S. Self-assembly dynamics of modular homoditopic bis-calix[5]arenes and long-chain r,ω-alkanediyldiammonium components. *J. Org. Chem.*, **2008**, *73*, 7280-7289; (d) Gargiulli, C.; Gattuso, G.; Notti, A.; Pappalardo, S.; Parisi, M.F. Supramolecular AA/BB-type oligomer formation from a heterotetratopic bis-calix[5]arene monomer and octanediyldiammonium dichloride. *Tetrahedron Lett.*, **2011**, *52*, 7116-7120; (e) Brancatelli, G.; Gattuso, G.; Geremia, S.; Notti, A.; Pappalardo, S.; Parisi, M.F.; Pisagatti, I. Probing the inner space of salt-bridged calix[5]arene capsules. *Org. Lett.*, **2014**, *16*, 2354-2357.

[118]   (a) Liu, Y.; Guo, D.S.; Zhang, H.Y.; Ding, F.; Chen, K.; Song, H.B. Supramolecular assemblies of sulfonatocalixarenes with phenanthroline: Factors governing capsule formation versus bilayer arrangements. *Chem. Eur. J.*, **2007**, *13*, 466-472; (b) Guo, D.S.; Su, X.; Liu, Y. Benzyl effects of supramolecular architectures constructed by *p*-sulfonatocalix[4]arene and viologen guests: from simple 2:1 complex to polymeric capsules. *Cryst. Growth Des.*, **2008**, *8*, 3514- 3517; (c) Wang, K.; Yang, E.C.; Zhao, X.J.; Dou, H.X.; Liu, Y. Molecular binding behaviors of sulfonated calixarenes with phenanthroline-diium in aqueous solution and solid state: Cavity size governing capsule formation. *Cryst. Growth Des.*, **2014**, *14*, 4631-4639.

[119]   Martin, A.D.; Boulos, R.A.; Hubble, L.J.; Hartlieb, K.J.; Raston, C.L. Multifunctional water-soluble molecular capsules based on *p*-phosphonic acid calix[5]arene. *Chem. Commun.*, **2011**, *47*, 7353-7355.

[120]   Ananchenko, G.S.; Udachin, K.A.; Dubes, A.; Ripmeester, J.A.; Perrier, T.; Coleman, A.W. Guest exchange in single crystals of van der Waals nanocapsules. *Angew. Chem. Int. Ed.*, **2006**, *45*, 1585-1588.

[121]   Ananchenko, G.S.; Udachin, K.A.; Pojarova, M.; Jebors, S.; Colemanb, A.W.; Ripmeester, J.A. A molecular turnstile in para-octanoyl calix[4]arene nanocapsules. *Chem. Commun.*, **2007**, (7), 707-709.

[122]   Ananchenko, G.S.; Moudrakovski, I.L.; Coleman, A.W.; Ripmeester, J.A. A channel-free soft-walled capsular calixarene solid for gas adsorption. *Angew. Chem. Int. Ed.*, **2008**, *47*, 5616-5618.

[123]   Li, G.K.; Yang, Y.; Chen, C.F.; Huang, Z.T. Heterodimer of tetraaryl- and tetratosylurea calix[4]arenes: First single crystal X-ray analysis and guest encapsulation properties in CDCl₃. *Tetrahedron Lett.*, **2007**, *48*, 6096-6099.

[124]   Corbellini, F.; Knegtel, R.M.A.; Grootenhuis, P.D.J.; Crego-Calama, M.; Reinhoudt, D.N. Water-soluble molecular capsules: self-assembly and binding properties. *Chem. Eur. J.*, **2005**, *11*, 298-307.

[125]   Corbellini, F.; Mulder, A.; Sartori, A.; Ludden, M.J.W.; Casnati, A.; Ungaro, R.; Huskens, J.; Crego-Calama, M.; Reinhoudt, D.N. Assembly of a supramolecular capsule on a molecular printboard. *J. Am. Chem. Soc.*, **2004**, *126*, 17050-17058.

[126]   Chas, M.; Gil-Ramírez, G.; Ballester, P. Exclusive self-assembly of a polar dimeric capsule between tetraurea calix[4]pyrrole and tetraurea calix[4]arene. *Org. Lett.*, **2011**, *13*, 3402-3405.

[127]   Cholewa, P.P.; Dalgarno, S.J. Metal-organic calixarene capsules: The evolution of controlled assembly. *CrystEngComm*, **2014**, *16*, 3655-3666.

[128]   Cotton, F.A.; Lei, P.; Lin, C.; Murillo, C.A.; Wang, X.; Yu, S.Y.; Zhang, Z.X. A calix[4]arene carceplex with four Rh24+ fasteners. *J. Am. Chem. Soc.*, **2004**, *126*, 1518-1525.

[129]   Ling, I.; Alias, Y.; Sobolev, A.N.; Raston, C.L. Constructing multicomponent materials containing cavitands, and phosphonium and imidazolium cations. *Cryst. Growth Des.*, **2009**, *9*, 4497-4503.

[130]   Erra, L.; Tedesco, C.; Vaughan, G.; Brunelli, M.; Troisi, F.; Gaeta, C.; Neri, P. A solid-state molecular capsule based on *p*-sulfonatocalix[7]arene and dicationic diquat guest. *CrystEngComm*, **2010**, *12*, 3463-3466.

[131]   Pasquale, S.; Sattin, S.; Escudero-Adán, E.C.; Martínez-Belmonte, M.; de Mendoza, J. Giant regular polyhedra from calixarene carboxylates and uranyl. *Nat. Commun.*, **2012**, *3*, 785-791.

[132]   Cholewa, P.P.; Beavers, C.M.; Teat, S.J.; Dalgarno, S.J. Directed assembly *via* selectively positioned host functionality. *Chem. Commun.*, **2013**, *49*, 3203-3205.

[133]   Cholewa, P.P.; Beavers, C.M.; Teat, S.J.; Dalgarno, S.J. Enhancing strategies for the assembly of metal-organic systems with inherent cavity-containing calix[4]arenes *Cryst. Growth Des.*, **2013**, *13*, 5165-5168.

[134]   Monnereau, L.; Sémeril, D.; Matt, D.; Toupet, L. Pseudo-capsular behavior of two *trans*-coordinated calixarenyl phosphines. *Transition Met. Chem.*, **2013**, *38*, 821-825.

[135]   Kerckhoffs, J.M.C.A.; ten Cate, M.G.J.; Mateos-Timoneda, M.A.; van Leeuwen, F.W.B.; Snellink-Ruël, B.; Spek, A.L.; Kooijman, H.; Crego-Calama, M.; Reinhoudt, D.N. Selective self-organization of guest molecules in self-assembled molecular boxes. *J. Am. Chem. Soc.*, **2005**, *127*, 12697-12708.

[136]   Kerckhoffs, J.M.C.A.; van Leeuwen, F.W.B.; Spek, A.L.; Kooijman, H.; Crego-Calama, M.; Reinhoudt, D.N. Regulatory strategies in the complexation and release of a noncovalent guest trimer by a self-assembled molecular cage. *Angew. Chem., Int. Ed.*, **2003**, *42*, 5717-5722.

[137]   Timmerman, P.; Vreekamp, R.H.; Hulst, R.; Verboom, W.; Reinhoudt, D.N.; Rissanen, K.; Udachin, K.A.; Ripmeester, J. Noncovalent assembly of functional groups on calix[4]arene molecular boxes. *Chem. Eur. J.*, **1997**, *3*, 1823-1832.

[138]   ten Cate, M.G.J.; Omerovic, M.; Oshovsky, G.V.; Crego-Calama, M.; Reinhoudt, D.N. Self-assembly and stability of double rosette nanostructures with biological functionalities. *Org. Biomol. Chem.*, **2005**, *3*, 3727-3733.

[139]   ten Cate, M.G.J.; Crego- Calama, M.; Reinhoudt, D.N. Formation of a hydrogen-bonded receptor assembly in niosomal membranes. *J. Am. Chem. Soc.*, **2004**, *126*, 10840-10841.

[140]   Crego-Calama, M.; Reinhoudt, D.N.; Mateos-Timoneda, M.A. Amplification of chirality in hydrogen-bonded tetra-rosette helices. *Chem Eur. J.*, **2006**, *12*, 2630-2638.

[141]   Piermattei, A.; Giesbers, M.; Marcelis, A.T.M.; Mendes, E.; Picken, S.J.; Crego-Calama, M.; Reinhoudt, D.N. Induction of liquid crystallinity by self-assembled molecular boxes. *Angew. Chem. Int. Ed.*, **2006**, *45*, 7543-7546.

[142]   Hardie, M.J.; Johnson, J.A.; Raston, C.L.; Webb, H.R. Cooperative hydrogen bonding and Yttrium(III) complexation in the assembly of molecular capsules. *Chem. Commun.*, **2000**, (10), 849-850.

[143]   (a) Drljaca, A.; Hardie, M.J.; Ness, T.J.; Raston, C.L. Rhodium(III) aqua ion salts of ambivalent self assembled superanion capsules. *Eur. J. Inorg. Chem.*, **2000**, (10), 2221-2229; (b) Dalgarno, S.J.; Raston, C.L. Rapid capture of 4,13-diaza-18-crown-6 molecules by *p*-sulfonatocalix[4]arene in the presence of trivalent lanthanide ions. *Dalton Trans.*, **2003**, (3), 287-290.

[144]   Dalgarno, S.J.; Raston, C.L. Capture of di-protonated [2.2.2]cryptand in the cavity of two *p*-sulfonated calixarenes as part of 2D bi-layer lanthanide coordination polymers. *Chem. Commun.*, **2002**, (19), 2216-2217.

[145]   Dalgarno, S.J.; Hardie, M.J.; Raston, C.L. pH-Dependent formation of molecular capsules and coordination polymers. *Cryst. Growth Des.*, **2004**, *4*, 227-234.

[146]   Dalgarno, S.J.; Fisher, J.; Raston, C.L. Interplay of *p*-sulfonatocalix[4]arene and crown ethers en route to molecular capsules and "Russian Dolls". *Chem. Eur. J.*, **2006**, *12*, 2772-2777.

[147]   Dalgarno, S.J.; Atwood, J.L.; Raston, C.L. Sulfonatocalixarenes: Molecular capsule and 'Russian Doll' arrays to structures mimicking viral geometry. *Chem. Commun.*, **2006**, (44), 4567-4574.

[148]   Dalgarno, S.J.; Hardie, M.J.; Raston, C.L. Conformation perturbation of *p*-sulfonatocalix[5]arene *via* complexation of 1,4-diazabicyclo[2.2.2]octane. *Chem. Commun.*, **2004**, (24), 2802-2803.

[149]   (a) Dalgarno, S.J.; Hardie, M.J.; Makha, M.; Raston, C.L. Controlling the conformation and interplay of *p*-sulfonatocalix[6]arene as lanthanide crown ether complexes. *Chem. Eur. J.*, **2003**, *9*, 2834-2839; (b) Makha, M.; Raston, C.L.; Sobolev, A.N.; White, A.H. Molecular capsules based on *p*-sulfonatocalix[6]arene shrouding two tetraphenylphosphonium cations. *Chem. Commun.*, **2005**, (15), 1962-1964.

## Oral communication at congress:

- Gangemi, C. M. A.; Tomaselli, G. A.; Purrello. R. *"Synthesis of new functionalized porphyrins and interaction with G-Quadruplex and proteasome".*
  "**VIII SCI Congress, Sicilia-Calabria**", December 6th-7th, 2012. Arcavacata di Rende, Cosenza, Italy.

- Gangemi, C. M. A.; D'Urso, A.; Tomaselli, G. A.; Purrello, R.; Yatsunyk, L. A.; *"Synthesis and characterization of porphyrins functionalized with polyamines for the interaction with the G-quadruplex".*
  "**IX SCI Congress, Sicilia-Calabria**", December 2nd-3rd, 2013. Catania, Italy

- Gangemi, C. M. A.; Berova, N.; Tomaselli, G. A.; D'Urso, A.; Purrello, R.; *"ZnTCPPSpm4: a single molecule as probe, catalyzer & stabilizer toward z-dna".*
  **Sigma-Aldrich Young Chemists Symposium (SAYCS 2015, XV Edition)**
  October 27th-29th, 2015. Rimini, Italy.

## Posters at congress:

- Gangemi, C. M. A.; D'urso, A.; Milardi, D.; Purrello, R.; Tomaselli, G.A.; Yatsunyk, L. A.; Di Fabio, G. *"Study of interactions between G-quadruplex and porphyrin bearing sperminate substituents".*
  "**European-Winter School on Physical Organic Chemistry (E-WiSPOC)**; February 2nd-7th, 2014. Brixen, South Tyrol, Italy.

- Gangemi, C. M. A.; Berova, N.; D'Urso, A.; Tomaselli, G. A.; Purrello, R. *"Interaction of ZnTCPPSpm4 with DNA. In a single molecule: probe, catalytic & stabilizing effects toward Z-form."*
  "**Italian meeting on porphyrins and phthalocyanines-2 (IMPP-2)**"; July 6th-8th, 2015. Rome, Italy

## Co-authors at congress:

- D'Urso, A.; Sabharwal, N.; Gangemi, C. M. A.; Tomaselli, G.; Di Fabio, G.; Milardi, D.; Yatsunyk, L. A.; Purrello, R.; *"G-quadruplex conformational selectivity by Zn(II) porphyrins bearing sperminate substituents"*.
  **"Convegno Nazionale della Divisione di Chimica dei Sistemi Biologici, 2013"** September 19th-20th, 2013. Bertinoro, Bologna, Italy. Oral communication.

- Milardi, D.; Santoro, A. M.; D'Urso, A.; Cunsolo, A.; Gangemi, C. M. A.; Tomaselli, G.; Gobbo, M.; Purrello, R.
  *"Proteasome inhibition by cationic porphyrins: tuning the potency by peripheral substitutions"*.
  **"Convegno Nazionale della Divisione di Chimica dei Sistemi Biologici, 2013"** September 19th-20th, 2013. Bertinoro, Bologna, Italy. Oral communication.

- Randazzo, R.; D'Urso, A.; Gangemi, C.; Fragalà, M. E.; Tomaselli, G. A.; Purrello, R. *"Spectroscopic characterization of porphyrin bearing sperminate substituents with polynucleotides"*.
  "**Convegno Nazionale della Divisione di Chimica dei Sistemi Biologici, 2013**" September 19th-20th, 2013. Bertinoro, Bologna, Italy. Poster.

- Cunsolo A., Santoro A. M., D'Urso A., Gangemi C. M. A., Stefanelli, M.; Tomaselli G., Gobbo, M.; Paolesse, R., Purrello R., Milardi D.
  *"The role of peripheral substituents in modulating the antiproteasome potential of porphyrins."*
  **"XXV congresso nazionale della societa' chimica italiana".** Arcavacata di Rende, Cosenza, Italy, September 7th-12th, 2014. Poster

- Randazzo R., Gangemi C. M. A., Oliviero G., Tomaselli G. A., Milardi D., Piccialli G., Di Fabio G., Purrello R., D'Urso A.
  *"Spectroscopic characterization of porphyrin bearing sperminate substituents with G-quadruplex."*
  "**Convegno Nazionale della Divisione di Chimica dei Sistemi Biologici, 2015**" September 24th-25th, 2015. Ortigia, Siracusa, Italy. Poster